AI-AEC-13079

ZIRCONIUM HYDRIDE REACTOR CONTROL SYSTEM BEARING DEVELOPMENT SUMMARY REPORT

AEC Research and Development Report

Atomics International Division
Rockwell International

P.O. Box 309
Canoga Park, California 91304

DISCLAIMER

AI-AEC-13079
SNAP REACTOR
SNAP PROGRAM
M-3679-R69
C92b

ZIRCONIUM HYDRIDE REACTOR CONTROL SYSTEM BEARING DEVELOPMENT SUMMARY REPORT

P. H. HORTON
W. J. KURZEKA

Atomics International Division
Rockwell International

P O Box 309
Canoga Park California 91304

CONTRACT: AT(04-3)-701
ISSUED: JUNE 14, 1973

DISTRIBUTION

This report has been distributed according to the catetory "Systems for Nuclear Auxiliary Power (SNAP) Reactor — SNAP Program," as given in the Standard Distribution for Classified Scientific and Technical Reports, M-3679.

CONTENTS

CONTENTS

TABLES

TABLES

TABLES

FIGURES

FIGURES

ABSTRACT

The technical history and development of bearings for the various SNAP reactor programs are traced from initial material selection through life testing and reactor operation. A reference bearing couple of flame-sprayed Al_2O_3 against carbon-graphite has successfully operated in individual tests of 20,000 hours and through a combined total of more than 120,000 hours. The self-aligning journal bearing design has provided low friction operation in temperatures to 1500°F in space vacuum (to 10^{-9} torr) without self-welding after long dwell periods. A variety of Al_2O_3 substrates have been used successfully for component requirements between 800 and 1500°F including Type 300 series stainless steels, Inconel-750, and tantalum - 10% tungsten alloys.

I. INTRODUCTION

A series of small nuclear reactors, designated "Systems for Nuclear Auxiliary Power" (SNAP), has been under development at Atomics International (AI) since 1957. These reactors have been designed to provide long-term uninterrupted power for space and remote terrestrial applications. Several generations of reactors: SNAP 10, SNAP 2, SNAP 4, SNAP 8, the Advanced ZrH Reactor, the Space Power Facility Test (SPF), and the 5 kwe Thermoelectric Reactor Systems have undergone design, development, testing, and operation to varying degrees. Technical developments of each generation have been utilized in succeeding generations, with the basic reactor concept modified for power and life requirements.

The reactors consist of a fueled core, through which a liquid metal coolant is circulated, surrounded by a beryllium moderator and reflector assembly. The control mode is by closing "windows" in the reflector assembly to regulate the amount of neutron loss and, therefore, maintaining the desired core and coolant temperatures.

The SNAP 10A, 2, 4, 8, SPF, and Advanced ZrH Reactors have movable reflector segments which are rotatable half cylinders parallel to the core centerline. Figure 1, the SNAP 8 Reactor System, illustrates this concept. The SNAP 10B and 5-kwe Thermoelectric Reactor movable reflectors consist of segments moved vertically along the plane parallel to the core. The 5-kwe design is illustrated in Figure 2.

Common to both reactor types are motors to drive the reflector segments, reflector drive and support fixtures, position sensors, and a variety of mechanical devices which require some form of movement and, consequently, bearings. The bearing environment is basically that of a space vacuum, pressures in the order of 10^{-10} torr air, high radiation, temperatures between 800 and 1500°F, and long periods of inactivity. Table 1 lists the environment requirements for specific reactor systems as they evolved.

At the beginning of the bearing development effort, it was determined that the most stringent requirements were for the movable reflector support bearings, and technology developed there could be utilized in the design of all other bearings.

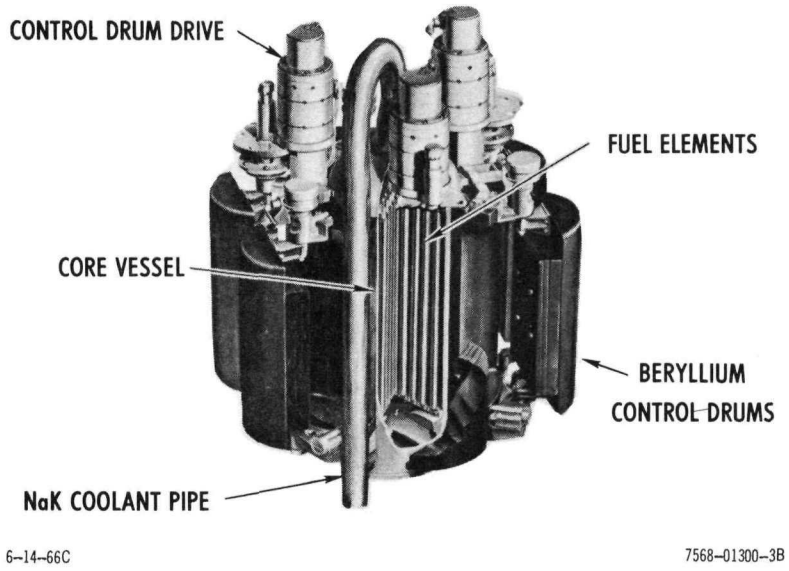

Figure 1. SNAP 8 Reactor System
(Rotating Control Drums)

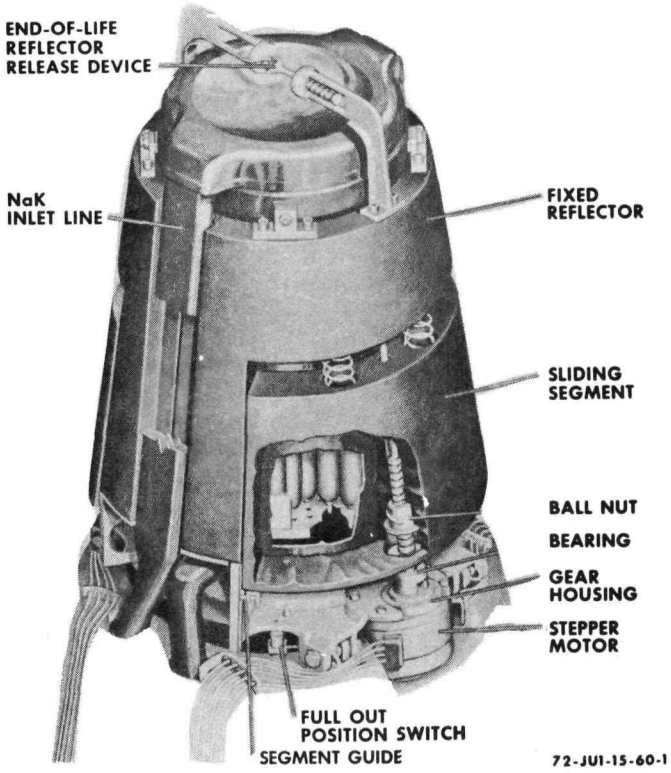

Figure 2. 5-kwe Thermoelectric Reactor System
(Sliding Reflector Segments)

TABLE 1

SNAP CONTROL DRUM BEARING DESIGN PARAMETERS

Parameter	SNAP 10A	SNAP 2	SNAP 8	Advanced ZrH Reactor	5 kwe
Temperature (°F)					
Maximum	700	900	1,150	1,500	800
Minimum	70	70	50	70	50
Pressure (torr)					
Space	10^{-6}	10^{-8}	10^{-13}	10^{-12}	10^{-8}
Ground Test	10^{-2}	10^{-4}	10^{-5}	10^{-5}	10^{-5}
Nuclear Radiation					
Neutrons (nvt)	7×10^{18}	1.5×10^{19}	10^{20}	1.9×10^{21}	1×10^{19}
Gammas, Carbon (rad)	1.5×10^{10}	3.9×10^{10}	10^{11}	-	5×10^{11}
Life (hr)					
Ground Test	8,700	10,000	12,000	20,000	44,000
Space Operation	8,700	10,000	12,000	20,000	44,000
Launch (maximum)					
Shock (g)	20	20	35	20	ND†
Acceleration (g)	9.4	9.4	7	6	16.25
Sinusoidal Vibration (g)	7.5	7.5	19 (max)	2	ND
Resonant Dwells (min)	5	5	5	5	ND
Random Vibration, Equivalent (g)	None	None	21	21	ND
Control Drum Weight (lb)					
Reflector Assembly	7	9	31	84	26
Allowable Drum Bearing Torque (shafts vertical, 1 g field)(in.-lb)					
System at 70°F	1.3	1.3	7.0	35.0	2.6
System at Maximum Temperature	1.3 (700°F)	1.3 (900°F)	3.5 at 1150°F	18 at 1350°F	7.0 at 875°F
Bearing Clearance, Nominal (in.)					
Diametral, maximum	0.0048	0.004	0.0012	0.012	0.005
Axial	0.0035 to 0.005	0.003 to 0.005	0.002 to 0.010	0.002 to 0.010	0.005 to 0.009
Operational Life					
Full Travel Cycles (angle or in., number of times)	135°, 10	150°, 10	135°, 200	180°, 50	2160°, 50 2160°, 40 in., 50*
Thermal Cycles (minimum)	10	10	200	50	50

*Combined Rotation and Translation †Not Determined

The initial effort was a search of the current literature to determine high temperature-vacuum bearing state of the art. Effort has continued throughout the program to maintain surveillance of industry-wide developments. The initial search showed that some material evaluations had been conducted for high temperature (above 400°F) bearings in air and for low temperature bearings in vacuum, but the combination of high temperature and vacuum operation was

basically unexplored. Early work by Bowden and associates,[1] among others, pointed the basic direction of research including satisfactory operation of graphite against various metals (Au, Ag, Cu, Ta, Fe, and Ni) and Al_2O_3 against TiC and graphite under various conditions. The use of contaminant films was also explored for their effect on friction and bearing seizure.

It was found, however, that little directly applicable data were available and that an extensive development program was necessary. The basic bearing performance requirements were to (1) provide low friction (friction coefficients less than 0.3) at operating temperatures, (2) prevent self-welding of the bearing mating surfaces after several hundreds of hours of nonoperation, and (3) have sufficient mechanical strength to support component loads, through reactor launch into space.

II. BASIC MATERIALS STUDIES

The bearing material evaluation program was divided into three separate phases. Potential materials and couples were studied for (1) self-welding of the couple under static conditions,[2] (2) static and dynamic sliding friction evaluations,[3,4] and (3) as an outgrowth of self-welding studies, basic material and coating metallurgical compatibility studies were conducted.[5] Studies were also conducted in phases as bearing temperature requirements increased from 1000 to 1250°F and to 1600°F.

A. SELF-WELDING STUDIES

1. Theoretical Factors

It has been shown that when two metals are heated in ultrahigh vacuum they will seize after some period of time. This is normally referred to as "self-welding." In general, before self-welding of metals can occur, the oxide film must be removed from the metal surface. If the film is not mechanically destroyed upon contact of the two surfaces, the onset of welding will be determined by some time rate process which removes the oxide.

In considering the mechanical destruction of the oxide film, the asperity mechanism reveals that extremely high pressures are obtained at the several points of contact. The adhesion theory as developed by Merchant[6] defines the real area of contact between metallic surfaces as the ratio of the applied load to the yield strength of the softer material. From this analysis, it can be shown that the real area of contact is very small. Thus, in a real case, if the load is high enough or if the oxide film is very thin, metal-to-metal contact may occur upon initial loading.

If the film is not destroyed initially, some other process will be responsible for its removal. Five possible rate mechanisms are (1) thermal decomposition, (2) sublimation, (3) reduction, (4) diffusion, and (5) free surface energy. One of the five mechanisms, or some combination of them, will eventually lead to metal-to-metal contact and adhesion will result.

2. Experimental Studies

Earlier studies on sliding block tests in vacuums to 10^{-6} torr and temperatures up to 1000°F showed interface adhesion occasionally resulted after short dwell periods between sliding cycles. Analysis of these tests indicated that galling, high starting friction, and seizure were direct results of this adhesion. Since most of the sliding surfaces in SNAP systems have relatively low sliding velocities, and in some cases long dwell times between sliding, it was necessary to study the static case.

Screening tests were conducted to determine the types of design materials which have the least adhesion when placed in static contact under moderate loading in the SNAP environment. The tests covered forty different combinations, mainly ceramic and metallic couples, that might have application in reactor components. These included not only the rotating or sliding mechanisms but also units such as springs, hinges, retaining band standoffs, and end-of-life devices that remain under static load for 10,000 hours and then separate. The tests were conducted at temperatures that simulated the operating range for the design involved. No tests were conducted at temperatures over 1300°F and none were conducted under 700°F. No tests were conducted for longer than 3400 hours and all tests were conducted in vacuum below 10^{-7} torr. In all, a total of 110 tests have been conducted.

In analyzing the combinations, it is convenient to classify them in five basic groups: A. metal vs metal, B. metal vs graphite, C. metal vs ceramic, D. ceramic vs ceramic, and E. ceramic vs graphite. A sixth group has been added which includes the use of contaminant films, such as dry-film lubricants, with the previous groups.

An analysis of the groups with respect to the average value of adhesion is shown in Table 2. The combinations, in which the adhesion force is immeasurable, were assigned to adhesion force equal to the accuracy of measurement (0.1 lb). It must be noted that the conditions of the tests vary considerably, and that they values do not represent a statistical analysis of materials under similar conditions. The data do indicate that in order to minimize adhesion, some contaminant film or low-shear material such as graphite must be placed between the mating surfaces. The results of the screening tests appear in Tables 3, 4, 5, and 6.

TABLE 2

SELF-WELD TEST RESULTS FOR ALL GROUPS

	Group	Average Adhesion Force (lb)	Maximum Adhesion Force (lb)	Number of Tests Evaluated
A	Metal vs Metal	0.57	3.56	47
B	Metal vs Graphite	0.10	0.10	2
C	Metal vs Ceramic	1.01	6.85	37
D	Ceramic vs Ceramic	0.37	0.9	3
E	Ceramic vs Graphite	0.10	0.10	2
F	Contaminant Films plus one of the previous combinations	0.28	3.50	19
	All Groups	0.41	-	110

The flame-sprayed coatings of LW-1N* and LC-1A contain an appreciable amount of metal; therefore, they are classified as a metal in material grouping. K-162B is also classified as a metal, because of the 30% metal binder (see Table 7 for composition of the coatings). Chromium plating that was applied to stainless-steel samples by an electrolytic process to thicknesses of 0.0003 to 0.0005 in. is also included with the metals.

The contaminant films used were sodium-silicate bonded dry-film lubricants, 0.0005 to 0.0008 in. thick. Both MoS_2 and WS_2 were tested; however, the shelf-life of the WS_2 material had been exceeded so these data are questionable. Colloidal graphite suspended in isopropyl alcohol and sprayed on surfaces 0.0002 to 0.0003 in. thick has also been effective in minimizing adhesion.

Other materials classified as contaminant films are Grafoil (pyrolytic graphite in sheet form) and woven graphite cloth. These materials are 0.005 to 0.010 in. thick and could be considered as separate materials rather than films. However, neither the foil nor the cloth contain binder materials, a factor which limits their physical strength. For this reason, they are classified as films.

*See Appendix for proprietary materials description.

TABLE 3

SELF-WELD DATA SUMMARY – METAL vs METAL

Material Combinations	Temperature* (°F)	Time (hr)	Contact Load (lb)	Adhesion Force (lb)	Vacuum (torr)
Inconel-X vs Inconel-X	900 1300 1300 1300 1000 1000 1000	2184 1272 302 528 1692 676 72	25.00 15.00 15.00 14.25 16.25 15.50 15.50	<0.10 0.78 <0.10 0.85 <0.10 <0.10 <0.10	10^{-8}
Ti-6Al-4V vs Stellite 6-B	800	1656	14.00	0.80	10^{-9}
Inconel-X vs A-286	1000 1000 1000 1300	144 676 1550 720	14.20 25.00 15.50 16.00	<0.10 0.32 2.50 1.68	10^{-9}
Beryllium vs Beryllium	900 1000 1000 1000 1000	1268 456 686 2400 72	11.50 11.50 11.50 11.50 11.50	<0.10 1.50 <0.10 <0.10 <0.10	10^{-9}
Ti-6Al-4V vs Beryllium	1000 1000	172 1104	15.00 15.00	<0.10 1.50	10^{-9}
Type 316 Stainless Steel vs A-286	1000 1000 1000 1000	192 672 2400 816	16.5 25.00 17.50 34.50	<0.10 <0.10 0.25 <0.10	10^{-8}
Beryllium vs Type 316 Stainless Steel	1000 900 1000 1000	216 1490 1178 728	16.00 16.00 35.00 25.00	<0.10 2.00 1.40 <0.10	10^{-9}
Beryllium vs Rene 41	900	936	12.50	0.50	10^{-9}
Tungsten vs Tungsten	1300 1300 1000	1300 672 1166	16.75 16.75 16.75	<0.10 <0.10 <0.10	10^{-9}
Inconel-X vs Relay Steel	1300 835	1258 1080	16.75 16.75	<0.10 <0.10	10^{-8}
Molybdenum vs Type 316 Stainless Steel	1300 1200	120 504	13.00 16.25	<0.10 3.56	10^{-8}
LC-1A vs K-162B	1000 850 1000 1000 700	192 1818 1032 670 1104	18.00 14.50 14.50 30.00 30.00	2.00 0.40 <0.10 <0.10 <0.10	10^{-9}
Ti-6Al-4V vs LW-1N	1000 1000 1000	3408 1128 2370	13.50 15.50 15.50	2.40 <0.10 <0.10	10^{-9}
LW-1N vs LW-1N	1000 1000	1512 2136	16.25 16.25	0.50 0.50	10^{-9}
K-162B vs K-162B	1200	1200	16.25	0.40	10^{-9}
Chrome Plate vs Chrome Plate	700	Together 72 hr; Apart 90 days; Together 72 hr	15.00	<0.10 <0.10	10^{-9}

*Approximate

TABLE 4

SELF-WELD DATA SUMMARY – METAL vs CERAMIC

Material Combinations	Temperature* (°F)	Time (hr)	Contact Load (lb)	Adhesion Force (lb)	Vacuum (Torr)
Beryllium vs BeO	1000	120	16.80	<0.10	10^{-8}
	1000	788	25.00	2.00	
K-162B vs LA-2	1000	2370	17.00	<0.10	
	1000	1780	17.00	0.50	
	1000	1556	17.00	<0.10	10^{-9}
	1000	1536	14.75	<0.10	
	875	1152	14.50	<0.10	
Type 316 Stainless Steel vs LA-2	1000	628	25.00	0.62	
	1000	792	15.50	<0.10	
	1000	1536	15.50	<0.10	10^{-9}
	1000	2510	15.50	<0.10	
	800	1326	15.50	0.40	
	1000	168	14.25	0.62	
Beryllium vs LA-2	1000	1104	15.00	1.50	
	1000	2018	12.50	6.85	
	950	1894	15.00	6.00	10^{-9}
	1000	812	25.00	4.50	
	1000	210	15.00	<0.10	
	1000	172	15.00	<0.10	
LC-1A vs LA-2	1000	3134	15.00	0.85	
	1000	1536	15.00	0.10	10^{-9}
Inconel-X vs LA-2	850	1512	25.00	0.38	10^{-9}
	1000	1020	25.00	<0.10	
Beryllium vs Mykroy	1000	1080	16.25	0.44†	10^{-7}
	1100	1200	16.25	1.00	
LA-2 vs LW-1N	1000	1540	25.00	0.50	
	1000	1128	15.50	<0.10	
	1000	2370	25.00	<0.10	10^{-9}
	1000	96	15.50	<0.10	
	1000	1954	15.50	<0.10	
	930	1128	15.35	<0.10	
Beryllium vs Micaceram	700	1324	25.00	<0.10	10^{-7}
	1300	1050	25.00	1.80	
Type 316 Stainless Steel vs Micaceram	900	1220	16.25	1.14	10^{-8}
	1115	1440	16.25	6.00	
Chrome Plate vs LA-2	700	2350	15.00	<0.10	10^{-9}
	700	2230	15.00	0.33	

*Approximate
†Mykroy decomposed and reacted with holder

TABLE 5

SELF-WELD DATA SUMMARY – OTHER MATERIALS

Material Combinations	Temperature* (°F)	Time (hr)	Contact Load (lb)	Adhesion Force (lb)	Vacuum (Torr)
		GROUP: METAL vs GRAPHITE			
Type 316 Stainless Steel vs Purebon P-5N	1000 1000	72 672	17.50 25.00	<0.10 <0.10	10^{-7}
		GROUP: CERAMIC vs CERAMIC			
LA-2 vs LA-2	1285 1280 1300	342 550 1560	16.75 16.25 20.00	0.90 <0.10 <0.10	10^{-9}
		GROUP: CERAMIC vs GRAPHITE			
LA-2 vs CDJ-83	1000 840	1780 1200	14.50 14.70	<0.10 <0.10	10^{-8}

*Approximate

TABLE 6

SELF-WELD DATA SUMMARY – CONTAMINANT FILMS

Material Combinations	Temperature* (°F)	Time (hr)	Contact Load (lb)	Adhesion Force (lb)	Vacuum (Torr)
Inconel-X with MoS_2 vs Type 316 Stainless Steel	850 900	2020 1056	13.25 13.25	<0.10 <0.10	10^{-9}
Type 316 Stainless Steel vs Molybdenum with WCG Graphite Cloth	900 1100 1100	2256 2500 2200	16.00 16.25 16.00	<0.10 <0.10 <0.10	10^{-9}
Type 316 Stainless Steel vs Molybdenum With Grafoil	1100 1100 1100	2178 2350 2300	15.00 16.25 16.25	<0.10 <0.10 <0.10	10^{-9}
LA-2 vs Type 316 Stainless Steel with Grafoil	1000 1000 1000	2328† 2280† 2234	16.25 16.25 15.00	<0.10 <0.10 <0.10	10^{-7}
Ti(6Al-4V) vs Molybdenum with Colloidal Graphite	700	120	25.00	<0.10	10^{-8}
Ti(6Al-4V) vs Mykroy with Colloidal Graphite	700	120	25.00	<0.10	10^{-8}
Type 316 Stainless Steel vs Type 316 Stainless Steel with Colloidal Graphite	1200	2112	16.2	<0.10	10^{-8}
Type 316 Stainless Steel vs Type 316 Stainless Steel with Bonded WS_2§	1300	2400	18.5	3.50	10^{-9}
Type 316 Stainless Steel vs Type 316 Stainless Steel with Bonded MoS_2	1200 1200 1200	2090 1260 1720	16.00 16.25 15.00	<0.10 <0.10 <0.10	10^{-9}
LA-2 vs K-162B with MoS_2	800	2160	10.00	<0.10	10^{-9}

*Approximate
†20-hr oxidation in air at 550°F before test
§6-month shelf life of the coating had been exceeded

TABLE 7

COMPOSITION OF SPECIAL COATINGS AND MATERIALS EVALUATED IN THE SELF-WELD PROGRAM

Coatings and Miscellaneous Materials	Composition
LW-1N	WC + 13 to 16% Co
LC-1A	85% Cr_3C_2 + 15% Ni-Cr
LA-2	99+% Al_2O_3
K-162B	25% Ni, 5% Mo, 64% TiC, 6% CbC (some TaC)
CDJ-83	Unknown — Impregnated carbon graphite
Mykroy	Unknown — Glass-bonded mica
Micaceram	Unknown — Mica-bonded mica

3. Discussion of Results

The program scope did not include the evaluation of the self-welding mechanism. Other investigators[7,8,9] have discussed this subject in some detail, with the conclusion that self-welding occurs by a very complicated process that includes several mechanisms. These mechanisms, as outlined in the introduction, have been observed as dependent variables to the self-welding process. It should be evident that an attempt to reduce even the simplest adhesion problem to a mathematical equation would involve so many unknowns that an evaluation becomes a major effort in itself.

In the Table 2, data were presented to show the relative self-welding between groups evaluated.

Only two tests were conducted in Groups B and E, but considerable information is available on these materials from other studies.[10] It is suggested that surface adhesion occurs between the material combinations in Groups B and E in the same manner as metal to metal in Group A. The strong bond observed with clean metals, however, does not occur with combinations in Groups B and

E. This is probably due to the mechanical and structural properties of the carbon-graphite materials. They have high penetration resistance but are relatively weak in shear. Visual inspection of the surfaces after test shows carbon-graphite transferred to the other surface. This indicates self-welding had occurred but the resultant bond strength is apparently insignificant.

The only material listed in Group D is "flame-sprayed" Al_2O_3. Three tests were conducted. One test resulted in 0.9-lb adhesion and the other two, both for longer time periods, had no adhesion. It is expected that more tests of this same combination would result in statistics favoring the no-adhesion case. On the other hand, this ceramic is applied to metal substrates by physically imbedding Al_2O_3 particles in the metal surface with a high-velocity detonation process. The microscopic process involved in the coating process is probably quite similar, thermodynamically, to the self-weld process. It is not surprising then that self-welding occurred — one out of three times — with this particular ceramic couple.

Almost all the combinations in Group A show self-welding. The pair with which one might expect the least adhesion in this group is tungsten vs itself and, in the three cases tested, the recorded value was below the reading accuracy of the test equipment. Photographs, however, show definite material transfer occurred between the mating interfaces. A similar result was obtained with Inconel-X vs No. 5 Relay Steel. In both cases the bond appears to be very brittle but nevertheless material transfer did occur. The obvious solution the designer must make to this problem is to employ the high-strength alloy materials he needs and then separate the moving parts with a thin film of low-shear contaminant that will not dissolve, sublimate, or otherwise allow intimate contact to occur during design life.

Only limited study on these contaminant films has been conducted. The sodium-silicate bonded dry-film lubricants appear to be satisfactory for limited use. These materials are radiation resistant but they oxidize at temperatures above 600°F in air, and they sublimate in space vacuum. The sublimation rate is directly a function of temperature, and films having vapor pressure below 10^{-9} Torr would be necessary to meet SNAP reactor environmental requirements of 1300°F for 10,000 hours.

The Grafoil or graphite cloth materials have much lower vapor pressures than the bonded dry films and would undoubtedly be satisfactory for 10,000-hr applications at 1300° F in space. They do, however, oxidize rapidly at 800° F in air; they may also carburize the contacting metal surfaces. Carbon diffusion, after long periods of time, could embrittle the structure, but this carburization requires extremely long times to cause any deleterious effects for the intended uses on SNAP components.

4. Test Techniques

General procedures for the self-welding tests conducted are described in the following paragraphs.

Attempts were made to provide optimum cleanliness in all tests to prevent undesirable contamination. Cleaning procedures were established not only for the test specimens but also for the test system. Both the test chamber and the ion pump are first ultrasonically cleaned in methylethylketone, then rinsed in 100% (200 proof) ethyl alcohol and allowed to air-dry at 150° F.

All test specimens, except carbon-graphites and those precoated with contaminant films, are cleaned by the following procedure: scrub in acetone, wash in tap water, scrub in 100% (200 proof) ethyl alcohol, wash in tap water, scrub with levigated alumina, wash in tap water, wash with distilled water, then dry in room air.

After cleaning, and just prior to testing, the specimens (except the carbon-graphites and precoated samples) are subjected to a wetting test. The samples are wet with distilled water and then tilted at a sufficient angle to allow excess water to drain off. If the water spreads readily and evenly over the surface, the specimens are allowed to air-dry and then are placed in test. An "unclean" condition allows an uneven pattern to form as the water runs off the surface; if the sample is not tilted, the water sets in droplet form on the surface. When this condition exists, the cleaning process is repeated. White nylon gloves and lint-free tissue are used at all times in sample handling to prevent contamination of the materials.

The test specimens are simple geometries designed to represent two flat surfaces in contact. The base is a square block with 1-in. sides and 3/8 in. thick. The rider specimen is a cube with 1/2-in. sides. Both the base and rider

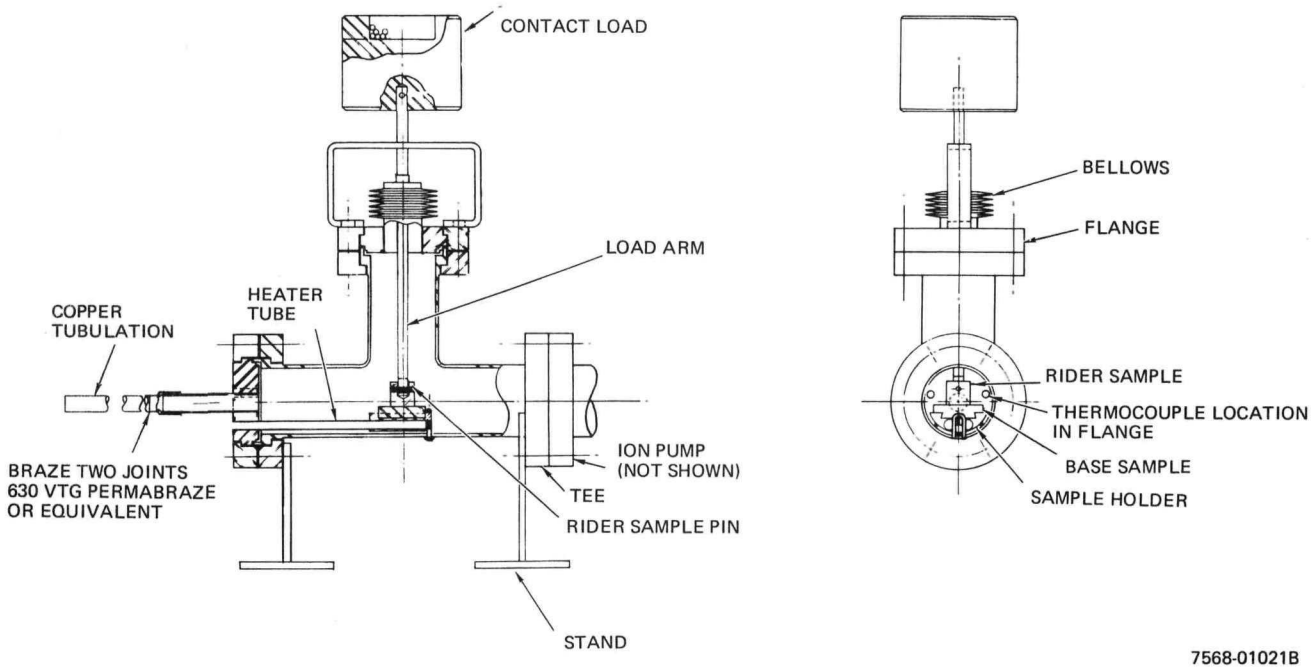

Figure 3. Self-Weld Test Assembly

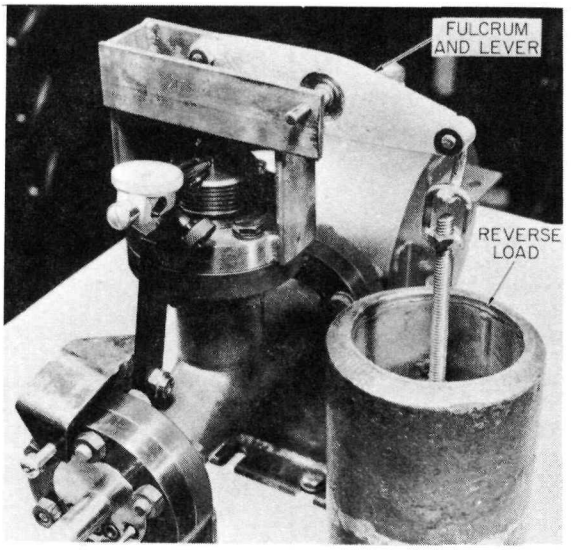

7568-18169b

Figure 4. Apparatus for Measuring the Self-Weld Adhesion Force

specimens are machined to fit holders that secure them inside the test chamber, as illustrated in Figure 3.

The specimens are secured in place initially with approximately 0.10-in. gap between the interfaces. This gap is maintained during bakeout and until ultrahigh vacuum has been established in the chamber.

The test began when the rider was placed in contact with the base specimen. The specimens were not allowed to "hit" together. The initial loading was a force of approximately 15 lb, determined by atmospheric pressure acting on the load arm bellows. (These loads vary from part to part, due to variances in the diameters of the bellows, which are designed for a 1-in.^{2} area.) Pre- and post-tare readings of the bellows load arm established the interface loading. The interface load could be increased by adding extra weights to the top of the load arm (as shown in Figure 3). Once the specimens were placed in contact and loaded they were not moved or unloaded until a test for self-welding was made. The check was made by reverse loading the bellows load arm with a fulcrum and lever. This is illustrated in Figure 4. The total net force required to separate the surfaces was recorded as the adhesion force. The contact time each material couple had in test is related to a particular design application. In cases where no adhesion occurred, longer contact time was used on the repeat tests. Repeat tests were conducted as required to provide significant self-weld information on particular material pairs.

5. Test Facilities

In designing a test facility for self-weld testing that would simulate the space temperature conditions of the SNAP program, the use of oil diffusion or oil fraction vacuum pumps (including mercury vapor pumps) was found to be impractical. These tests require unattended operation for periods of 3000 hours or more and all possible contamination with foreign materials from oil back-streaming must be avoided. Ion getter pumps, however, are ideally suited for providing the "clean," ultrahigh vacuums desired. The ion pump, in combination with the absorbent type (molecular sieve) roughing pump, has proved to be the cleanest and simplest system available for this type of work.

Twenty independent test chambers (Figure 3) were used to conduct the self-weld tests described. Each chamber has a 9-liter/sec ion pump. The test

chamber and all associated fittings, including the pump, are Type 300 series stainless steel. The chamber is a tee-fitting 1-1/2 in. in diameter by 6 in. long. A bellows and load arm are attached to the leg of the tee. The ion pump is connected to one side of the tee and the opposite side is connected to the molecular sieve roughing pump. A 3/8-in.-diameter copper tubulation connects the roughing pump and test chamber. The tubulation is pinched off after ion pump startup to provide an independent, closed system for each test. The test samples are heated by conduction from small resistance wire heaters located inside sealed tubes that come through the end of the test chamber.

Thermocouples are used to sense the temperature of the base sample. The couples are chromel-alumel, packed in alumina and encased in a 1/16-in.-diameter protective stainless-steel sheath. The hot point of the couple is welded to the end of the sheath and located 0.060 in. below the surface of the test surface.

The systems provide an oil-free environment and maintain pressures in the 10^{-9} Torr range with temperatures up to 1000°F. Temperatures up to 1300°F may be obtained with a slight degradation in vacuum due to increased outgassing above the bakeout temperature.

6. Summary

Self-welding or interface adhesion may be expected to occur on metal couples, ceramic couples, and metal-ceramic couples when the materials are heated to SNAP environmental temperatures in ultrahigh vacuum.

Any combination of materials in couple with carbon-graphites may be expected to have low interface adhesion.

Contaminant films such as sodium-silicate bonded dry lubricants are effective in reducing or preventing self-welding as long as the film remains between the material surfaces.

B. SLIDING FRICTION

1. Theory and Application

The adhesion theory, as postulated by Merchant[6], Bowden and Tabor,[1] and more recently by Bisson,[11] is developed from Amonton's law which may be generally stated as: frictional force is proportional to load and independent of the surface.

Dry sliding friction appears to be caused by at least three factors operating at the sliding junction. This may be shown schematically as follows:

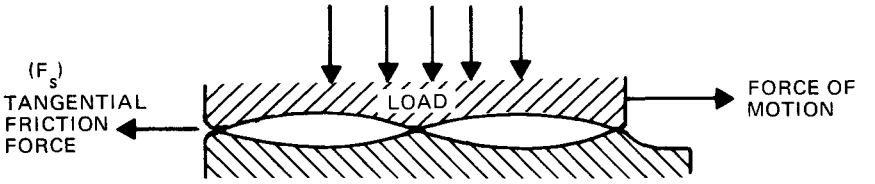

1) One cause of friction is bonding, or self-welding occurring between the sliding junctions.

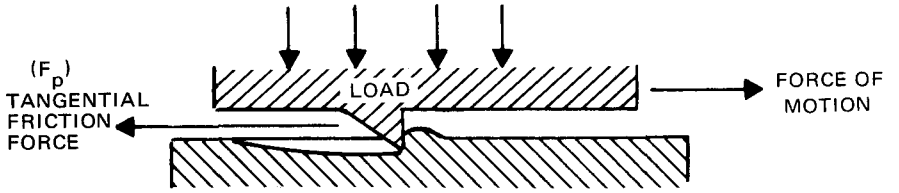

2) A second cause of friction is ploughing, occurring between the sliding junctions.

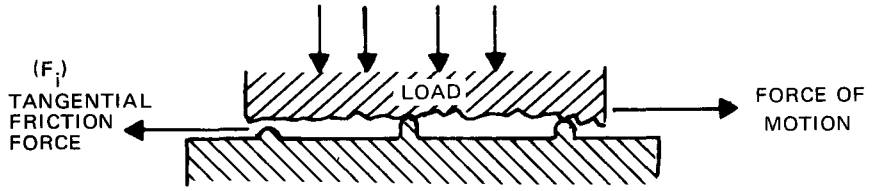

3) A third cause of friction is the interference of asperities between the sliding junctions.

A summation of the forces gives

$$F_f = F_s + F_p + F_i$$

In practically all cases of elastic bearing surfaces that have relative sliding, the friction due to shearing of the bonded junctions is many times greater than the ploughing or interference terms. This is explained where the F_i and F_p terms result in fusion welding at initial loading. Then for sliding to occur, the bonds must shear or break away; for a practical analysis, F_p and F_i become F_s. Thus the mathematical representation of the mechanics of the system is

$$F_f = F_s$$

Furthermore, the frictional force due to shear is equal to the shear stress of the weaker material times the area of the bonded junctions (this area is termed the real area). Thus,

$$F_f = A_r s.$$

Since the real area is equal to the load (W) divided by the yield strength or flow pressure (P) of the softer material, we have

$$A_r = \frac{W}{P}$$

Thus, as Amonton has stated, F_f is proportional to load and independent of the apparent area of the surface. The coefficient of friction may then be defined as

$$\mu = \frac{F_f}{W} = \frac{Ws}{WP} = \frac{s}{P}$$

This equation defines the coefficient of friction as being equal to the shear stress (s) of the weaker material divided by the flow pressure of the weaker material.

It is interesting that very small loads may cause the onset of plasticity in the asperity contact of metals. Bowden[1] calculated the load required to cause plastic flow for various radii of asperities of steel-on-steel as shown below:

Radius	Load
10^{-4} cm (10^4 Å)	4.7×10^{-5} gm
10^{-2} cm (10^6 Å)	0.47 gm
1 cm (10^8 Å)	700 gm

This may lead to the false conclusion that surface finish is the most important factor in controlling friction level. However, the best laboratory techniques reduce surface roughness to within 100 to 1000 angstroms, while the range of molecular attractions is only a few angstroms. Experiments have shown that even with this degree of surface preparation, the real area of contact will be much less than the apparent area and asperities or irregularities will still exist in contact.

In practically all cases, there will be at least three major contact points between the asperities of mating surfaces, and the real area will be proportional to the load and independent of the size or shape of the surface. In such a case for elastic materials, plastic deformation will occur until the contact area is sufficient to support the load. For all tests in normal atmosphere and for virgin tests in vacuum, the contacting interfaces are contaminated with inherent films.

Studies in ultrahigh vacuums in which the partical pressure of oxygen is less than 10^{-9} Torr have shown repeated bonding between the contact points as this contaminating film is broken down. The breakdown usually is a mechanical destruction process at the asperity contact. However, diffusion of the metal substrate through the contaminant film as well as sublimation of the oxides can yield the same result. These results appear to be time- and temperature-dependent and reproducible only to the degree that the contaminant or "healing" films can be controlled. On the other hand, the predominant reactive residual gas in an ion pumped space simulator or vacuum chamber is shown to be hydrogen.[12] The reducing action of hydrogen tends to "super" clean the friction surfaces. This effect may not be too unrealistic since hydrogen (H_2, H_1, H^+) is also the predominant constituent of space atmosphere.

2. Surface Film Effects

The most significant single factor affecting friction in vacua is the partial pressure of oxygen. Other gases and contaminant films may also act as "healing" agents but to a much lesser degree than oxygen. The "healing" results from a buildup of residual gas molecules on the surfaces which may react physically or chemically to form a contaminant film. For a particular absolute pressure, the ideal rate of formation of a particular film may be calculated.

Figure 5 is a theoretical curve for the time required to form a monomolecular film of O_2 on a surface. For these data, it is assumed that the O_2 molecules have a diameter of 3.0 Å and the O_2 is physically absorbed with no molecules restriking the existing film. It is quite possible that in simulated space chambers, monolayer formation may occur faster than in space, which could result in misleading friction data. It is therefore important to conduct friction tests so the time between dwell and relative motion of the surfaces is less than the rehealing time established by the pressure level of the vacuum chamber.

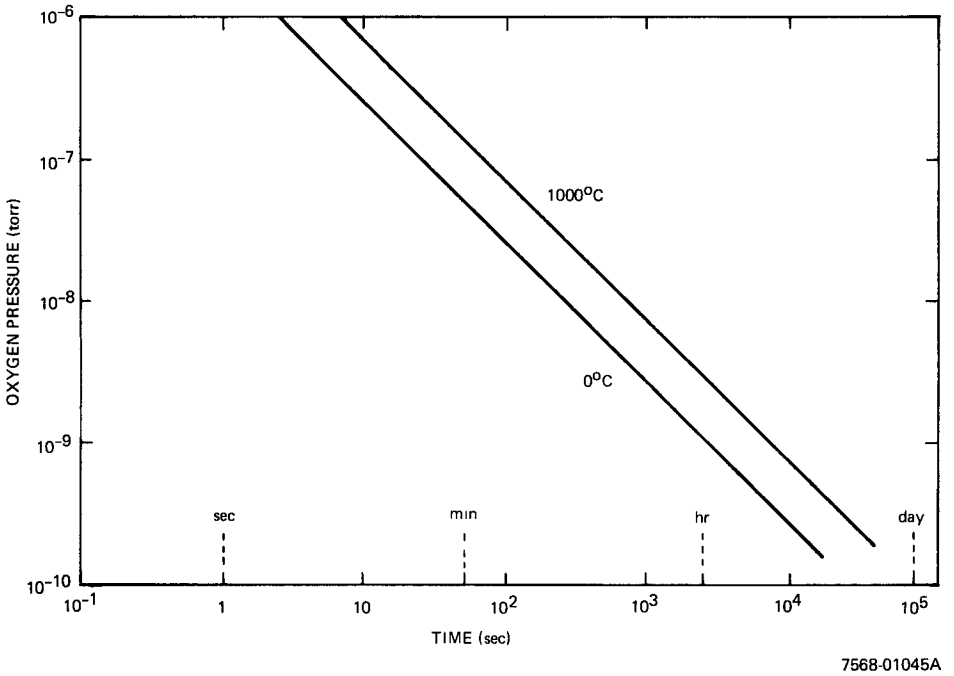

Figure 5. Time Required to Form Theoretical Monomolecular Film of O_2 on a Surface

Calculations show that potential solid-surface lubricant films must have vapor pressures below 10^{-9} torr at 1300°F to meet the environmental requirements. These films must have a strong bond to the substrate but have low shear between the moving parts. To establish the ability of the films to meet these requirements, a simple vapor pressure curve for each compound can be constructed from sublimation rate studies. Compounds of the refractory metals with sulfur, tellurium, or selenium appear to form a low-vapor-pressure, low-shear solid film when mixed with a sodium-silicate binding agent. Selection of the binding agent is all-important and is based on stability while in the environment, and on the reaction of the agent with the substrate. It must also demonstrate low-shear strength properties. The application thickness of these films is important in that they serve to prevent contact of the selected mating materials and reduce film loss by sublimation.

The sublimation rate is a function of temperature, increasing with temperature. However, the binders may act as a mechanical barrier to reduce the total rate. The investigator must be careful in evaluating the sublimation rates of sodium-silicate bonded dry-film lubricants since the binding agent may vary from

25 to 50% of solid volume. The chemical composition both by weight and volume must be known before a correct analysis can be made. The cure or bakeout of the coating is also an important variable in the finished coating.

3. Solid Carbon-Graphites

It has already been shown that specially impregnated graphites provide film contamination with the contacting interface.

Without the impregnants, the graphites exhibit considerable wear and have coefficients of friction of ~0.3 to 0.5. There is some doubt about the mechanics of the friction process of carbon vs the friction process of graphite, but with an impregnant both systems yield similar results. This indicates that the impregnant influences the lubrication. This might be explained by the formation of a low-shear compound or transfer film between the interfaces resulting from a chemical reaction between the impregnant and the mating metallic surface. However, the mechanics of the friction process appear to be dependent more on the shear qualities of the carbon-graphite than on the impregnant. Nevertheless, the impregnant does provide a better surface texture, and surface wear is greatly reduced by its use.

Carbon graphite without an impregnant was used for bearings operating for long periods of time above 1100°F after it was observed that the impregnant reacted with the Al_2O_3-coated mating surface. This change will be discussed in detail later in this report.

Figure 6 shows the variation of the friction coefficient with the graphite content of carbon-graphite when in sliding contact with Al_2O_3 at 1000°F in ultrahigh vacuum. The minimum friction is obtained with graphite content between 30 and 60%. The reference bearing material, Purebon P-5N, which is approximately 60% graphite and 40% carbon, was selected on this basis.

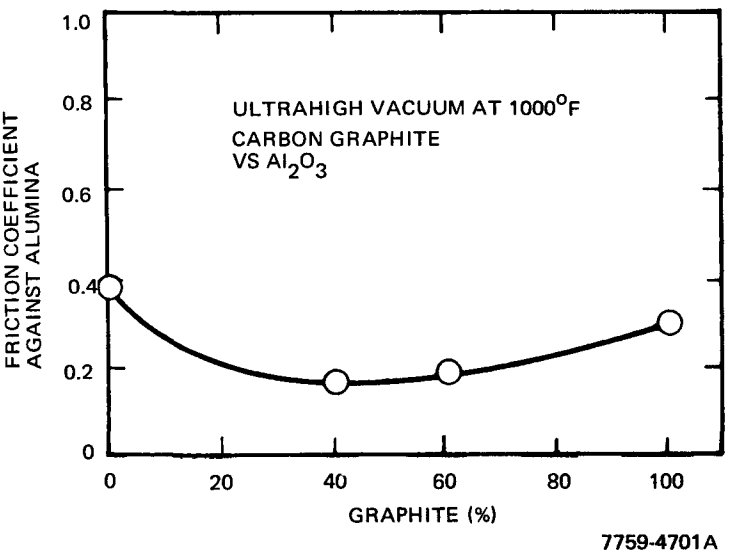

Figure 6. Friction Variation With Graphite Content

TABLE 8

FRICTION TEST MATERIALS AND TEST RESULTS
(Sheet 1 of 2)

Test No.	Material Combinations		Observed Friction Coefficients											
	Small Rider Sample	Stationary Base Sample	Initially at Room Temperature and Pressure		After 10 to 20 hr at 10^{-5} mm Hg and Room Temperature		After 24 hr at 10^{-5} mm Hg and 600°F		After 24 hr at 10^{-5} mm Hg and 1000°F		After 7 days at 10^{-5} mm Hg and 1000°F		Finally at Room Temperature and Pressure	
	Description	Description	Starting	Dynamic	Starting	Dynamic	Starting	Dynamic	Starting	Dynamic	Starting	Dynamic	Starting	Dynamic
I	Ni Base – Inconel X	Ni Base – Inconel X	Equipment shakedown test. High friction samples used.											
II	WC – Kennametal K96	TiC – Kentanium K162B	†	0.22	†	0.65	†	0.68	†	0.64	†	0.78	†	0.71
III	Co Base – Haynes Alloy 25	Co Base – Haynes Stellite 3	†	0.63	†	0.61	†	0.82	†	0.94	†	0.63	†	0.71
IV	Cr_3C_2 on Type 316 Stainless Steel - Linde LC-1A	Al_2O_3 on Type 316 Stainless Steel - Linde LA-2	†	0.18	†	0.63	†	0.49	†	0.43	†	0.37	†	0.65
V	MoS_2 on Type 316 Stainless Steel - Electrofilm	MoS_2 on Type 316 Stainless Steel - Electrofilm	†	0.21	†	0.36	†	0.81	Stopped because of excessive friction					
VI	MoS_2 on Type 316 Stainless Steel - Electrofilm	MoS_2 on Type 316 Stainless Steel - Electrofilm	†	0.20	Stopped because of excessive friction									
VII	MoS_2 on Ni Base Alloy Electrofilm on Inconel X	MoS_2 on Ni Base Alloy Electrofilm on Inconel X	†	0.32	Stopped because of excessive friction									
VIII	MoS_2 on Co Base Alloy Electrofilm on Haynes 25	MoS_2 on Co Base Alloy Electrofilm on Haynes 3	†	0.19	Stopped because of excessive friction									
IX	Al_2O_3 on Type 316 Stainless Steel - Linde LA-2	TiC - Kentanium K-162B	†	0.22	†	0.33	†	0.34	†	0.25	†	0.39	†	0.89
X	Graphite - Nat'l Carbon CDJ-83	Co Base - Haynes Stellite 3	†	0.18	†	0.21	0.27	0.11	0.21	0.11	0.47	0.24	0.29	0.21
XI	Al_2O_3 Hot Pressed - Norton LA 687	SiC - Norton	†	0.51	†	0.88	†	0.69	†	0.45	†	0.57	†	0. 95
XII	BN - Carborundum Co.	Cr_3C_2 - Firth CR2	0.37	0.23	0.39	0.37	0,53	0.42	0.55	0.40	0.66	0.47	†	0.23*
XIII	WC - Kennametal K96	SiC - Norton	†	0.50	†	0.42	†	0.79	†	0.57	†	0.54	†	0.47
XIV	Al_2O_3 Hot Pressed - Norton LA 687	Graphite - National Carbon CDJ-83	0.19	0.27	†	0.30	0.13	0.05	0.23	0.20	†	0 09	†	0.22

4. Preliminary Testing

Initial sliding friction studies were conducted on the following basic material groups as friction pairs, with and without dry-film lubricant as contaminant film.*

1) Metals
   a) Cobalt Base Alloys
   b) Nickel Base Alloys
   c) Iron Base Alloys
   d) Stainless Steel
2) Carbides (WC, Cr_3C_2, TiC)
3) Nitrides (BN)
4) Oxides (Al_2O_3)
5) Carbon-graphite
6) Metal-graphite (12%) Composite (Deva metal)

Friction tests were conducted at temperature to 1000°F in 10^{-5} torr environment produced by an oil-diffusion-pumped vacuum system. Test sequences were designed to duplicate reactor operation (SNAP 10A and SNAP 2) as close as possible, during the short-term testing with friction measurements being made as follows:

1) In air at ambient temperature
2) In vacuum after 10 hr
3) In vacuum after 24 hr at 600°F
4) In vacuum after 24 hr at 1000°F
5) In vacuum after 7 days at 1000°F
6) In air at ambient temperature.

Table 8 shows friction levels for all couples tested. Table 9 indicates the low friction combinations which can be broken down to basically (1) couples with carbon-graphite or (2) couples with Al_2O_3.

*The sources of various proprietary materials described in this report are listed in the Appendix.

TABLE 8

FRICTION TEST MATERIALS AND TEST RESULTS
(Sheet 2 of 2)

Test No.	Material Combinations		Observed Friction Coefficients											
	Small Rider Sample	Stationary Base Sample	Initially at Room Temperature and Pressure		After 10 to 20 hr at 10^{-5} mm Hg and Room Temperature		After 24 hr at 10^{-5} mm Hg and 600°F		After 24 hr at 10^{-5} mm Hg and 1000°F		After 7 days at 10^{-5} mm Hg and 1000°F		Finally at Room Temperature and Pressure	
	Description	Description	Starting	Dynamic	Starting	Dynamic	Starting	Dynamic	Starting	Dynamic	Starting	Dynamic	Starting	Dynamic
XV	Cr_3C_2 on Type 316 Stainless Steel - Linde LC-1A	TiC - Kentanium K-162B	†	0 29	†	0.42	†	0 48	0.53	0.39	0.63	0 43	†	0 74
XVI	Al_2O_3 on Type 316 Stainless Steel - Linde LA-2	Co Base - Haynes Stellite 3	†	0.21	†	0.45	†	0.90	Stopped because of excessive friction					0.85
XVII	Al_2O_3 on Type 316 Stainless Steel - Linde LA-2	Fe Base - Haynes Alloy 90	†	0.16	†	0.16	†	0.31	Equipment failure after 8 hours at 600°F					
XVIII	Al_2O_3 on Type 316 Stainless Steel - Linde LA-2	Fe Base - Haynes Alloy 90	†	0.15	†	0.15	†	0.29	(Equipment failure at 800°F, 0 36)				†	0.75
XIX	C-Graphite - Graphitar 16	Al_2O_3 Hot Pressed - Norton LA 687	†	0.24	(Special Test		(Overnight at 10^{-5} and 500°F, Coefficient = 0.16 (5 hr at 500°F & N_2 atmosphere Coefficient - 0.10)							0.29
XX	C-Graphite - CDJ-83	Fe Base - Haynes Alloy 90	†	0.20	†	0.22	0.19	0.10	†	0.05	†	0.18		0.17***
XXI	Al_2O_3 on Type 316 Stainless Steel Linde LA-2	Carbon CDJ-83	†	0.14	0.21	0.15	(Temperature raised to 1000° in one step)							
XXII	TiC - Kentanium K-162B	Fired PbO coat on Type 304 Stainless Steel	†	0.18	†	0.25	†	0.07	Stopped because of excessive friction					
XXIII	Al_2O_3 on Type 316 Stainless Steel - Linde LA-2	Carbon Graphite CDJ-83	†	0.15	(Temperature to 1000°F in one step)				†	0.05	†	0.05	†	0 20***
XXIV	Deva 3-N-12	Al_2O_3 Hot Pressed	†	0.50	0.29	0.23	0.14	0.12	0.37	0.21	0.40	0.30	0.48	0 31
XXV	Deva 3-F-12	Al_2O_3 Hot Pressed	†	0.30	†	0 40	†	0 26	†	0.21	†	0 23	†	0 26

†Means starting friction same as running friction
*BN showed excessive wear
**A variation in test procedure was used in this test in that after 7 days at 1000°F, a 48-hour dwell period was added. After no operation for 48 hours and with a 10^{-6} mm Hg pressure at 1000°F, a starting friction of 0.27 was observed with a subsequent dynamic or running friction of 0.10
***After 3 days at 1000°F and 10^{-6} to 10^{-7} mm Hg, ion pump was turned "on" and the diffusion pump valve was closed for 3 days No change in friction was noted

TABLE 9

LOW FRICTION COMBINATIONS

Test No.		Friction Coefficient Maximum at Vacuum and 1000°F
XX	C Graphite CDJ-83, Haynes 90	0.22
XIV	Al_2O_3 (Hot Pressed, or LA-2), C Graphite (CDJ-83)	0.23
XXV	Deva 3-F-12, Al_2O_3 (Hot Pressed)	0.23
IX	Al_2O_3 (LA-2), TiC (K-162B)	0.39
XXIV	Deva 3-N-12, Al_2O_3 (Hot Pressed)	0.40
IV	Cr_3C_2 (LC-1A), Al_2O_3 (LA-2)	0.49
X	C Graphite (CDJ-83), Haynes Stellite 3	0.47

The oil diffusion vacuum systems in which these tests were conducted permitted some backstreaming of oil vapor and possible contamination of bearing surfaces affecting friction results. All subsequent sliding friction testing was conducted with ion pumping systems which provide contaminant-free testing to 10^{-9} torr or less pressure.

5. Screening Tests

The second and major series of bearing couple screening tests were conducted in conjunction with and parallel to the previously discussed self-weld studies. Sixty-seven material pairs in sliding couples were tested in ultrahigh vacuum at temperatures ranging from 70 to 1000°F. For convenience of comparison, the data are categorized into seven groups: metal vs metal, metal vs metal with dry lubricants, metal vs carbon, ceramic vs ceramic, ceramic vs ceramic with dry lubricants, metal vs ceramic, and ceramic vs carbon. Special tests have been conducted using MoS_2 powder (unbonded) with all groups. Tests were continued for approximately 1000 hours. Some tests, however, were run 3000 hours to obtain additional data.

The coefficient of friction is recorded as the highest value obtained for both starting and running at the operating temperature. The temperature recorded is

an average value during operation when data were recorded. In some cases the operating temperature had an effect on the friction force and in some cases it did not. Each test is accordingly marked YES or NO in the table for each group. The run time in cycles is also recorded. The linear travel may be approximated since each cycle represents about 5 in. displacement of the rider sample.

All tests were conducted in ultrahigh vacuum (below 10^{-7} torr) except those noted. The pressure was not recorded for each test but in all cases it was decreasing with time. In many tests the pressure dropped below the lower reading limit of the gage (2×10^{-9}).

The flame-sprayed coatings such as LW-1N, LC-1N, and LA-2 are included with the ceramics since they represent refractory type hard faces. K-162B is also classed with the ceramics although this material is a solid cermet with approximately 30% metal binder. All these materials except LA-2 (Al_2O_3) could be grouped with the metals; in other studies[4] of the static case they are so grouped. Table 10 is included to present the composition of the coatings. Chromium plating that was applied to Type 316 stainless steel 0.0003 to 0.0005 in. thick by an electrolytic process is included with the metals.

TABLE 10

COMPOSITION OF SPECIAL COATINGS AND MATERIALS EVALUATED

Coatings and Miscellaneous Materials	Composition
LW-1N	WC + 13 to 16% Co
LC-1A	85% Cr_3C_2 + 15% Ni-Cr
LA-2	99+% Al_2O_3
K-162B	25% Ni, 5% Mo, 64% TiC, 6% CbC (some TaC)

The contaminant films used were sodium-silicate bonded dry-film lubricants 0.0005 to 0.0008 in. thick. The surfaces to be coated required special preparation for optimum bonding of the dry film. The friction coefficient was independent

of the substrate preparation or coating cure but surface wear, bonding strength, and sublimation rate appear to be affected. The dry-film lubricants tested were MoS_2, WS_2, and $MoSe_2$. All lubricants, when properly applied and cured, showed similar friction properties.

All uncoated samples were finish-ground to approximately 8 rms on the test surface and then diamond-lapped to a mirror finish. No attempt was made to evaluate the effects of surface finish on friction coefficient, since early results indicated plowing and seizure occurred at the start of sliding with metallic couples regardless of surface finish.

a. Friction Data

Details of testing by group are presented in Tables 11 through 17. The bar charts of Figure 7 summarize the results of all 67 tests run illustrating friction as a function of temperature for the five material groups tested. Significant reduction in the friction of noncarbon interfaces can be seen in the two bar charts. Most tests were of medium duration, less than 1000 hours, and the results do not significantly verify the wear life of the dry lubricants. Thus, should the dry-film be worn through the friction level of the noncarbon interfaces would escalate dramatically.

b. High-Friction Materials for Brakes

From the screening tests several material combinations exhibited relatively high values for sliding friction without plowing or seizure. Ten combinations of materials that might work as brake materials for mechanical devices in SNAP environments were evaluated in special screening tests. Table 18 is a tabulation of the test data summarizing each combination. The rider sample covered approximately 75 in. travel during this temperature ramp; thus, the friction coefficient vs rider travel data represents a continuation of each test after sample temperature had stabilized. The material combinations for brake surfaces, should exhibit the following characteristics:

1) Relatively constant friction coefficient in the 0.4 to 0.8 range

2) Little or not effect of temperature on friction coefficient

3) Very little, or no material transfer or wear

4) No self-welding after long-term dwell.

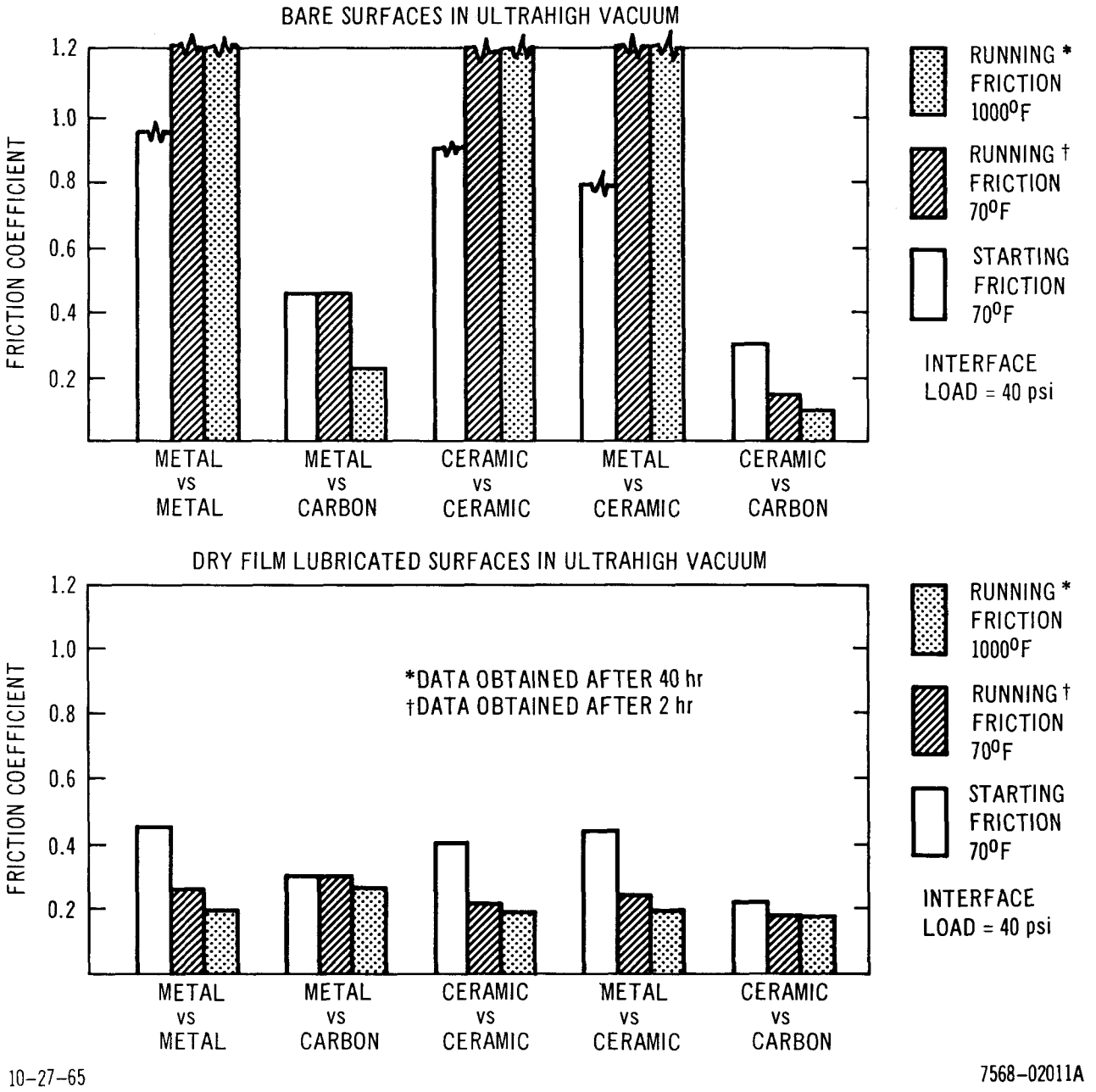

Figure 7. Summary of Ultrahigh-Vacuum Sliding Friction Studies

TABLE 11

SCREENING TEST RESULTS, GROUP A – METAL vs METAL

No.	Sample Combinations	Maximum Starting Friction	Dynamic Friction	Operating Temperature (°F)	Temperature Effect On Friction	Run Time (cycles)	Remarks
1	Titanium (6Al-4V) Stellite 6-B	0.95	0.4 to 0.5	950	No	76 and 27	Typical results for 2 tests. First test involved a 100-hr dwell and a 300-hr dwell. Samples seized after 300-hr dwell.
2	Titanium (6Al-4V) Titanium (6Al-4V) nitrided	>1	0.4	70	No	7	Galling of bare Ti occurred.
3	Titanium (6Al-4V) nitrided Titanium (6Al-4V) nitrided	>1	0.38	700	No	48	Rub marks on surface but no galling occurred. 16-hr dwell after 24 cycles had no effect.
4	Titanium (6Al-4V) nitrided ASTM A-286 nitrided	>1	0.85	70	No	2	The nitrided case failed on both samples. (Typical results for 2 tests)
5	Titanium (6Al-4V) nitrided ASTM A-286 annealed	>1	-	70	No	1	Samples galled – large metal transfer.
6	Titanium (6Al-4V) nitrided Stellite 6-B	0.9	0.58	700	No	60	Samples galled and seized. Typical results for 3 tests, 60 cycles shown is for longest run time.
7	Titanium (6Al-4V) nitrided Stellite 25	>1	0.9	950	No	12	Samples galled and seized. Typical results for 2 tests, 12 cycles shown is for longest run time.
8	Titanium (6Al-4V) nitrided Vicalloy (FeCo)	>1	-	70	No	1	Samples galled, metal transfer occurred.
9	Titanium (6Al-4V) nitrided Inconel-X	>1	-	70	No	6	Seizure occurred after 1 cycle. Samples were separated, the load reduced to 5 lb. Five more cycles resulted in galling.
10	Titanium (6Al-4V) nitrided Silver plate on H-11 Tool Steel	>1	0.9	70	Yes	3	The nitride case was not damaged. Large silver plating transferred to the nitride. Plating became soft under load.
11	Titanium (6Al-4V) Silver plate on H-11 Tool Steel	>1	0.9	70	Yes	3	Same results as No. 10.
12	H-11 Tool Steel, Heat Treated Stellite 6-B	>1	0.57	70	No	5	Galling and seizure occurred.
13	Inconel-X ASTM A-286	>1	0.8	70	No	2	Galling and seizure occurred.
14	Inconel-X Inconel-X	>1	0.85	70	No	2	Galling and seizure occurred. Typical for 2 tests.
15	Stellite 6-B Copper	0.4	0.36	68	-	30	Maximum temperature = 68°F. After approximately 150 in. of travel there was no galling or seizure.

Note: All combinations have a polished pretest surface.
Bearing Load = 40 psi (10 lb)

TABLE 12

SCREENING TEST RESULTS, GROUP B – METAL vs METAL WITH DRY LUBRICANT

No.	Sample Combinations	Maximum Starting Friction	Dynamic Friction	Operating Temperature (°F)	Temperature Effect on Friction	Run Time (cycles)	Remarks
1	H-11 Tool Steel, Heat Treated + Lubeco 6001 (MoS_2) Inconel-X	0.27	0.18	850	No	204	480 hr in test. Galling occurred, however, the lubricant provided film protection and prevented seizure. A 72-hr dwell had no effect.
2	H-11 Tool Steel + Lubeco 6001 (MoS_2) H-11 Tool Steel Heat Treated	0.6	0.14	750	No	87	288 hr in test. Considerable dry film transfer. Seizure did not occur, considerable asperity contact resulted in gradually increasing μ.
3	H-11 Tool Steel, Heat Treated + Molykote X-15 (MoS_2) Inconel-X	0.3	0.2	800	Yes	540	1093 hr in test. Note μ = 0.15 at room temperature. Wear was negligible. Molykote applied by brush.
4	Inconel-X + Lubeco 6001 (MoS_2) Inconel-X	0.2	0.1	900	No	1542	3096 hr in test. No surface damage or wear occurred.
5	H-11 Tool Steel + Lubeco 6001A (MoS_2) H-11 Tool Steel, Heat Treated	0.3	0.13	950	Yes	225	508 hr in test. Wear was negligible. Note μ = 0.08 at room temperature.
6	Inconel-X with pure MoS_2 H-11 Tool Steel, Heat Treated	0.9	0.22	950	Yes	10	This test was conducted in air, continuous run for 10 hr. X-ray diffraction shows no trace of MoS_2.
7	Titanium (6Al-4V) with Drilube 861 (WS_2) Stellite 6-B	0.7	0.12	1000	Yes	120	After 6 days at 1000°F, starting friction was 0.7 and running friction was 0.5.
8	Inconel-X ASTM A-286 with Lubeco 6021 (MoS_2)	0.8	0.08	800	Yes	144	High friction and sticking occurred above 750°F, 15 days in test had no effect on coating wear.
9	Type 316 Stainless Steel with Drilube 867N ($MoSe_2$) Inconel-X	0.3	0.08	1000	No	1109	90 days continuous operation at 1000°F. Surfaces were highly burnished
10	Titanium (6Al-4V) with Molykote X-15 (MoS_2) Stellite 6-B	0.17 0.43	0.12	700	No	710	3-day operation, then 90-day dwell at 700°F, then 7-day operation. Slight stiction noted (μ = 0.43 start) after the sixth day.

Note All combinations have a polished pretest surface.
Bearing load = 40 psi (10 lb)

TABLE 13

SCREENING TEST RESULTS, GROUP C – METAL vs CARBON

No.	Sample Combinations	Maximum Starting Friction	Dynamic Friction	Operating Temperature (°F)	Temperature Effect On Friction	Run Time (cycles)	Remarks
1	Titanium (6Al-4V) Purebon P-5N	0.25	0.2	975	Yes	264	Typical results for two tests. Considerable graphite transfer to the metal. μ = 0.65 at 75°F but drops to 0.25 above 600°F.
2	Inconel-X Purebon P-5N	0.34	0.21	850	Yes	800	1584 hr in test. Gradual reduction in μ with operation. Considerable graphite transferred to the metal. μ = 0.51 at 75°F. Weight loss of P-5N -0.6%.
3	Inconel-X Purebon P-5N with pure MoS_2 powder	0.34	0.2	900	No	545	1056 hr in test. Two temperature cycles show low μ at ambient temperature but μ = 0.34 at 800°F. Final cool-down cycle resulted in μ = 0.36 at 100°F.
4	Inconel-X Pyrolytic graphite (Normal to "C" plane)	0.84	0.61	1010	Yes	200	Continuous operation resulted in a wear track -1/32 in. DP after 83 ft of travel. Friction was gradually increasing during test.
5	Titanium (6Al-4V) Purebon P-03NHT	0.9	0.34	1000	Yes	600	Considerable graphite transferred to the metal. Friction coefficient decreased from 0.7 to 0.4 at 600°F.
6	Inconel-X Purebon P-03N	0.58	0.33	1000	No	288	Erratic friction data, i.e., μ oscillated between 0.35 and 0.45 for first 4 days of test. Considerable graphite transfer to the metal rider occurred.

Note: All combinations have a polished pretest surface.
Bearing load = 40 psi (10 lb)

TABLE 14

SCREENING TEST RESULTS, GROUP D – CERAMIC vs CERAMIC

No.	Sample Combinations	Maximum Starting Friction	Dynamic Friction	Operating Temperature (°F)	Temperature Effect On Friction	Run Time (cycles)	Remarks
1	TiC (Kentanium, K-162B) Solar Glass on Type 316 Stainless Steel	>1	0.62	980	Yes	28	Glass becomes soft and transfers to the TiC above 500°F
2	TiC (Kentanium, K-162B) Al_2O_3 (LA-2)	0.78	0.3	950	No	65	Steadily increasing μ from start to finish. Typical results for 3 tests. Results are for best test.
3	Al_2O_3 (LA-2) Al_2O_3 (LA-2)	0.74	0.6	1000	No	70	Both rider and pad were galled and worn from a grinding type action.
4	Al_2O_3 (LA-2) Al_2O_3 (LA-2)	>1	0.96	75	-	41	Results similar to No. 3.

Note: All combination have a polished pretest surface.
Bearing load = 40 psi (10 lb)

TABLE 15

SCREENING TEST RESULTS, GROUP E – CERAMIC vs CERAMIC WITH DRY LUBRICANT

No.	Sample Combinations	Maximum Starting Friction	Dynamic Friction	Operating Temperature (°F)	Temperature Effect On Friction	Run Time (cycles)	Remarks
1	TiC (Kentanium, K-162B) Al_2O_3 (LA-2) + MoS_2 powder	0.18	0.15	700	No	42	72 hr with 1 cycle every 2 hr. 90-day dwell had no effect on friction. The MoS_2 minimized self-welding.
2	Al_2O_3 (LA-2) Al_2O_3 (LA-2) + MoS_2 powder	0.74	0.34	750	Yes	108	216 hr in test. Steadily increasing μ from start to finish. Results similar to No. 2-D. μ = 0.25 at ambient start. μ = 0.34 at ambient finish.
3	TiC (Kentanium, K-162B) with X-15 Al_2O_3 (LA-2)	0.3	0.3	650	No	60	Special test to simulate SNAP 10A bearings. 20-hr oxidation in air at 550°F. High vacuum for 90 days at dwell and then one week autocycle at 650°F. No galling, seizure, or welding occurred.

Note All combinations have a polished pretest surface.
Bearing load = 40 psi (10 lb)

TABLE 16

SCREENING TEST RESULTS, GROUP F – METAL vs CERAMIC

No.	Sample Combinations	Maximum Starting Friction	Dynamic Friction	Operating Temperature (°F)	Temperature Effect On Friction	Run Time (cycles)	Remarks
1	Titanium (6Al-4V) TiC (Kentanium, K-162B)	0.54	0.34	950	No	44	Continuous operation for 72 hr. Seizure occurred after a 10-hr dwell.
2	Titanium (6Al-4V) Al_2O_3 (LA-2)	>1	0.5	830	No	72	Continuous operation for 144 hr. Seizure did not occur after a 90-hr dwell but large metal transfer did occur.
3	Titanium (6Al-4V) WC (LW-1N)	>1	0.48	880	No	108	Continuous operation for 144 hr. Seizure occurred after a 48-hr dwell.
4	Titanium (6Al-4V) Sapphire, Single Crystal	0.78	0.17	900	No	144	Typical for two tests. Both conducted in air. Catastrophic failure of sapphire in first test. Metal transferred to the sapphire.
5	Tungsten Al_2O_3 (LA-2)	0.7	0.54	1050	No	168	Continuous operation for 12 days. Seizure occurred after a 2-hr dwell.

Note All combinations have a polished pretest surface.
Bearing load = 40 psi (10 lb)

TABLE 17

SCREENING TEST RESULTS, GROUP G – CERAMIC vs CARBON

No.	Sample Combinations	Maximum Starting Friction	Dynamic Friction	Operating Temperature (°F)	Temperature Effect On Friction	Run Time (cycles)	Remarks
1	Al_2O_3 (LA-2) Purebon P-5N	0.1	0.09	950	Yes	748	2700 hr in test. μ = 0.3 at 70°F. μ = 0.1 above 600°F. 300-hr dwell after 30 days autocycle. Then 1 cycle per day for 40 days. Very small graphite transfer.
2	Al_2O_3 (LA-2) Purebon P-5	0.19	0.13	900	Yes	1140	2282 hr in test. μ - 0.58 at 70°F. Graphite transferred to the Al_2O_3.
3	Al_2O_3 (LA-2) National Carbon CDJ-83	0.32	0.23	950	Yes	648	1400 hr in test μ = 0.58 at 70°F. Graphite transferred to the Al_2O_3.
4	Al_2O_3 (LA-2) National Carbon CDJ	0.32	0.16	870	Yes	756	1560 hr in test. μ = 0.57 at 70°F. Graphite transferred to the Al_2O_3.
5	Al_2O_3 (LA-2) National Carbon ZTA	0.28	0.12	850	Yes	470	940 hr in test. μ = 0.57 at 70°F. Galling of the graphite surface occurred.
6	TiC (K-162B) National Carbon CDJ-83	0.28	0.08	1000	Yes	240	528 hr in test. μ = 0.58 at 75°F. Graphite transferred to the TiC.
7	Al_2O_3 (LA-2) Purebon P-5N	0.17	0.10	550	Yes	612	1272 hr in test. μ = 0.68 at 70°F. Small graphite transfer to the Al_2O_3. Trace of zinc found in P-5N by x-ray diffraction.
8	Al_2O_3 (LA-2) Purebon P-03NHT	0.57	0.23	1000	Yes	695	840 hr in test. μ = 0.62 at 70°F. Graphite transferred to the Al_2O_3. Trace of zinc found in P-03 by x-ray diffraction.
9	Al_2O_3 (LA-2) Pyrolytic Graphite ("A-B" plane)	0.52	0.04	1000	Yes	1380	Erratic friction during test. Low friction at 1000°F with occasional 'jumps' from 0.04 to 0.3. Slight material transfer to the Al_2O_3.
10	Al_2O_3 (LA-2) Purebon 3293	0.65	0.1	1000	Yes	1400	Erratic friction during temperature ramp. Smooth operation during 30-day operation at 1000°F. Severe plowing of the graphite occurred.
11	Al_2O_3 (LA-2) Pyrolytic Graphite (C' plane)	0.7	0.05	1000	Yes	462	Friction reduced gradually at 1000°F. Slight surface wear.
12	Sapphire Purebon P-5N	0.38	0.15	1000	Yes	502	Friction decreased with temperature. Erratic friction at 1000°F, coefficient varied from 0.15 to 0.2.

Note All combinations have a polished pretest surface.
Bearing load = 40 psi (10 lb)

TABLE 18

SLIDING FRICTION TESTS ON BRAKE MATERIALS

No.	Combination	Coefficient of Friction Range (μ)	Temperature (°F)	Vacuum (Torr)	Load (lb)	Time (days)	Remarks
1.	Al_2O_3 vs Electrolyzed Chrome Plate	0.5 to 0.86	70 to 1010	$\sim 10^{-7}$	10	16	Rider sample covered 2200 in. of linear travel. No material transfer.
2.	Al_2O_3 vs Relay 5 Steel	0.4 to 0.80	70 to 1000	$\sim 10^{-7}$	10	7	1134 in. of linear travel. No seizure or welding.
3.	Al_2O_3 vs Purebon P-02 Carbon	0.5 to 0.1	70 to 1000	$\sim 10^{-8}$	10	60	6606 in. of linear travel. Not suitable for a brake.
4.	Al_2O_3 vs Pyrolytic Graphite ("C" plane)	0.5 to 0.2	70 to 1100	7×10^{-8}	10	22	"C plane provides least amount of lubrication from outgassing.
5.	Al_2O_3 vs Purebon 3293	0.65 to 0.1	70 to 1000	2×10^{-8}	10	30	μ increased when temperature was lowered.
6.	Inconel-X vs "Blue Oxide" on Inconel-X	1.0 to 1.6	70 to 1300	1×10^{-3}	10	1	Specimens galled severely after 16 in. of travel.
7.	Al_2O_3 vs Al_2O_3	0.6 to 1.5	70 to 1000	1×10^{-8}	10 and 5	1	203 in. of travel. Severe galling.
8.	Inconel-X vs Pyrolitic Graphite ("C" plane)	0.45 to 0.62	70 to 1000	5×10^{-9}	10	12	1000 in. of travel. Considerable wear.
9.	Cr vs Cr	1.3 to 1.8	70 to 1000	1×10^{-8}	5	7	Severe galling, but did not weld together.
10.	Inconel-X vs Purebon P-02 Carbon	0.44 to 0.58	100 to 1000	2×10^{-8}	10	35	Carbon transfer to the metal riders; no severe damage. 4296 in. of travel.

NOTE: Area of contact = 0.25 in.^{2}

Using the above criteria, the Combinations 1, 2, 8, and 10 show the acceptable variation in friction through the temperature range from room ambient up to 1000°F; The friction variations of Combination 2 and the indicated wear of Combination 8 would limit them to applications with short total travel of perhaps 100 in. This leaves 1 and 10 as possible candidates. Long-term static adhesion tests of Al_2O_3, LA-2 vs electrolyzed chrome plate, however, show 0.32-lb adhesion (self-weld) in one out of two tests.[2] This leaves only Inconel-X vs P-02 carbon, as the combination meeting the criteria. There are no long-term static adhesion tests on Inconel-X vs P-02 carbon, but several other tests of Type 316 stainless steel vs P-5N (a materially similar pair) show no "stiction" (i. e., static adhesion) after long-term dwells in the high-temperature, high-vacuum environment. Similar results are also obtained in static adhesion tests with both Type 316 stainless steel and molybdenum against graphite cloth.

It should be pointed out that the results of these tests, both the static adhesion tests and the sliding friction tests, are obtained with small blocks loaded over a 0.25-in.^{2} area. This system may or may not be realistic in terms of representing a real component geometry. These tests do, however, serve to define the wear characteristics and dynamic friction that may be expected from each couple. Several other combinations beside Inconel-X vs P-O2 carbon, such as Al_2O_3 vs chrome, Al_2O_3 vs No. 5 Relay steel, or chrome vs chrome, may work equally well as brake surfaces depending upon a particular design. Since the motions in a particular component employing a brake are different from the motion of the sliding blocks, and interactions between bearings, encapsulants, and the braking surfaces themselves are possible in a real case, final selection of the optimum braking surfaces must be made in a real component or prototype test.

c. Test Facilities and Techniques

The test coupon preparation and test facilities were identical with those used for the self-welding studies, except coupons were subjected to an oscillating motion against each other under load instead of the static load used in self-welding tests.

Figure 8 shows the rider and base sample relationship during test; the chamber is removed in this view. Note that the location of the base sample is upside down with respect to the rider. This allows debris and wear particles to fall to the bottom of the chamber during sliding and not "ball-up" between the interfaces. Loading was accomplished by means of a load arm extending into the test chamber through a bellows seal and a gimbal. The bellows-gimbal arrangement allows for a two-degree freedom of motion about a common axis; thus, the rider sample may be oscillated back and forth on the base sample with an externally applied drive mechanism.

Input motion is provided by a small high-torque electric motor driving a bell-crank mechanism through a yoke that is connected to a force transducer. The output of the transducer is recorded on a high-speed, direct-writing oscillograph.

A simple calibration procedure before and after testing allows for the inherent friction and spring constant of the facility to be calibrated and corrected for in the test results. The external mounting of the testing components allows

for lubrication of the bearings and sliding joints without contamination of the test facility. Figure 9 shows this test facility in operation.

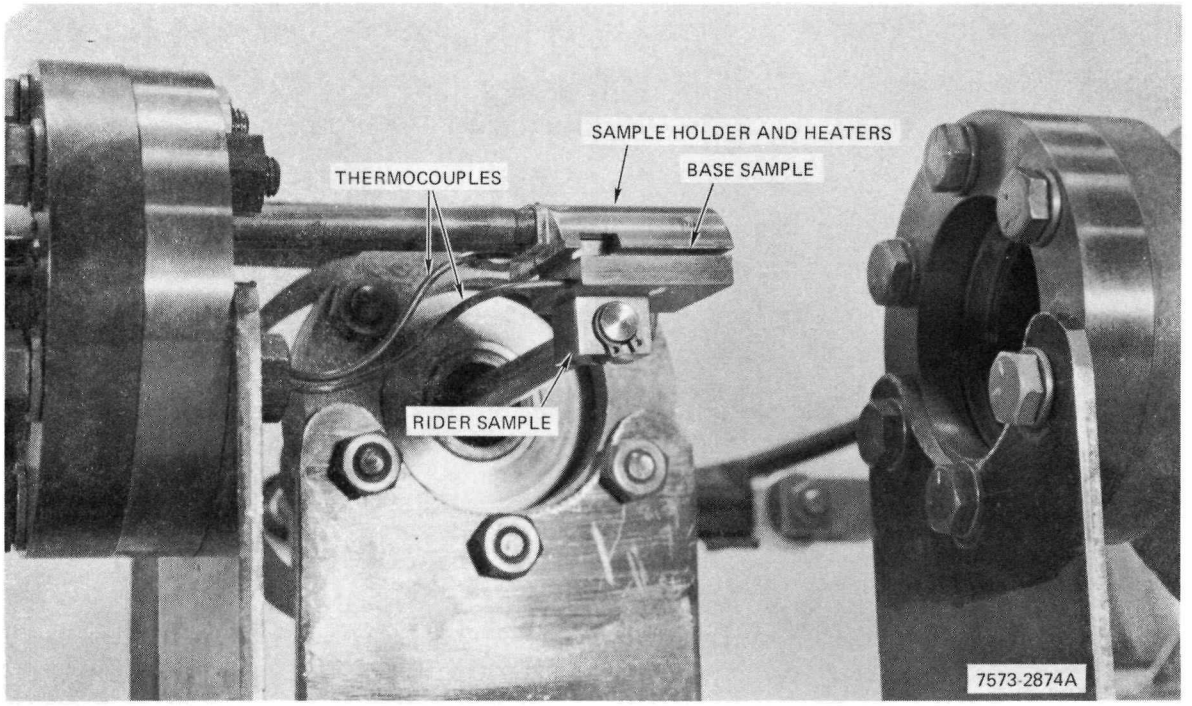

Figure 8. Friction Test Setup (Exposed)

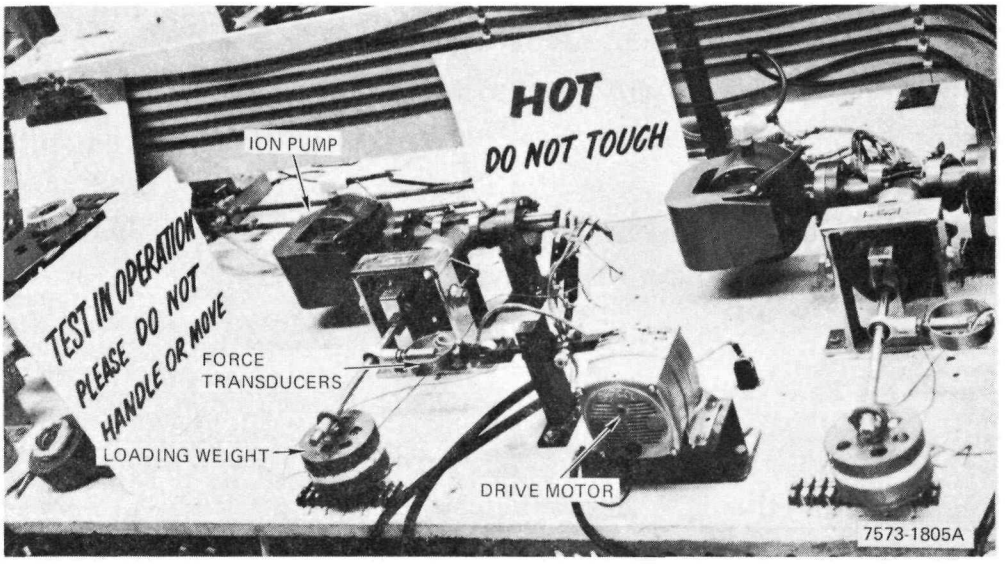

Figure 9. Sliding Block Friction Test Facilities

6. 1250°F Friction Evaluation

Development of the SNAP 8 reactor required the operation of control drum bearings in the 1150 to 1250°F temperature range, some 250°F above previous friction couple evaluations. A series of tests was conducted, utilizing the test fixtures and techniques of the previous 1000°F UHV investigations. [5]

These tests evaluated the SNAP 8 reference design P5-N carbon-graphite and P5 carbon-graphite (identical, but without a LiF impregnant) against a series of coatings on Inconel-750 and to solid materials. Table 19 presents the results of all testing with couples rated best to worst in reference to friction levels. Tests again substantiated that the Al_2O_3 vs carbon-graphite couple provides the most consistently low friction couple above 700°F. The MoS_2-coated couples showed low friction, but with some inconsistency. Galling occurred with WC, Cr_3C_2, and Haynes 90 specimens in some cases. Friction values of TiC-coated and solid specimens were moderately low and presented no galling material problems. Some transfer of chrome to the carbon-graphite was found after the Cr_3C_2 tests were completed. Figure 10 illustrates typical Al_2O_3 vs P5 carbon-graphite, Cr_3C_2 vs P5-N, and TiC vs P5-N carbon-graphite test coupons after testing.

7. 1600°F Friction Evaluations

Testing of candidate materials for operation to 1600°F was a continuing task. An initial group was selected and then other couples were tested as they became known.

a. Initial Tests

Development of the Advanced ZrH Reactor required bearing operation between 1500 and 1600°F, well above the previously developed 1250°F maximum for SNAP 8 bearings. Based on thousands of hours of successful operation of the Al_2O_3 vs P5 carbon-graphite bearing couple, that combination was retained as the reference design. Due to the increased temperature, it was necessary to replace the Inconel-750 substrate material with a material having good mechanical properties of 1600°F. A study was conducted and tantalum - 10% tungsten was selected. In conjunction with material and coating compatibility tests, sliding friction testing at 1600°F and 10^{-8} torr was initiated on the P5 vs Al_2O_3 on Ta-10W couple to verify its selection.

TABLE 19

FRICTION COEFFICIENTS OF MATERIALS
(1250°F and 10^{-6} torr)

Base	Coating	Rider	Time (hr)	Maximum Friction Coefficient
Inconel-750	Al_2O_3 (LA-2)	P5 Carbon-graphite	403	0.12
Inconel-750	Al_2O_3 (LA-2)	P5 Carbon-graphite	1200	0.33
Inconel-750	Al_2O_3 (Noroc)	P5-N Carbon-graphite	1010	0.28
Inconel-750	MoS_2	P5-N Carbon-graphite	72	0.15
Inconel-750	MoS_2	P5-N Carbon-graphite	616	0.62
WC	MoS_2 (in-situ)	P5-N Carbon-graphite	1487	0.25
Inconel-750	Chrome	P5-N Carbon-graphite	192	0.32
K-162B	None	P5-N Carbon-graphite	898	0.35
Inconel-750	TiC	P5-N Carbon-graphite	1018	0.42
Inconel-750	TiC	P5-N Carbon-graphite	1068	0.62
Inconel-750	WC (LW-5)	P5-N Carbon-graphite	1080	0.39
Inconel-750	WC (LW-5)	P5-N Carbon-graphite	1005	1.05
Inconel-750	Cr_3C_2 (LC-1)	P5-N Carbon-graphite	1193	0.78
Inconel-750	Cr_3C_2 (LC-1)	P5-N Carbon-graphite	--	>2.0
Inconel-750	None	P5-N Carbon-graphite	192	1.25
Inconel-750	Haynes 90	P5-N Carbon-graphite	96	1.05
Inconel-750	Haynes 90	P5-N Carbon-graphite	30	1.25
Inconel-750	Haynes 90	P5-N Carbon-graphite	329	>2.0

A second carbon-graphite, denoted as grade AXF-5Q, was selected for testing due to its fine grain and good mechanical properties. In addition, several other materials were studied as potential backup bearing couples. Eight material couples were tested at 1600°F and 10^{-8} torr air through 900 in. of travel under a 150-psi apparent load. Table 20 lists the eight couples.

Of the eight couples, only the carbon-graphites against Al_2O_3 and K-162B did not show severe wear or galling. These four couples were then subjected to 2000-hour tests at 1600°F to study friction after long-term dwells (up to 2 weeks). Tables 21 and 22 present results of the wear and dwell tests. At 1600°F, the carbon-graphite against Al_2O_3 exhibited the lowest friction values

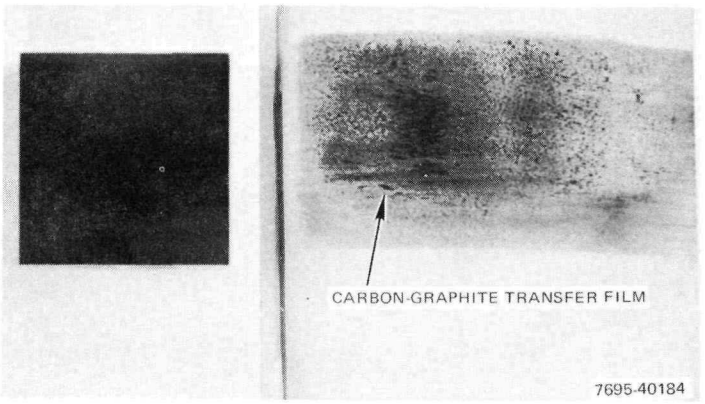

a. Al_2O_3 vs P5 [1200 hr, μ(max.) = 0.33]

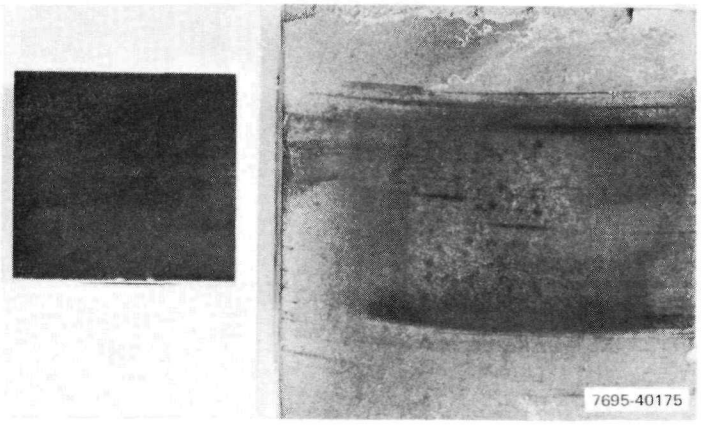

b. TiC vs P5-N [1010 hr, μ(max.) = 0.42]

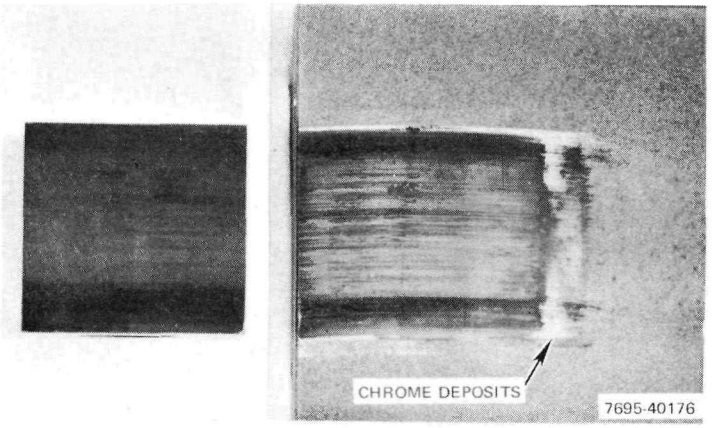

c. Cr_3C_2 vs P5-N [1193 hr, μ(max.) = 0.78]

Figure 10. Test Coupons, 1250° F Friction Test

TABLE 20

CANDIDATE MATERIALS FOR 1600°F BEARINGS

Couple No.	Couple Materials
1 and 2	P5 and AXF-5Q Carbon-Graphite vs Al_2O_3 on Ta 10-W
3 and 4	P5 and AXF-5Q vs K-162B (TiC+Ni Binder)
5 and 6	P5 and AXF-5Q vs LT-2 (W, Cr, Al_2O_3 cermet)
7	LT-2 vs solid Al_2O_3
8	LT-2 vs LT-2

TABLE 21

WEAR TEST SUMMARY, POTENTIAL 1600°F BEARING COUPLES

Couple		Maximum Static Friction Coefficient			Remarks
Base	Rider	Ambient	800°F	1600°F	
LA-2	P5	0.56	0.35	0.17	Light carbon-graphite transfer film
LA-2	AXF-5Q	0.56	0.43	0.15	
K-162B	P5	0.61	0.61	0.42	Heavy carbon-graphite transfer film, some metallic coating on K-162B surface.
K-162B	AXF-5Q	0.65	0.52	0.70	
LT-2	P5	0.25	0.34	--	Seized at 1600°F, chrome transfer from LT-2 to carbon graphite at interface.
LT-2	AXF-5Q	0.39	0.36	--	
LT-2	Al_2O_3	0.61	0.76*	0.60*	Severe wear of LT-2 transfer of material to Al_2O_3 severe chattering during operation.
LT-2	Al_2O_3	0.61	0.61	0.74	
LT-2	LT-2	0.65	0.71*	0.61	Severe wear of LT-2, material transfer to riders, severe chattering during operation.
LT-2	LT-2	0.69	0.61	0.78	

*Run under 75-psi load due to $\mu > 1.0$ with 150-psi load.

TABLE 22

LONG-TERM-FRICTION TESTS OF ACCEPTABLE 1600°F BEARING COUPLES

Event	Bearing Couple Friction Coefficient at 150-psi Load			
	LA-2 vs P5	LA-2 vs AXF-5Q	K-162B vs P5	K-162B vs AXF-5Q
Maximum				
At ambient	0.60	0.59	0.56	0.43
At 800°F	0.37	0.58	0.71	0.63
At 1600°F	0.31	0.32	0.56	0.57
Average at 1600°F				
Pre-dwell	0.19/0.22	0.22/0.26	0.30/0.37	0.38/0.48
Post-dwell	0.26/0.30	0.16/0.18	0.44/0.52	0.32/0.37
Total travel (in.)	275	275	400	400
Time (hr)				
At 1600°F	1760	1760	3240	3240
At 10^{-8} torr	2010	2010	3490	3490

and was retained as the reference bearing couple. The carbon-graphite against K-162B was retained, without further testing, as the backup bearing design.

Figures 11 and 12 show the post-test condition of the wear test samples. The carbon-graphite transfer-films are evident on both Al_2O_3 and K-162B which exhibited low friction. The material transfer of the LT-2 responsible for seizing and high friction is probably related to high vapor pressure chrome.

b. Al_2O_3 vs Al_2O_3

Tests were then initiated on solid Al_2O_3 against Al_2O_3-coated Ta-10W as a potential bearing combination.

Two duplicate test couples were subjected to a series of friction vs time and vs temperature tests following different dwell periods. In both cases, friction showed a steady increase with time and one couple showed excessive friction (0.6 or greater) particularly below 800°F. Data were recorded at 1500, 800, and 400°F and ambient temperature after dwells at 1500°F of 400, 400, 2000, 1200, 400, and 400 hours (4800 hours total). Table 23 summarizes test data.

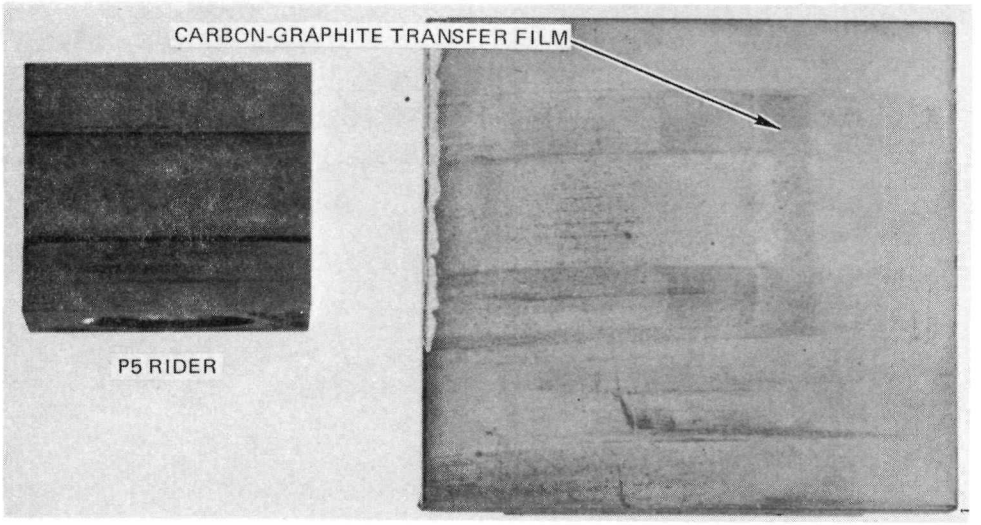

5-3-68 7695-55634a

a. Al_2O_3 on Ta-10W vs P5 Carbon-Graphite

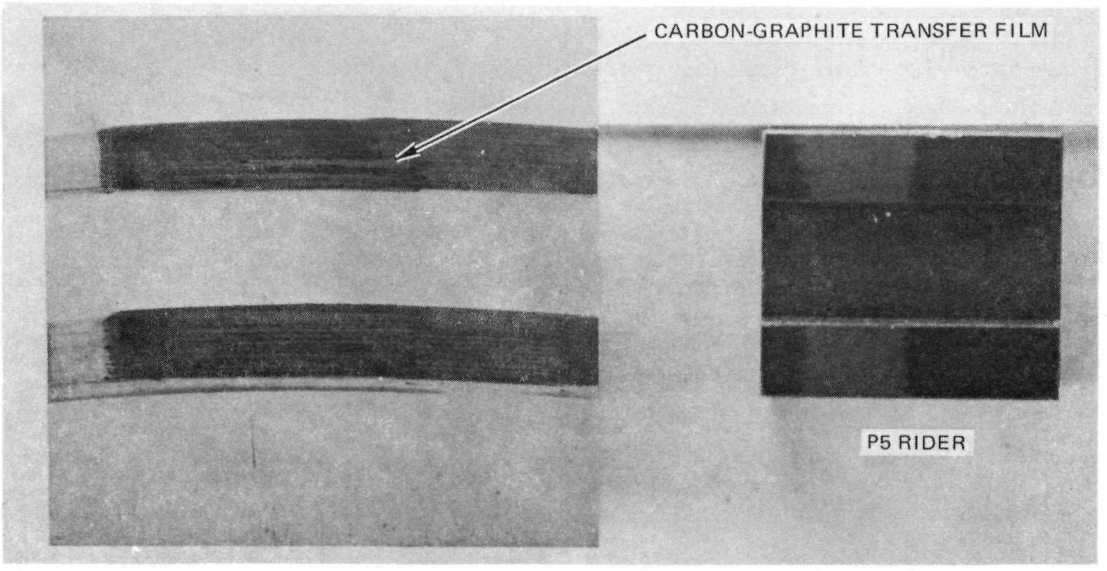

5-17-68 7696-4027a

b. TiC vs P5 Carbon-Graphite

Figure 11. 1600° F Wear Test Samples With Acceptable Friction and Wear

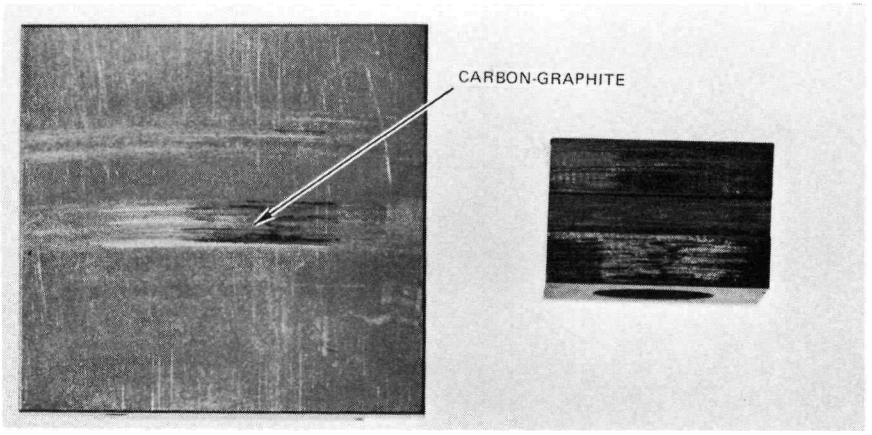

10-1-68 7759-4013

a. LT-2 Cermet vs Carbon-Graphite

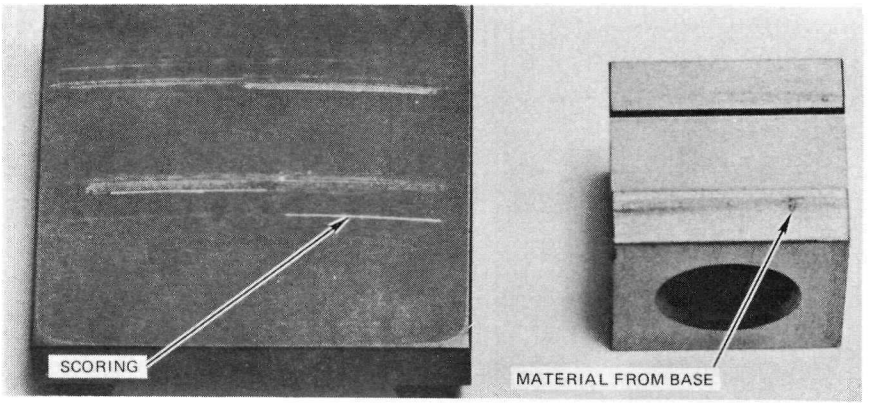

10-1-68 7759-1004a

b. LT-2 Cermet vs LT-2

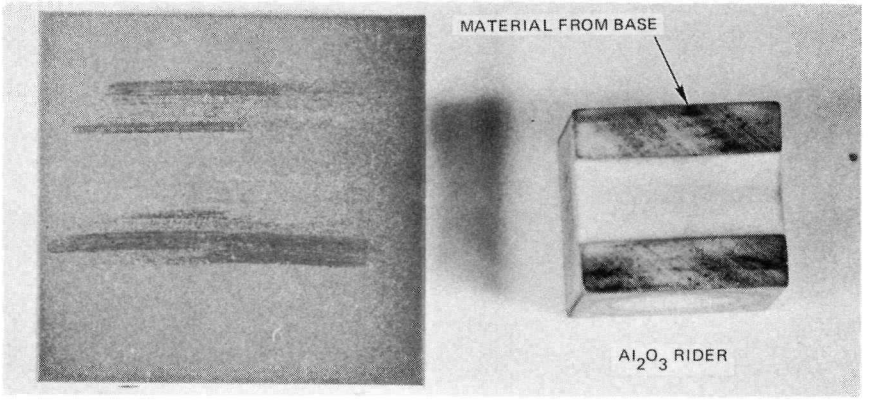

10-1-68 7759-4016a

c. LT-2 Cermet vs Solid Al_2O_3

Figure 12. 1600°F Wear Test Samples With Excessive Wear

TABLE 23

Al_2O_3 VS Al_2O_3 FRICTION TO 1500°F

Temperature (°F)	Time at 1500°F (hr)	Friction Coefficient	
		Couple A	Couple B
RT	Initial	0.21	0.17
800		0.10	0.11
1500		0.10	0.12
RT	2800	0.11	0.23
800		0.24	0.30
1500		0.30	0.26
RT	4000	0.91*	0.47
800		0.58	0.36
1500		0.47	0.36
RT	4800	0.99*	0.48
800		0.71*	0.44
1500		0.49	0.34

*Half load due to excessive friction.

c. MoS_2 Compact Studies

In a continuing study of wear rate and friction of potential Advanced ZrH Reactor bearing materials, a series of tests was conducted on a molydisulfide-tantalum compact material. The compact was developed by Boeing Company, Seattle, Washington, under an Air Force Contract, and is designated 108M.[14] The composition is 65 wt % MoS_2, 25 wt % Ta, and 10 wt % Mo. Tests were run on the compact against Al_2O_3-coated Ta - 10 W and against bare Ta - 10 W to study possible replacement of the P5 carbon-graphite with the self-lubricating compact and possible elimination of the Al_2O_3 coating. The material is approximately three times as strong as P5 and the thermal expansion rate is close to Ta - 10 W (4.9 vs 3.9 x 10^{-6} in./in./°F).

Two test couples, one each of the MoS_2-Ta compact against Al_2O_3-coated Ta - 10 W and MoS_2-Ta against bare Ta - 10 W, were subjected to testing at 1600° F and 10^{-8} torr pressure.[15] Table 24 shows the friction coefficients as a function of time under vacuum.

TABLE 24

STATIC FRICTION COEFFICIENTS

Temperature (° F)	Time at Dwell (hr)	MoS_2-Ta vs Al_2O_3		MoS_2-Ta vs Ta - 10 W	
		Pre-Dwell	Post-Dwell	Pre-Dwell	Post-Dwell
1600	50	0.39	0.48	0.42	0.95
1200	75	0.25	0.24	0.21	0.20
1600	75	0.26	0.46	0.24	0.87
	20		0.39		0.69
1300	75	0.23	0.24	0.24	0.24
	20		0.25		0.26
1400	75	0.27	0.34	0.26	0.39
1500	75	0.25	0.35	0.26	0.53
	75		0.32		0.60
1600	75	0.31	0.71	0.34	1.10
	75		0.73		0.90
	80		0.60		>1.1

An initial friction coefficient reading was taken at 1600° F and a second taken following a 50-hour dwell. While the MoS_2-Ta vs Al_2O_3 couple showed only a moderate increase in friction (0.39 to 0.48), the MoS_2-Ta vs Ta - 10 W resulted in a doubling of friction (0.42 to 0.95). Continued operation resulted in substantial drops in friction (0.33 and 0.35 for Al_2O_3 and Ta - 10 W, respectively). Friction coefficients were then taken at 1300, 1200, and 800° F with friction levels between 0.20 and 0.35. A 75-hour dwell at 1200° F was run with no increase in friction coefficients. A second set of readings at 1600° F was taken with a 75-hour dwell between readings. Friction following the dwell period again showed a moderate increase (0.26 to 0.46) for the MoS_2-Ta vs Al_2O_3 couple and a substantial increase (0.24 to 0.77) for the MoS_2-Ta vs Ta - 10 W couple.

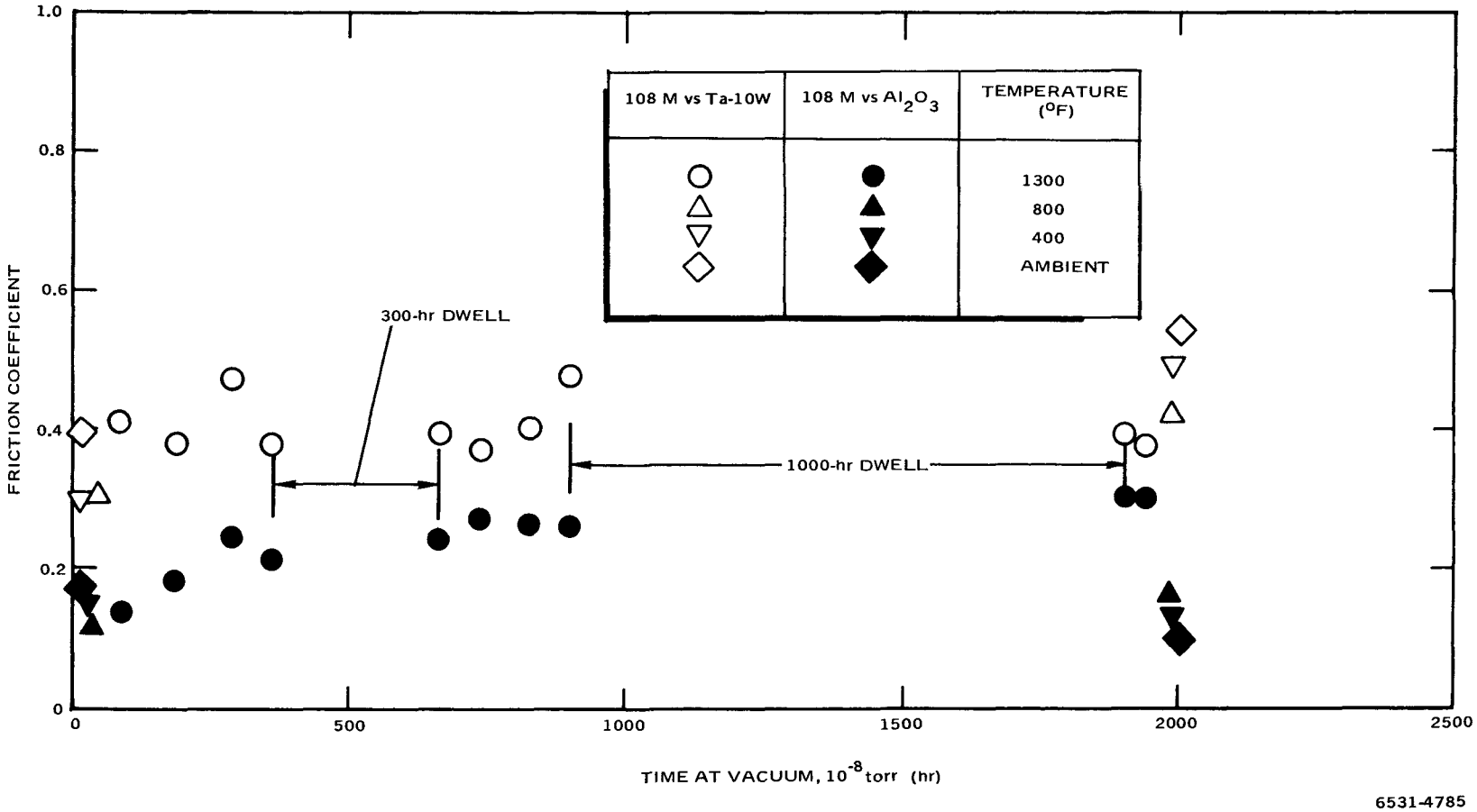

Figure 13. Friction vs Time (MoS_2 Compacts)

The temperature was lowered to 1300° F, and a series of 75-hour dwell periods was initiated to study the relationship between friction and temperature above 1200° F. There was no appreciable increase in friction for either couple following the dwell at 1300° F. As temperature was increased to 1600° F, the increase in post-dwell friction was considerable. While both couples showed increased friction, the MoS_2-Ta vs Al_2O_3 couple showed less increase than the MoS_2-Ta vs Ta - 10 W couple. The final test at 1600° F resulted in a friction coefficient greater than 1.0 for the couple with bare Ta - 10 W. Following the final 1600° F dwell, the test was disassembled and all specimens were visually inspected. All mating surfaces were in excellent condition, with light MoS_2 transfer films on the Al_2O_3 and Ta - 10 W.

The test couples were reassembled in the test fixture and a long-term 1300° F test initiated. From the previous tests, 1300° F was determined to be the highest operating temperature with no appreciable short-term temperature effects. Figure 13 shows the friction coefficients vs time for both the MoS_2-Ta vs Al_2O_3 and MoS_2-Ta vs Ta - 10 W couples. For the 2000-hour test, the friction coefficients at 1300° F varied between 0.14 and 0.30 for the Al_2O_3 couple and between 0.37 and 0.48 for the Ta - 10 W couple. Dwells of 300 and 1000 hours were included in the test sequence without any significant increase in friction. Friction at the conclusion of the test at 1300° F was 0.30 and 0.38 for the Al_2O_3 couple and the Ta - 10 W couple, respectively.

The post-test condition of both couples is shown in Figure 14 and indicates the heavy uniform transfer film buildup for the bare Ta - 10 W. A uniform, but thinner, transfer film is present on the Al_2O_3 surface.

Tests have shown friction to be low during periodic oscillation and uneffected by long-term dwell periods at temperatures up to 1300° F. Above 1300° F, friction showed an increasing effect due to dwells at temperature. While both couples, MoS_2-Ta vs Al_2O_3 and MoS_2 vs Ta - 10 W, had acceptable results at 1300° F and below, friction for the Al_2O_3 couple was consistently lower during all testing. Either couple, however, shows promise for long-term periodic operation at 1300° F or below.

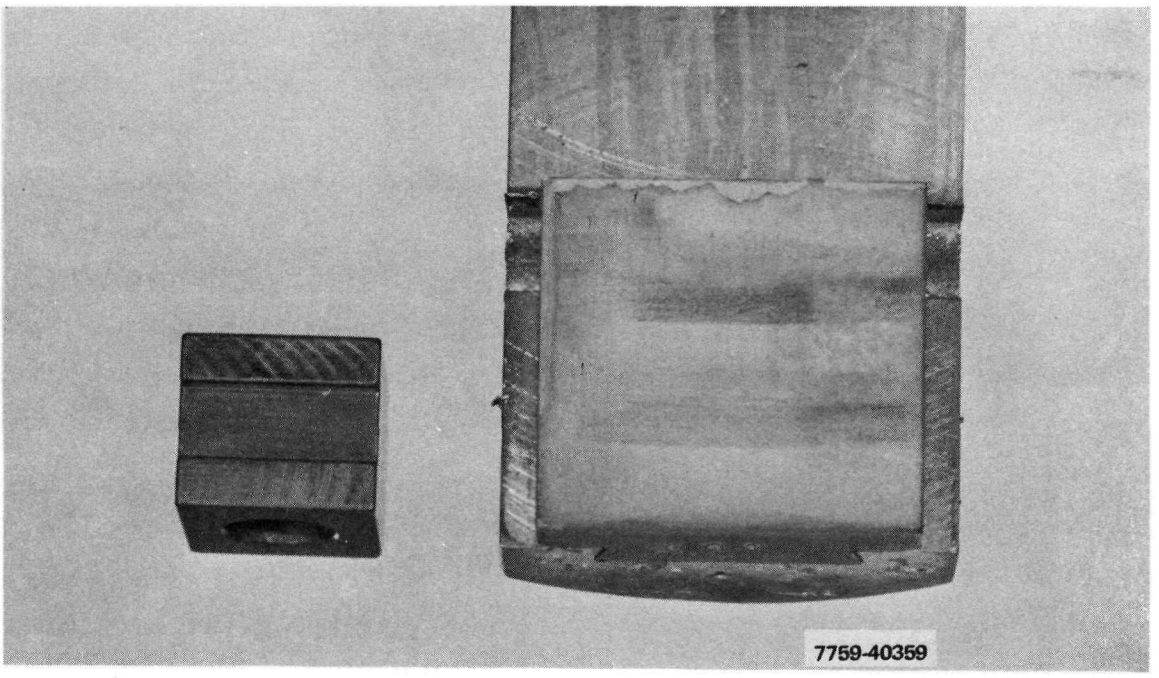

a. MoS_2-Ta vs Al_2O_3 on Ta - 10 W 1800 Hours at 10^{-8} torr and 1300° F

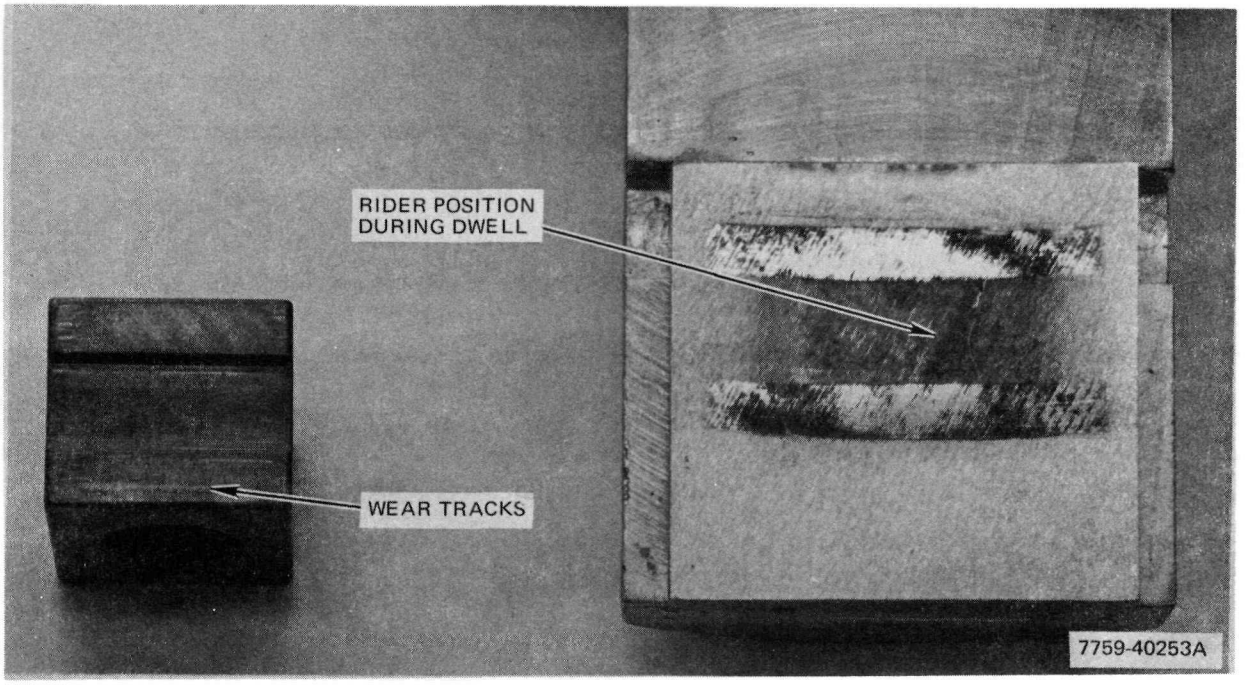

b. MoS_2-Ta vs Ta - 10 W

Figure 14. Post-Test Photos of MoS_2 Compacts

d. Test Fixture

While retaining the same test specimen configuration as previous tests, it was necessary to fabricate a fixture capable of operating for long periods of time under load at 1600°F and under pressures of 10^{-8} torr or less. The resulting fixture, Figure 15, uses the same operating technique as the small 1000 to 1250°F fixtures, but will test two couples independently and simultaneously. All internal fixturing in the test chamber, including the heater, was fabricated from tantalum or Ta - 10 W to withstand the high temperatures and to preclude sublimation of chrome and nickel contaminants onto the test specimens. The chamber is mounted on a 400 liter/sec ion pump to ensure a contaminent free environment under operation.

8. MoS_2 Coatings

When the first bearing material couples were tested, the dry lubrication coating techniques were still under development. Because of possible loss of coating by wear or by evaporation (rate was unknown), the early coatings were relatively thick. Dry lubrication was used only to enhance low friction with couples that in themselves produced low friction. When methods of bonding MoS_2 using a sodium silicate binder were developed, extended use of this material came into play as evidenced by its use in gears, cams, ball screws, and shafts.

Coated cylindrical surfaces that rubbed against a flat surface to simulate cam configurations were tested at various temperatures, vacuum levels (to evaluate oxidation effects) and contact stresses (calculated for base materials). Table 25 shows the results of the testing. The friction remained relatively low during all testing and was not seriously affected by temperature or contact stresses but did show an increase at 1000°F after 650 hours in 1×10^{-3} torr, air. The surfaces showed only a burnishing or polishing and no deterioration after the test. It was concluded that sodium-silicate-bonded MoS_2 on René 41 (or similar substrate) was suitable for use to 900 or 1000°F in a moderate vacuum (1×10^{-5} torr) and high vacuum for long periods of time at Hertz stresses up to 51,800 psi. Work by Brainard[13] demonstrated the thermal stability of MoS_2.

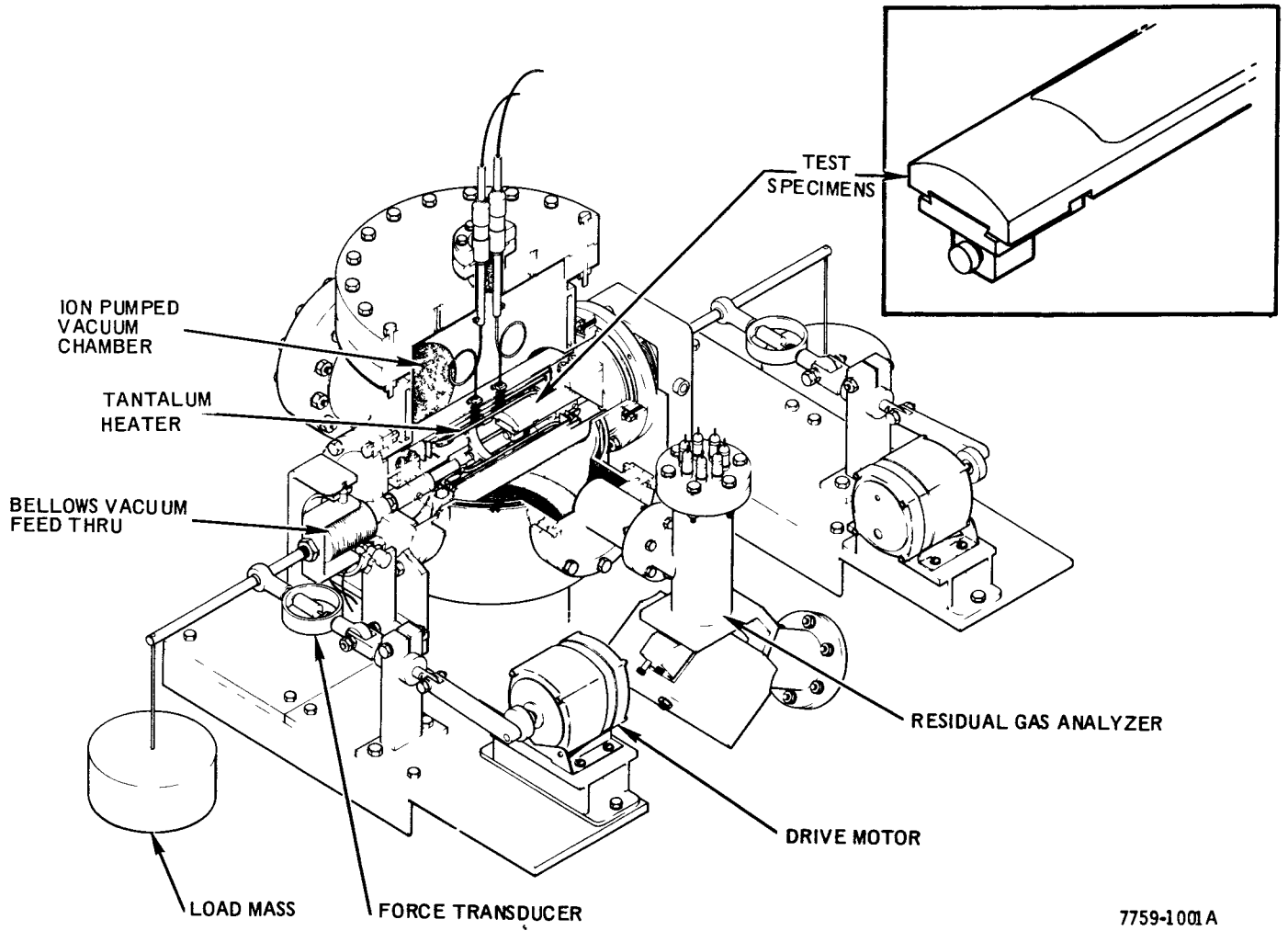

Figure 15. Sliding Friction Test Fixture

TABLE 25

FRICTION OF MoS_2 vs MoS_2 ON RENÉ 41 SUBSTRATE
(Sodium-Silicate-Bonded MoS_2, 0.0004 to 0.0010-in. thick)

Test No.	Test Variable	Contact Stress* (psi)	Pressure (torr)	Temperature (°F)	Total Time (hr)	Total Accumulated Travel (in.)	Friction Coefficient	
							Static	Dynamic
1-a	Temperature	12,500	$<1 \times 10^{-5}$	70 to 1150		500	0.12	0.07
1-b	Contact Stress	29,600 to 51,800	1×10^{-7}	1000		800	0.13	-
2	Contact Stress	12,500 to 25,000	1×10^{-7}	500		1000	0.13	0.07
3	Oxidation	35,500	1×10^{-3}†	600	411	32	0.22	0.14
4-a	Oxidation Time,	35,500	1×10^{-3}	800	433	410	0.16	0.10
4-b	Travel, and	35,500	1×10^{-3}	900	541	560	0.22	0.14
4-c	Temperature	35,500	1×10^{-3}	1000	650	640	0.30	0.20

*Calculated Hertzian stress between a 0.188-in. radius cylindrical surface and a flat surface of the René 41 base material.

†A 400-hr test in 1×10^{-3} torr using a metered air leak was assumed to closely simulate the quantity of O_2 encountered during a reactor 40,000-hr life test in 1×10^{-5} torr.

C. MATERIAL COMPATIBILITY

1. Al_2O_3 vs P5 and P5-N Carbon Graphite

The selection of bearing couples for acceptable friction properties was based on the extensive self-weld and sliding friction studies as previously described. Tests designed specifically to study interaction between coating, substrates, and mating surfaces were initiated upon the failure of the SNAP 8 bearing as a result of Al_2O_3 separation from the Inconel-750 bearing shafts.[5]

Test specimens representing all applications of an Al_2O_3-coated bearing either against carbon-graphite or against itself were collected. These specimens, 65 in number, included SNAP 8 control drum bearings (Al_2O_3 on Inconel-750 substrate), SNAP 8 actuator bearings (Hiperco-27 substrates), and SNAP 10A drum bearings (Ti-6Al-4V substrates) which had been exposed to the temperature range of 1000 to 1250° F for test periods to 10,000 hours. All specimens underwent sectioning and metallographic examination of the Al_2O_3-substrate interface and the surfaces of Al_2O_3 coating specimens were studied by x-ray diffraction. The most significant discovery was that the Al_2O_3, applied as 99% gamma (γ) phase Al_2O_3, had a small, but definite transformation to alpha (α) phase. The phase shift (1) occurred when the Al_2O_3 was in contact with the P5-N carbon-graphite, (2) occurred only on specimens tested above 1100° F, and (3) appeared to be time dependent. Table 26 shows the transformation of Al_2O_3 to α phase.

TABLE 26

ALPHA Al_2O_3 AS A FUNCTION OF TIME AND MATING SURFACE

Time at 1150° F and 10^{-5} Torr (hr)	Alpha Phase Al_2O_3	
	Against P5-N	Against Al_2O_3
Pre-Test	1.7, 3.2*	1.7, 3.2
3,000	1.4, 3.2	-
5,000	4.8, 13.6	-
10,000	9.8, 15.7	1.6, 3.2

*Friction surface, substrate surface

Material compatibility testing of bearing couples was initiated in support of the SNAP 8 bearing failure analysis. Tests were conducted using coupons 0.5 in. square and 0.37 in. thick stacked under load in vacuum furnaces to simulate bearing test conditions. The initial test was conducted to study the effect of the LiF impregnant in the P5-N carbon-graphite on the stability of the alumina coatings and its reactions with the substrate material. The matrix, shown in Table 27, was designed to allow comparison of (1) the effects of different graphites or no graphite against Al_2O_3 on the Inconel-750 substrate and, (2) the effects of different substrates with the P5-N and Al_2O_3 interface.

TABLE 27

SNAP 8 BEARING MATERIAL COMPATIBILITY TEST

Graphite	Coating	Substrate
None	Al_2O_3	Inconel-750
P5	Al_2O_3	Inconel-750
P5-N	Al_2O_3	Inconel-750
P5-N	Al_2O_3	Inconel-600
P5-N	Al_2O_3	Ta - 10% W

Tests were conducted at 1250, 1350, and 1450°F for 500, 1000, 2000, and 5000 hours at 10^{-7} torr air. The Al_2O_3 coating separated from the substrate in all cases where it was in contact with the P5-N (LiF impregnated) carbon-graphite. In no case did the coating or coating-to-substrate bond deteriorate or separate when the LiF impregnant was absent. Figure 16 shows typical cases of Al_2O_3 on the Inconel-750 substrate against (1) the P5 (unimpregnated graphite) and (2) the P5-N graphite. Inspection under 250X magnification also showed a definite change in the Al_2O_3 microstructure. The unimpregnated P5 carbon-graphite was therefore selected to replace the LiF impregnated P5-N.

2. Alternate Materials for SNAP 8 (1250°F)

Concurrent with the evaluations of the effect of impregnated and non-impregnated carbon-graphite other candidate coatings for shafts were selected and tested in vacuum at various temperatures for compatibility.[5]

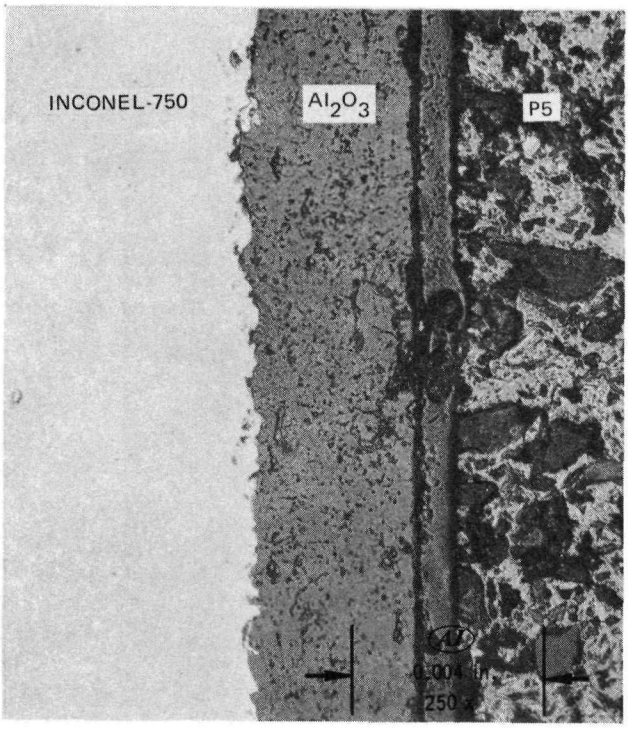

8148-7-1

a. 1450° F Against P5

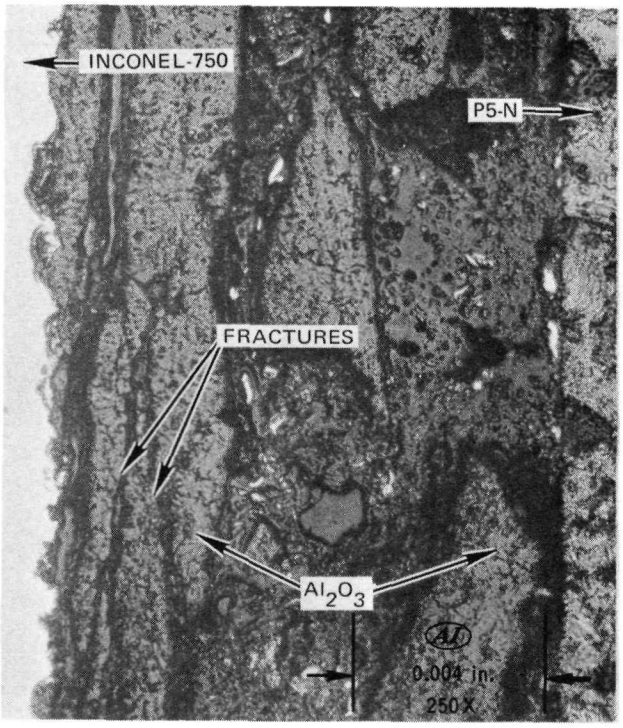

8148-5-3

b. 1450° F Against P5-N

Figure 16. Alumina vs Carbon-Graphite Metallurgical Results — 2000 hr

The materials and couples evaluated were P5-N carbon-graphite against:

1) LC-1C (Cr_3C_2) flame-spray coating (Cr_3C_2 93%, Co 7%)
2) LW-5 (WC) flame-spray coating (WC 25%, Ni 7%, W, Cr Carbides 68%)
3) TiC plasma-spray coating (TiC 99%, trace of Cu)
4) LA-2 (Al_2O_3) flame-spray coating (Al_2O_3 99+ in gamma phase)
5) Haynes Alloy 40 hard facing.

Tests were conducted at 1250, 1350, 1450° F to accelerate any effects of temperature, and were run for 500, 1000, 2000, and 5000 hours. Post-test specimens were sectioned and examined for reaction at the carbon-graphite or substrate interfaces or for any deterioration of the coating itself.

1) The Cr_3C_2 coatings remained intact with good coating-substrate bonds, but a chrome-rich layer was deposited on the carbon-graphite. The chrome thickness increased with both time and temperature and was not present in two coupon tests without the carbon-graphite. Figure 17 illustrates these conditions.

2) The WC coatings remained well bonded to the substrates, but again showed a chrome-rich deposit on the carbon-graphite mating surfaces, Figure 18. The layer was thinner than on the Cr_3C_2 specimens but was a function of time and temperature.

3) As shown in Figure 19, the TiC coating substrate bond was excellent and no transfer of material to the contacting carbon-graphite was present. Porosity of the coating increased as a result of testing, but no effect of time or temperature could be established. The porosity is postulated to have been caused by sectioning and polishing for metallographic examination, but indicates coating strength may be effected by exposure. There was some evidence that the presence of the carbon-graphite increased the porosity. Pre-test porosity was estimated at 10.8%, while average post-test values increased to 26.8% "pull out."

4) The Al_2O_3 coating severely broke up and separated from the substrate when in contact with the P5-N carbon-graphite. The Al_2O_3 not exposed to the carbon-graphite was unaffected by testing as can be seen in Figure 20.

5) Haynes 90 sliding friction tests running concurrently exhibited extremely high friction, material transfer, and self-welding. Examination of the metallurgical specimens was therefore eliminated.

From these tests it was concluded that only TiC rated consideration as a potential bearing surface coating for use with the P5-N carbon-graphite.

3. High Temperature Materials (1600° F)

A third series of compatibility tests was conducted at 1600° F in support of the 4π shielded reactor study. Specimens were again exposed for 500, 1000,

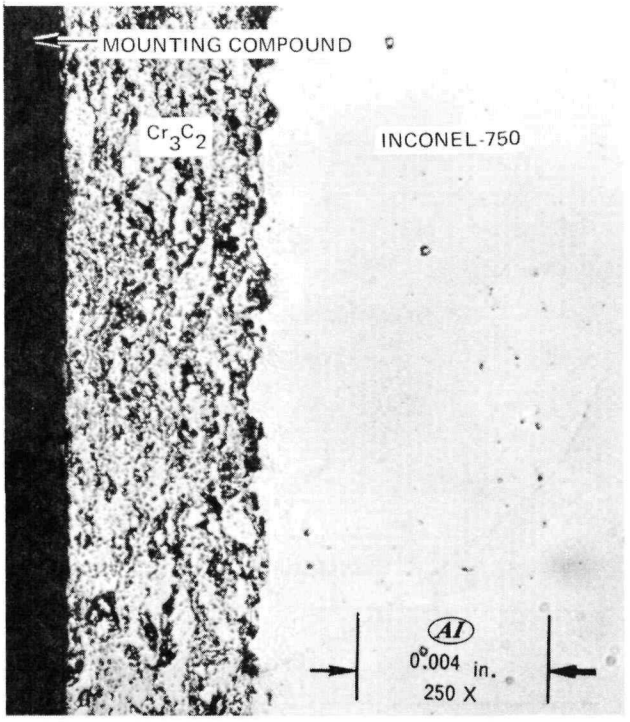

8085-4-1

a. 1450° F Without Graphite

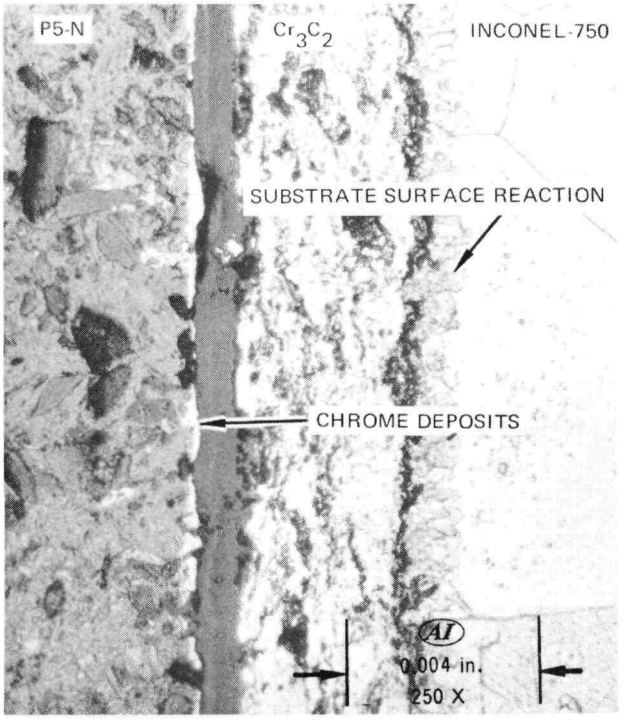

8083-5-2

b. 1450° F With P5-N

Figure 17. Cr_3C_2 1000-hr Metallurgical Specimens

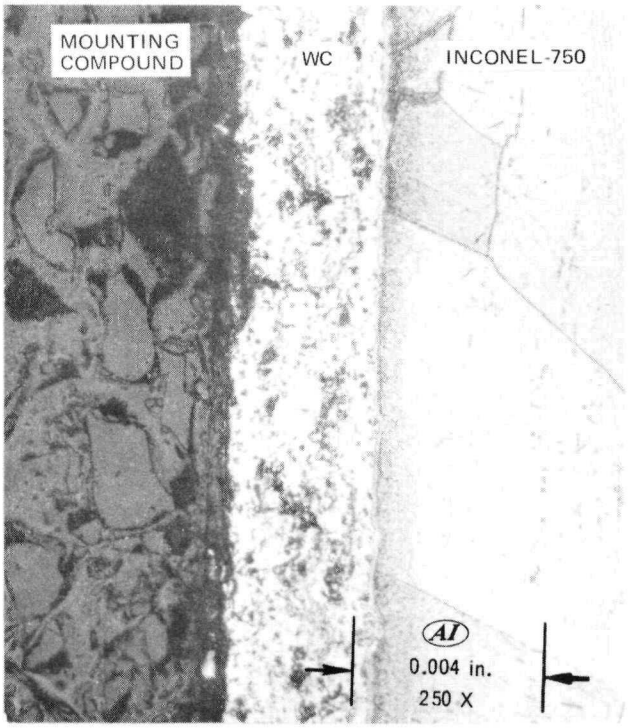

8085-5-1

a. 1450° F Without Graphite

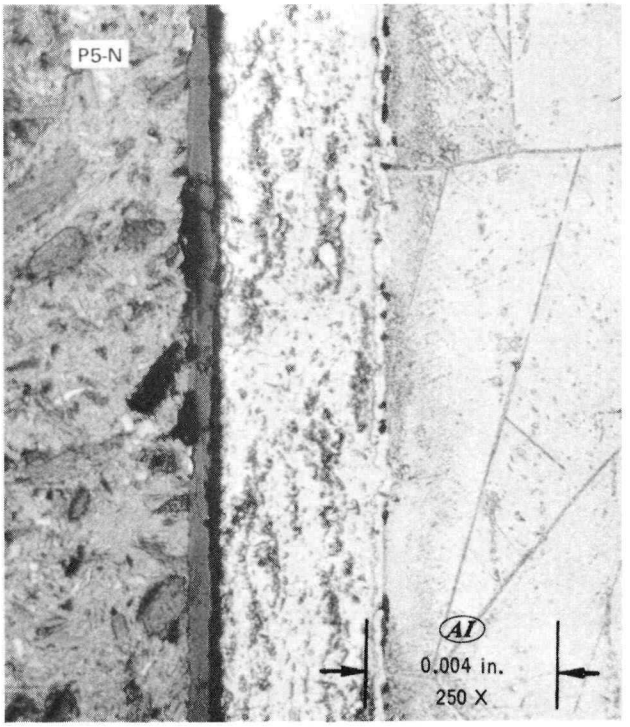

8083-4-2

b. 1450° F With P5-N

Figure 18. WC 1000-hr Metallurgical Specimens

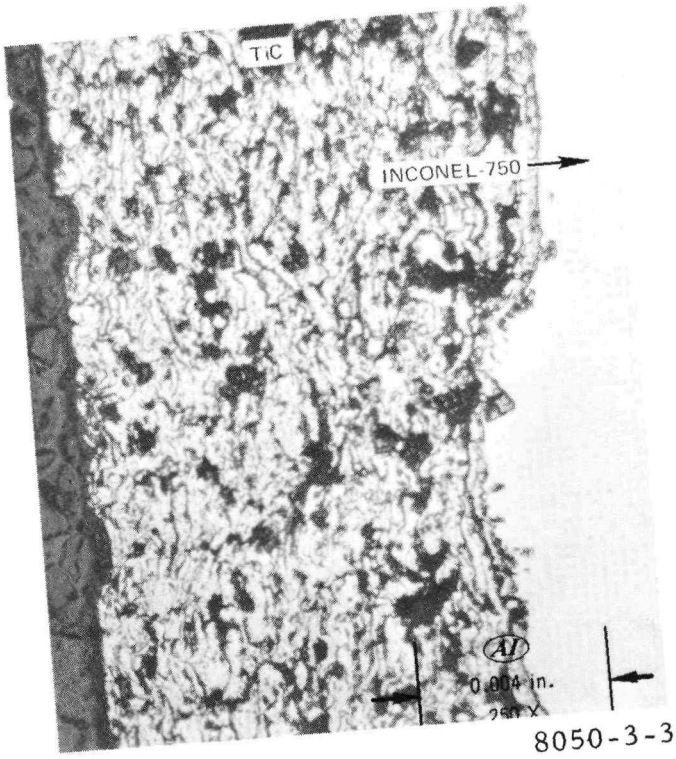

8050-3-3

a. As-Coated

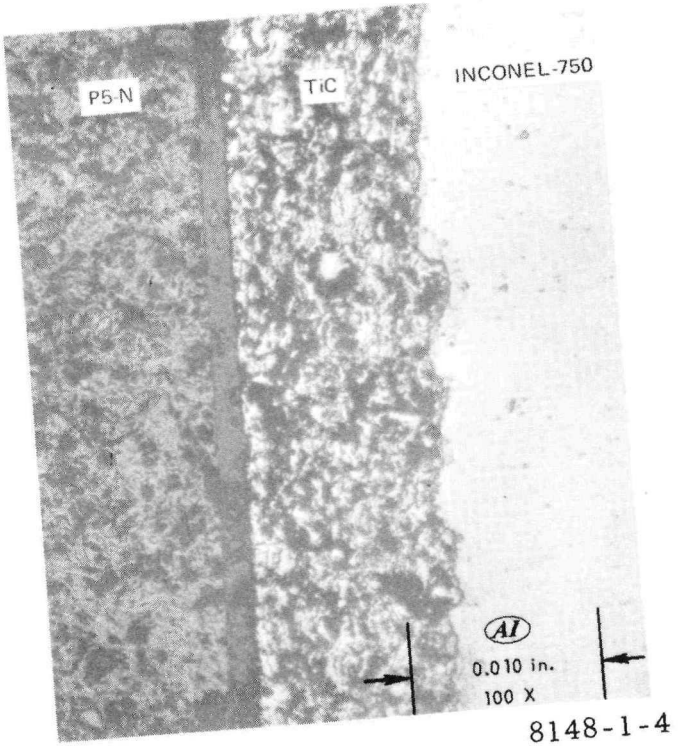

8148-1-4

b. 1250° F With P5-N

Figure 19. TiC 2000-hr Metallurgical Specimens

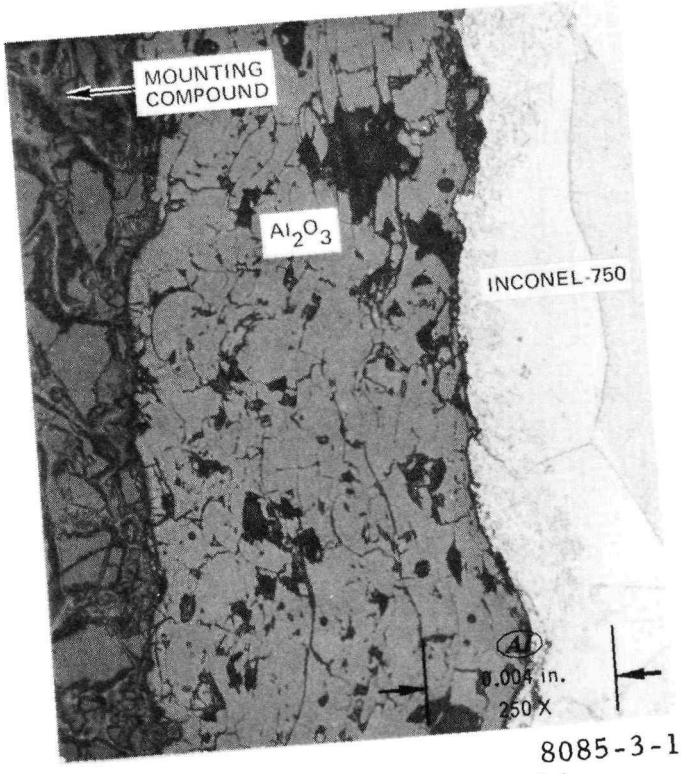

8085-3-1

a. 1450° F Without Graphite

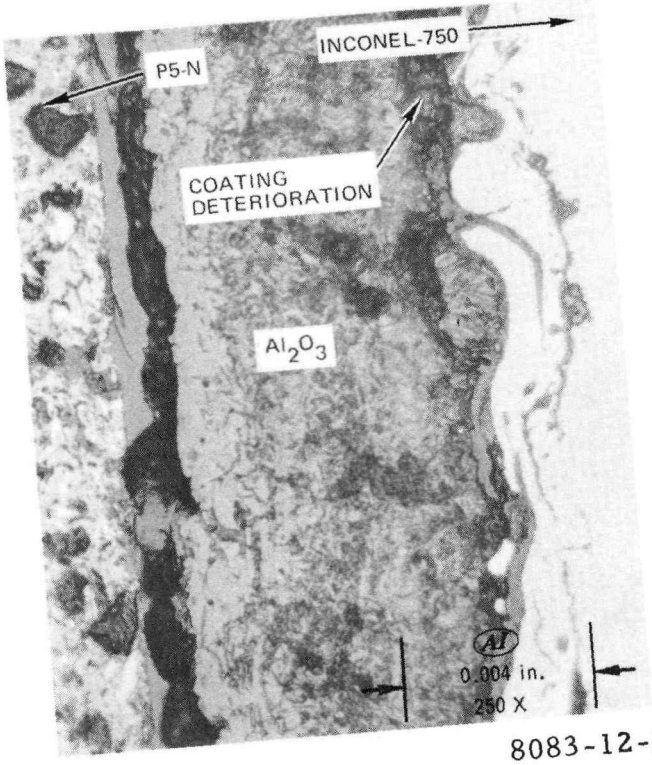

8083-12-2

b. 1450° F Against P5-N

Figure 20. Al_2O_3 2000-hr Metallurgical Specimens

TABLE 28

CHEMICAL COMPOSITION OF MATERIAL COMPATIBILITY SPECIMENS

Composition (wt %)

Kentanium K-162B	Haynes LT-3 Cermet	Linde LA-2 Flame Plate	Centralab Al_2O_3	Union Carbide Ta - 10 W Alloy
TiC 64	W 60	Al_2O_3 99.5	Al_2O_3 99.5	Ta 90
Ni 25	Al_2O_3 25	(γ phase)	(γ phase)	W 10
NbC 6	Cr 15			
M 5				
P5 Carbon-Grahite: Unimpregnated 60% graphitized				
AXF-5Q Carbon-Graphite: Unimpregnated 60% graphitized				

TABLE 29

PROPERTIES OF AXF-5Q AND P5 CARBON GRAPHITE

Property	Graphite	
	AXF-5Q	P5
Density (gm/cc)	1.84	1.70
Strength (psi)		
Tensile	4,000	6,000
Compressure	16,000	25,000
Transverse		8,500
Flexure	9,000	
Hardness (shore)	70	85
Coefficient of Expansion (10^{-6} in. /in. /°F)		
RT-212	3.7	
RT-500		2.2
RT-1500	4.3	
Porosity (0/0)	15	18
Oxidation Threshold (°F)*	950	
Temperature Limit (°F)*		500

*at ambient pressure air

2000, and 5000 hours in a 10^{-7} torr vacuum. The following couples were tested and analyzed:

1) Carbon-graphite (Types P5 and AXF-5Q) vs Al_2O_3 (on Ta - 10 W and Inconel-750 substrates)
2) Carbon-graphite (P5 and AXF-5Q) vs solid Al_2O_3
3) Carbon-graphite (P5 and AXF-5Q) vs solid K-162B

Two additional material couples were tested, but not examined because of poor friction characteristics exhibited during concurrent sliding friction tests.

4) Carbon-graphite (P5 and AXF-5Q) vs LT-2
5) LT-2 vs solid Al_2O_3

Table 28 gives the chemical composition of the materials and Table 29 compares the properties of the two carbon-graphites.

There was no deterioration of materials and no signs of incompatibility or interaction on any specimen couple. The Inconel-750 substrate is not satisfactory for a bearing substrate at 1600° F due to material strength limitations but was included for further study of the Al_2O_3 to substrate thermal expansion difference.

Figures 21, 22, and 23 respectively show the Al_2O_3 coating, K-162B, and solid Al_2O_3 specimen couples, respectively. No difference in exposure to the two graphites was discernible and all couples are considered acceptable on a compatibility basis.

D. RECOMMENDATIONS

Table 30 lists material combinations that have been used in bearing design or are considered as backup combinations. Sodium-silicate-bonded MoS_2 should be used to reduce friction where carbon-graphite is not one of the mating surfaces. Rubbing powdered MoS_2 into the machined carbon balls also reduces friction.

Carbon will oxidize above 800 to 900° F in O_2 partial pressures above 10^{-3} torr to form CO_2, and thus increase bearing clearances. This is a function of time, temperature, O_2 level, and bearing configuration. Figure 24 shows the surface loss vs pressure (air assumed). The attenuated curve was calculated for a monoball bearing as used in reactor control drums. The correlation of the 10,000-hour test data with the curve adds a measure of validity.

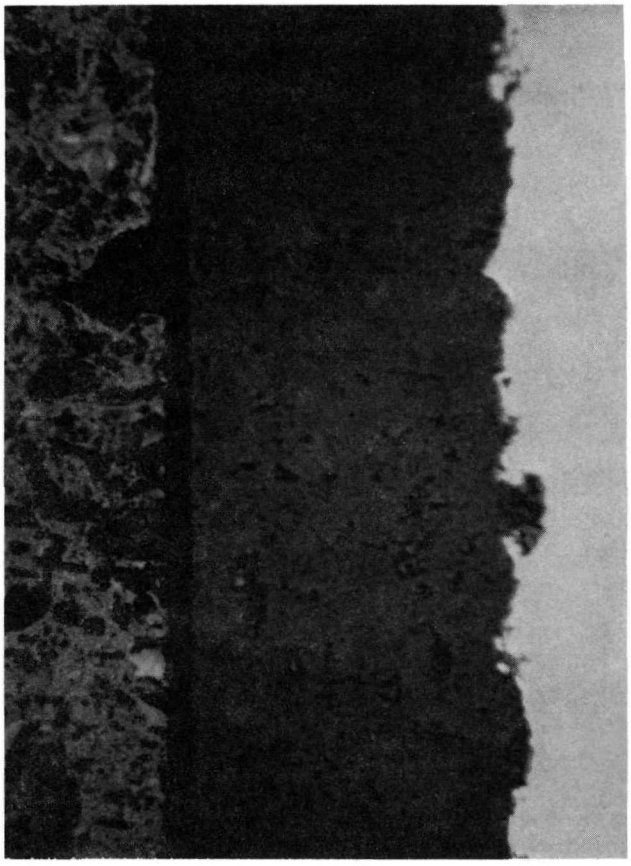

a. LA-2 (on Ta - 10 W) Against P5

8516-7-2 500X

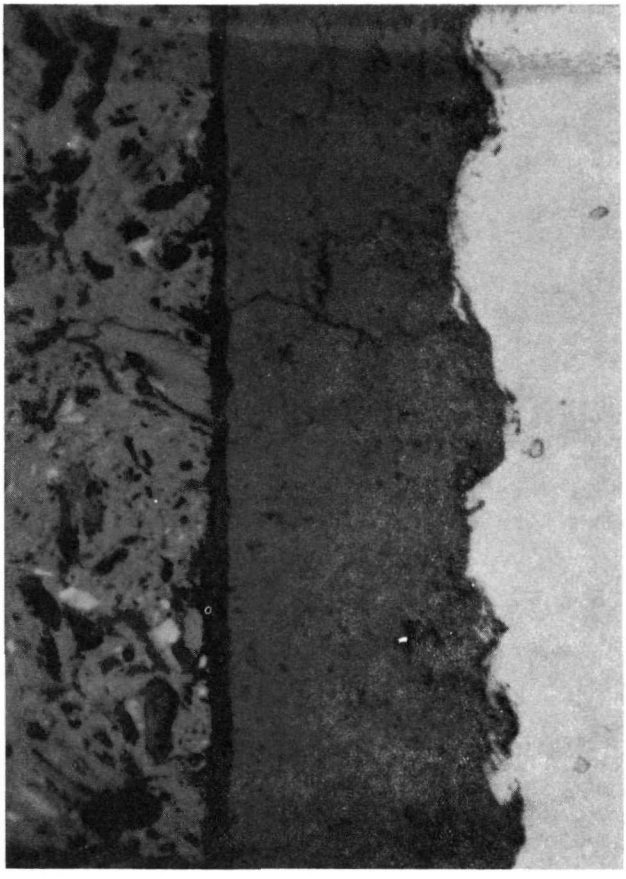

b. LA-2 (on Inconel-750) Against P5

8516-1-2 500X

Figure 21. Al_2O_3 vs P5 After 5000 hr

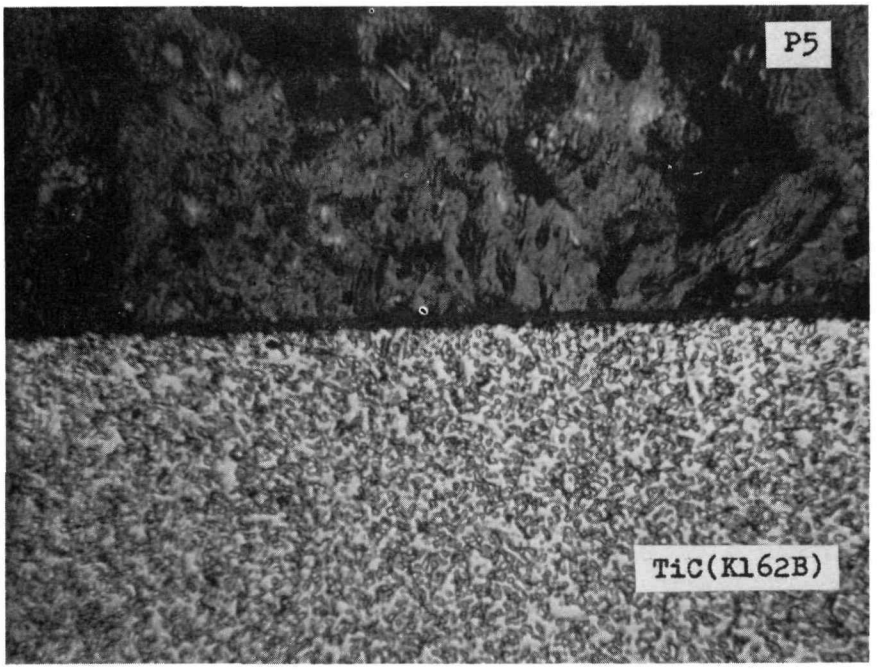

8428-3-1 500X

Figure 22. K-162B vs P5 After 2000 hr at 1600° F and 10^{-6} torr

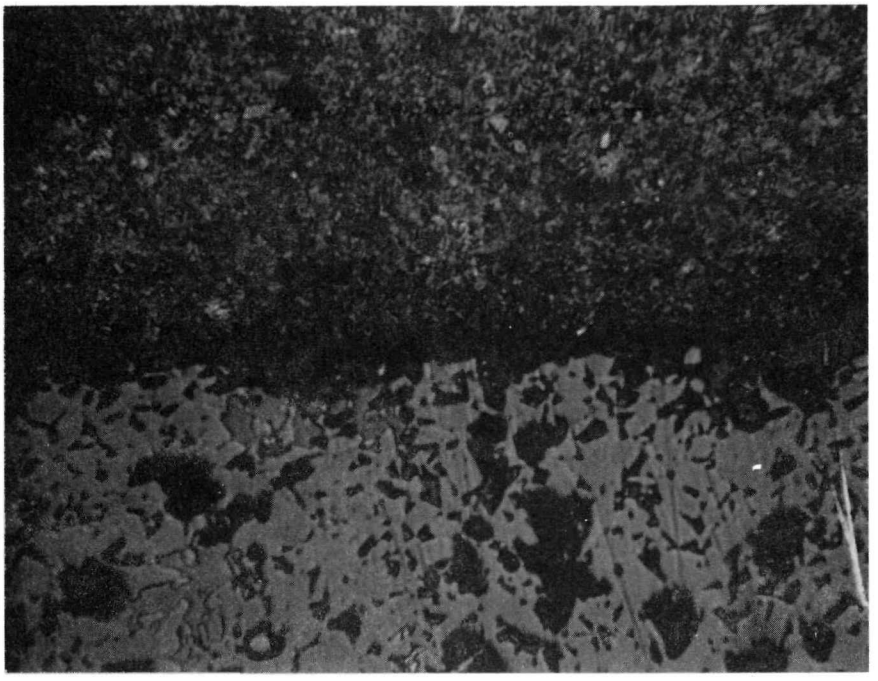

8428-4-1 500X

Figure 23. Solid Al_2O_3 vs AXF-5Q After 2000 hr at 1600° F and 10^{-6} torr

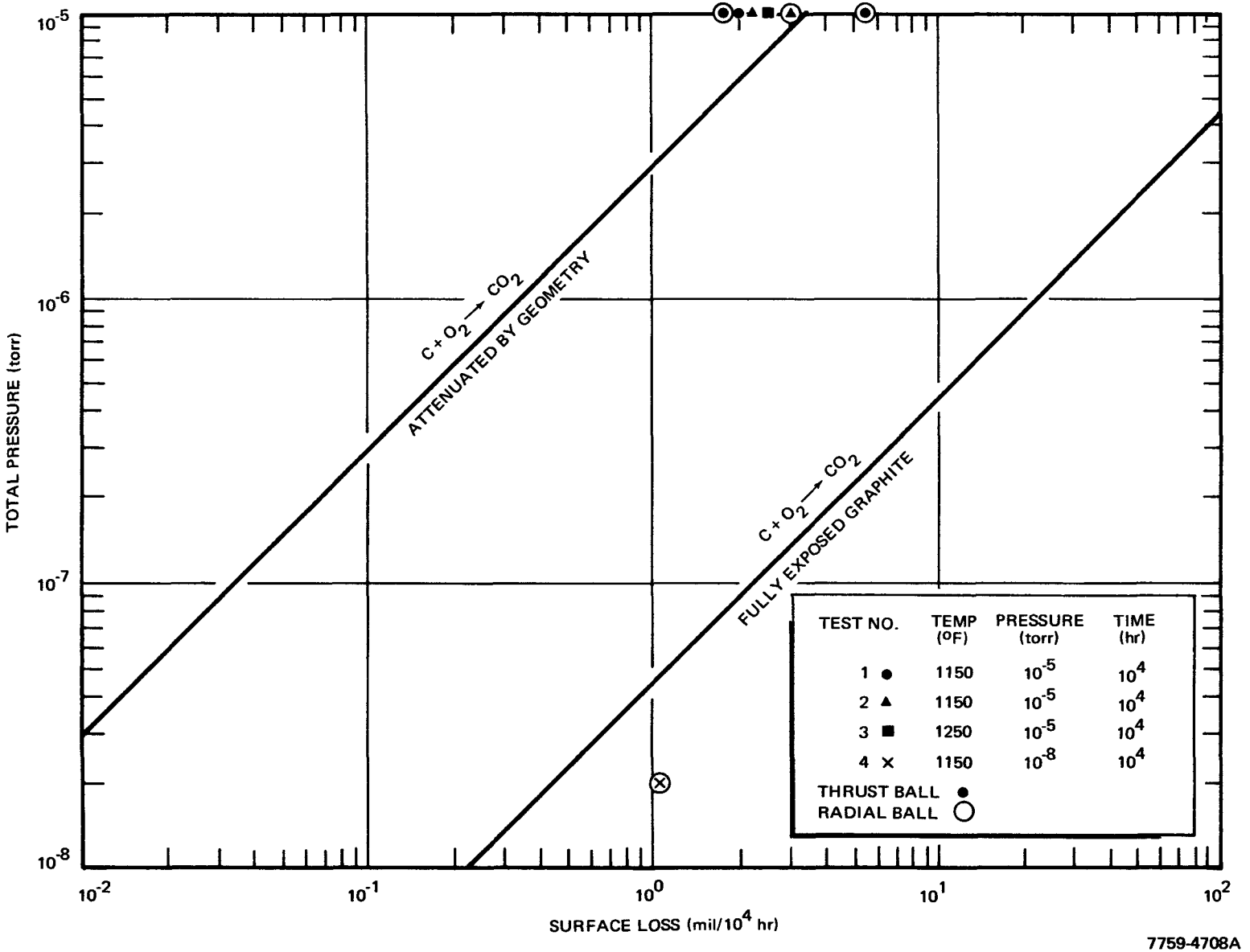

Figure 24. P5 Carbon-Graphite Oxidation Loss Rates at 1150° F

TABLE 30

MATERIAL COMBINATIONS FOR SPACE REACTOR BEARINGS

Materials Combinations and Substrates			Maximum Temperature (°F)	Maximum Friction	Tested for Compatibility
$Al_2O_3 + MoS_2$ Ti - 6 Al - 4V	vs	K162B	900	0.2	No
Al_2O_3 Inconel 750	vs	$Al_2O_3 + MoS_2$ Inconel 750	1250	0.3	Yes
Al_2O_3 Inconel 750	vs	P5N --	1000	0.3	Yes
Al_2O_3 Inconel 750	vs	P5 --	1250	0.3	Yes
TiC Inconel 750	vs	P5N --	1250	0.6	Yes
Al_2O_3 Ta - 10 W	vs	P5 or AXF-5Q	1600	0.2	Yes
K-162B	vs	P5	1600	0.4	Yes
MoS_2 - Ta Compact	vs	Al_2O_3 Ta - 10 W	1300	0.2	No
MoS_2 Rene 41	vs	MoS_2 Rene 41	900 1000	0.2	No

BLANK

III. SNAP REACTOR BEARING HISTORY

A. CONTROL DRUM BEARINGS

1. Basic Design Concept

The SNAP reactors were designed for long-term uninterrupted operation with no maintenance. Control drums must be capable of slow continuous rotation during reactor startup, rapid rotation during shutdown or scram, and periodic small angle steps during full temperature operation for power level corrections. The criteria for bearing operation under these conditions include low friction rotation without self-welding following hundreds of hours of dwell in the reactor high temperature-vacuum environment. The bearing must also be capable of surviving, without damage, the shock and vibration loads of launch into space.

The need for a simple, reliable bearing resulted in the selection of a journal-sleeve bearing as the primary rotation element.[16] One bearing at each end of the control drum carries the radial load, and one of the two carries the axial or thrust load. To prevent binding of the bearing from thermal distortion of the control drum, the journal sleeves have spherical OD's and are captured in a socket to provide self-alignment. The ball-to-socket combination also provides a backup rotational bearing in the event of journal-to-sleeve seizure. The basic bearing concept is illustrated in Figure 25.

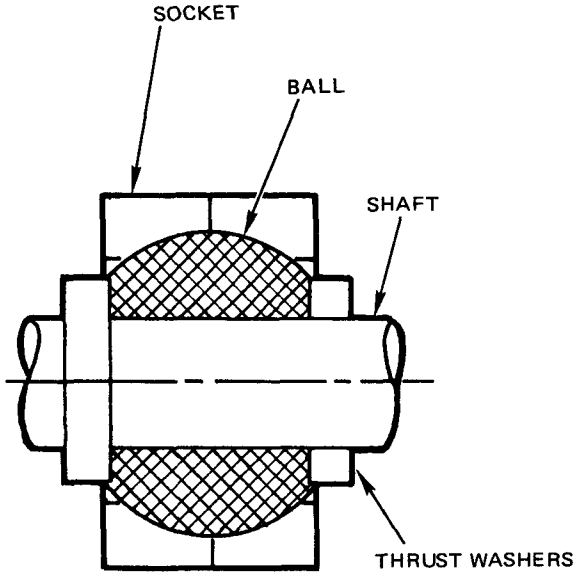

Figure 25. Basic Self-Aligning Monoball SNAP Bearing

2. Design Variations

The first bearing sets were fabricated while initial 1000° F sliding friction and wear studies were in progress. The bearing sets were tested under thermal-vacuum operational and vibration environmental conditions to evaluate relative performance. Each reactor system had slightly different requirements which required different bearing materials and configurations. The differences were primarily temperature, pressure, and load considerations, particularly during launch.

a. Solid Cermet Ball (SNAP 10A)

Bearing sets were fabricated using a solid Kennametal K-162B ball and Al_2O_3-coated titanium shaft and sockets.[17] No galling occurred during testing, but friction showed a steady increase with operation. Based on sliding friction tests, a MoS_2 dry-film lubricant was bonded to the shaft and socket Al_2O_3 surfaces. This resulted in a low friction couple under all test conditions and was selected as the SNAP 10A reference control drum bearing. A backup design of a composite ball, consisting of carbon-graphite bushings inserted into a K-162 ball, was also tested with satisfactory performance. The specific reference and backup designs are given in Table 31.

TABLE 31

COMPONENT MATERIALS COMBINATIONS

Component	Reference Bearing	Backup Bearing
Socket	Titanium with Al_2O_3 coating lubricated with $NaSiO_3$ bonded MoS_2	Same as Reference Socket
Shaft	Same as Reference Socket	Titanium with Al_2O_3 Coating
Ball	Solid K-162B	Same as Reference with P5-N Carbon-Graphite Bushings

b. Coated Metallic Ball (S8ER)

The S8ER ground test was designed to operate under an atmosphere of N_2 with 1% oxygen with bearing temperatures to 1100° F. Investigation of this

regime showed that dry films and carbon-graphites were unsatisfactory due to high oxidation. Two bearing material combinations were investigated. Both bearing sets utilized Hastelloy B shaft and socket sets with the Linde LA-2 Al_2O_3 coating. One bearing set used a solid chrome carbide (Carboloy 608) ball, and the second used a Hastelloy B ball coated with Linde LC-1A Cr_3C_2. Both exhibited satisfactory friction results ($0.22 > \mu > 0.35$) during ~3000-hr testing at 1100° F, but as indicated by test data post-test inspection, the solid carbide ball was becoming tighter in the socket and exhibiting greater wear than the plated ball. Consequently, the solid Cr_3C_2 ball was eliminated from further consideration because of the indicated loss of clearance with time.

c. Composite and Solid Carbon-Graphite Ball

Development of the SNAP 8 bearings was based on the SNAP 10A backup design, and studies were continued on the Al_2O_3 vs carbon-graphite and other combinations with and without dry-film lubricant.[18] To meet the increased temperature, the titanium shaft and socket material was replaced with Inconel-750. The cermet of the composite ball was also replaced with Inconel-750 for thermal expansion match with the socket. Dry-film lubrication was added to the ball OD to improve the ball-to-socket friction properties. Inconel-750 was selected because of its mechanical properties at 1100 to 1250° F and because its thermal expansion coefficient was close to that of the beryllium control drums.[19] This combination exhibited low friction and passed shock and vibration testing. A backup design using a solid P5-N carbon-graphite ball was also tested under thermal-vacuum and vibration conditions. While it exhibited somewhat greater friction, it was considered an adequate substitute.

During the latter stages of SNAP 8 bearing testing, a series of Al_2O_3 coating failures occurred when in contact with the carbon-graphite. Investigation of the problem described previously established that the presence of the LiF oxidation inhibitor in the P5 carbon-graphite had sufficient catalytic action to cause a phase change (from γ to α) in the Al_2O_3 under its already stressed condition and, consequently, fracture. Several alternate fixes were studied and the decision was made to replace the composite ball with a solid P5 carbon-graphite ball (identical to P5-N, but without the LiF). Additional testing showed that with MoS_2 burnished into the ball surfaces, satisfactory low friction operation was obtained.

The basic bearing design — sockets and shafts of Inconel-750 with Al_2O_3 coatings and a solid P5 carbon-graphite ball with MoS_2 burnished into the surfaces — was used on the space power facility test and the 5-kwe thermoelectric reactor systems with redesign being limited to bearing sizing for loads.

Development of the 4π shielded Advanced ZrH Reactor, however, resulted in requirements for a bearing environment temperature to 1500 or 1600° F and a control drum weight up to ~80 lb. Based on friction tests and a material investigation, a tantalum - 10 % tungsten alloy was incorporated as the Al_2O_3 substrate material.

3. Development and Verification Tests

Proof of design tests and system tests provided an abundance of data on the various bearing configurations and materials.

a. SNAP 10A Bearings

Reflector control drum bearings of similar configurations but various materials were subjected to shock and vibration tests, thermal cycle tests, and endurance tests in 10^{-6} and 10^{-9} torr vacuum at elevated temperatures.(16)

Eight of the bearing sets were subjected to thermal cycle tests with no observable deleterious effects. The thermal cycle tests consisted of placement of the unloaded assembled bearing sets in a vacuum chamber at 10^{-6} mm Hg and varying the temperature from 200 to 1000° F for the recorded number of cycles. The rate of temperature change was limited by existing vacuum facilities. Single temperature cycles were also induced during each of the twelve vacuum-elevated temperature-torque tests.

Vibration tests were conducted on eight bearing sets to SNAP 10A design levels. Detailed results are discussed later in this report.

Twelve bearing sets of various material combinations were subjected to simulated loading at elevated temperatures in vacuum. Duration of tests varied from 100 to 2160 hours. Operation temperatures ranged from 585 to 950° F. Operation vacuums ranged from 10^{-6} to 10^{-9} mm Hg. Torque values of the loaded drum bearing sets were less than the maximum allowable 2.5 in.-lb torque requirement. Description of bearing materials, test conditions, and results are

outlined in Table 32. The vacuum-temperature-torque tests show higher friction at low temperatures. Similar friction variations with temperature were exhibited with sliding block tests.

The reference developmental test configuration of the bearings is shown in Figure 26.

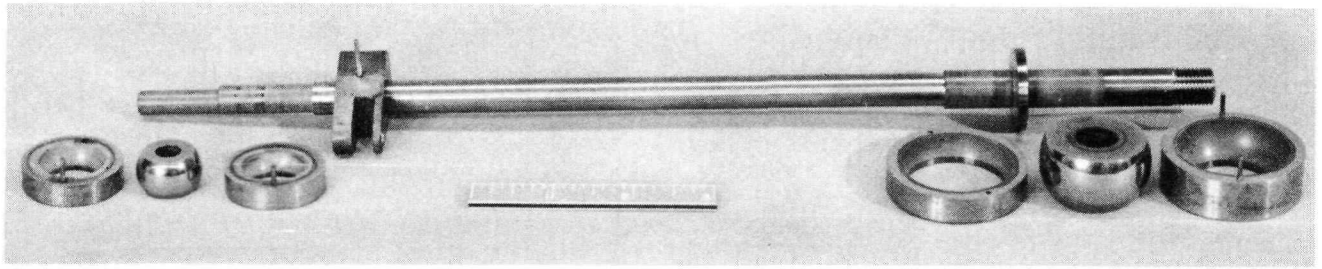

Figure 26. SNAP 10A Test Bearing Set

b. S8DRM Bearings

The first SNAP 8 flight configuration bearing assemblies fabricated were designed for the S8DRM, a mockup reactor for nonnuclear testing. The bearings were subjected to simulated reactor tests, to study design compatibility during thermal cycling and intermittent operation at temperature. Additional sets were subjected to shock and vibration loads which would be encountered on launch of a space reactor.

Three tests were initiated to study alternate ball concepts, using: (1) the composite Inconel ball with alumina-coated OD and carbon-graphite bushings, (2) the same ball, with a sodium-silicate-bonded MoS_2 dry-film lubricant on the ball OD to decrease friction and to act as a vibration cushion between the ball and socket alumina surfaces, and (3) a solid carbon-graphite ball, in place of the composite Inconel ball.[15] Figure 27 illustrates the composite ball concept. The tests were run under identical test conditions of 1150° F and 10^{-5} torr pressure, and were scheduled to run for 2,000 hours, minimum. Test parameter and torque readings are summarized in Table 33. Bearing friction-torque was measured through actuation sequences consisting of driving the bearing shaft 70° CCW and 35° CW at a rate of ~5°/sec. Using a force ring transducer and a mechanical linkage, the resistance to rotation of the bearings was measured and recorded (see test fixture in Figure 28).

TABLE 32

SNAP 10A DRUM BEARING TEST DETAIL RESULTS

Bearing Test No.	Bearing Set No.	Materials	Thermal Cycles (200° to 1000°F)	Shock and Vibration to Design Specifications	High Vacuum, Elevated Temperature Drum Torque Tests								
					Test Duration (hr)	Actuation Cycles	Torque (in.-lb)			Temperature (°F)		Vacuum (mm Hg)	Remarks
							Initial	Maximum	Final	Radial Bearing	Thrust Bearing		
1	1	Balls-K-162B Shafts-T_1 + Al_2O_3 Sockets-T_1 + Al_2O_3	5	Yes	330	8500	1.0	1.1	1.1	950	780	1×10^{-6}	Breakdown of Al_2O_3 coating on socket edges after vibration.
2	3	Balls-K-162B + CDJ-83 Bushings Shafts-T_1 + Al_2O_3 Sockets-T_1 + Al_2O_3	5	None	270	1900	0.1	0.3	0.25	960	780	7×10^{-7}	
3	2	Balls-K-162B + CDJ-83 Bushings Shafts-T_1 + Al_2O_3 Sockets-T_1 + Al_2O_3	5	Yes	270	2600	0.05	0.05	0.05	900	730	1×10^{-6}	
4	4	Balls-K-162B + CDJ-83 Bushings Shafts-T_1 + Al_2O_3 Sockets-T_1 + Al_2O_3	5	Yes	300	2650	0.2	0.5	0.5	910	730	1×10^{-6}	A number of operation problems occurred during this test. An additional run was made for 70 hours and 350 more actuation cycles. No change resulted.
5	5	Balls-K-162B + CDJ-83 Bushings Shafts-T_1 + Al_2O_3 Sockets-T_1 + Al_2O_3	5	Yes	270	2600	0.1	0.5	0.5	900	720	7×10^{-7}	
6	6	Balls-K-162B Shafts-T_1 + Al_2O_3 Sockets-T_1 + Al_2O_3	10	Yes	100	680	1.0	2.5	2.5	890	730	1×10^{-6}	Thrust washer became tight. This was an assembly problem, not a bearing problem. TiC + Ni deposits on thrust face.
6B	6	Same set as above			290	2500	0.5	1.0	0.9	890	730	1×10^{-6}	Ball thrust face reversed.
7	13	Balls-K-162B Shafts-T_1 + Al_2O_3 Sockets-T_1 + Al_2O_3	None	None	190	120	0.3	0.70	0.70	920	750	8×10^{-7}	
8	13A	Same set as above plus X-15 on all Al_2O_3 surfaces	None	None	1487	570	0.2	0.65	0.5	930	750	8×10^{-7}	
9	14	Balls-K-162B + CDJ-83 Bushings Shafts-T_1 + Al_2O_3 Sockets-T_1 + Al_2O_3 + X-15	None	None	2340	770	0.05	0.35	0.35	710	585	2×10^{-7}	
10	15	Balls-K-162B + P5N Bushings Shafts-T_1 + Al_2O_3 Sockets-T_1 + Al_2O_3 + X-15	None	Yes	2160			0.1		710	585	2×10^{-7}	Balls became tight in sockets. SNAP 10A backup design
11	7	Balls-K-162B Shafts-T_1 + Al_2O_3 Sockets-T_1 + Al_2O_3	5	Yes									Tested in SNAP 10A reflector shock and vibration at one end and two times design specification
12	10	Balls-T_1 + Cr_3C_2 with P5N Bushings Shafts-T_1 + Cr_3C_2 Sockets-T_1 + Cr_3C_2	10	Yes			1.5	1.7	1.5	600	600		
13	12	Balls-K-162B Shafts-T_1 + Al_2O_3 + X-15 Sockets-T_1 + Al_2O_3 + X-15	None	None	2784	230	2.2	2.2	1.9	During 70° to 600°		2×10^{-9} ion pump system	Included 90-day dwell

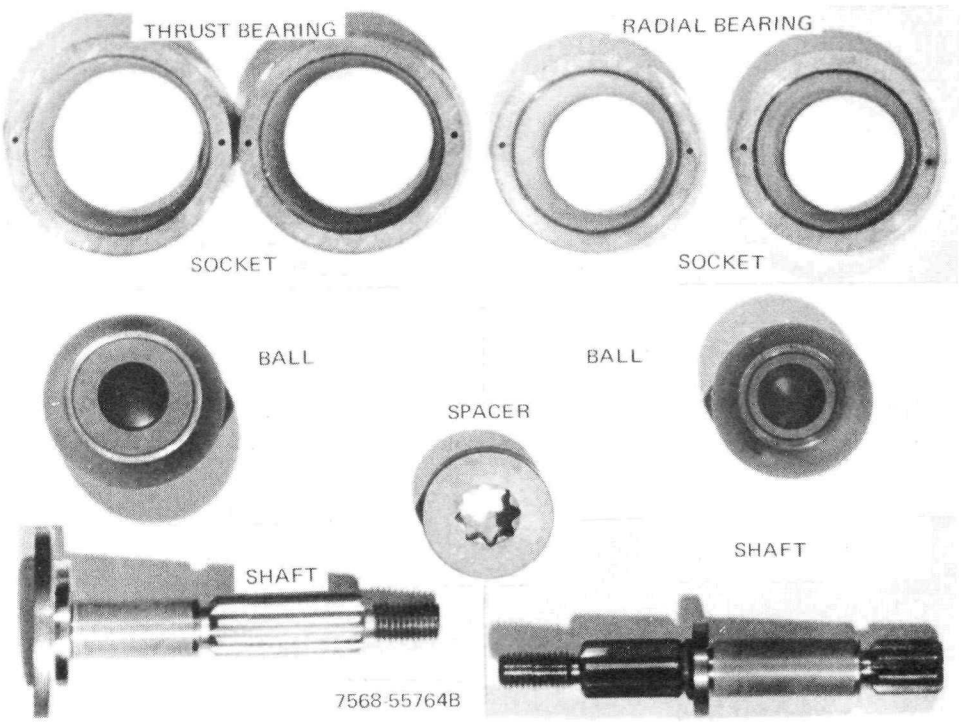

Figure 27. SNAP 8 Composite Bearing

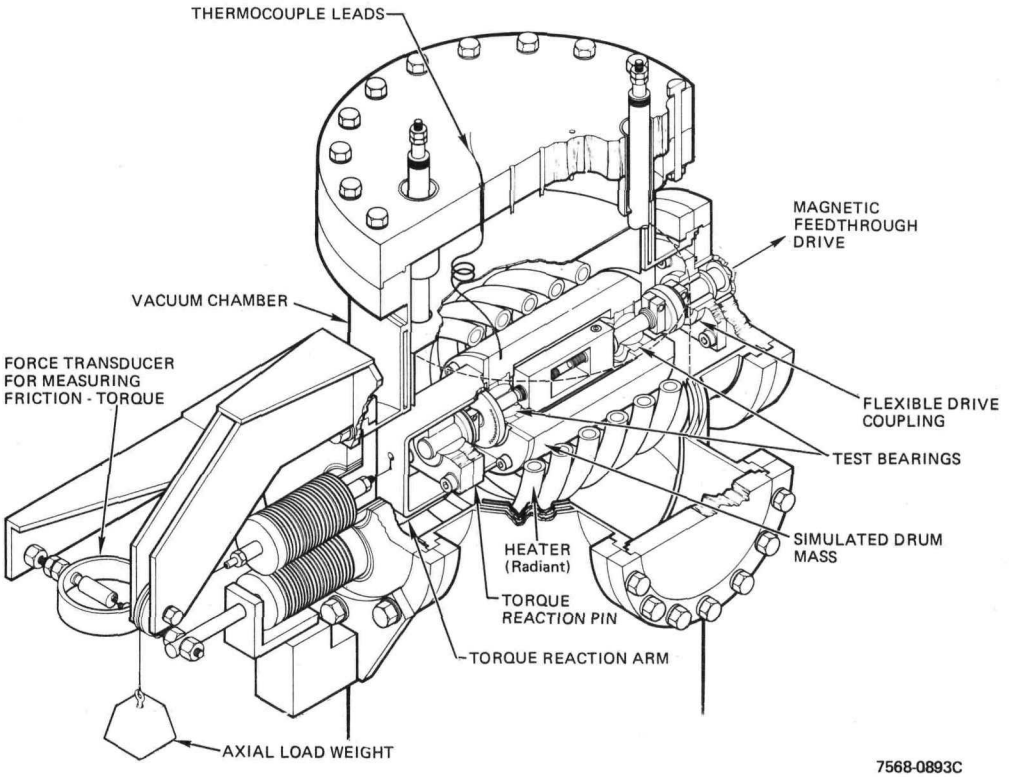

Figure 28. Bearing Development Test Fixture

TABLE 33

SNAP 8 BEARING TEST SUMMARY

Material Combination (All sockets are alumina coated. Composite ball is alumina coated with P5N bushings in bore.)		Test No.	Pressure (torr)	Temperature (°F)	Time at Temperature (hr)	Equivalent Life Times	Static Dwell (hr)	Thermal Cycles	Maximum Friction Torque (in.-lb)	
Ball Type	Shaft Coating								Ambient	At Temperature
S8DRM Development Testing										
Composite	Alumina	1	10^{-5}	1150	5,050	370				1.5
Composite + MoS_2	Alumina	2	10^{-5}	1150	1,060	225				2.0
Solid P5N	Alumina	3	10^{-5}	1150	2,230	291				1.6
Composite + MoS_2	Alumina	4	10^{-9}	1150	9,600	800		7	3.6	1.8
Composite + MoS_2	Alumina	5	10^{-5}	1150	10,094	132		13	3.7	2.3
S8DR Original Verification Tests										
Composite + MoS_2	Alumina	1	10^{-5}	1150	2,928	3,480	1,000	210	3.9	3.2
Composite + MoS_2	Alumina	2	10^{-5}	1150	3,830	2,218	1,000	218	5.8	5.1
Composite + MoS_2	Alumina	3	10^{-5}	1150	1,592	1,068	1,000	210	3.7	1.6
Composite + MoS_2	Alumina	4	10^{-5}	1150	10,000	1,454	1,700	32	5.0	2.8
Composite + MoS_2	Alumina	5	10^{-5}	1150/1250	5,000/2,500	562	1,000	29	8.0	3.4
Composite + MoS_2	Alumina	6	10^{-5}	1150	84	260		17	3.6	0.9
Prototype Shaft Tests (After Alumina vs P5N Failure)										
Composite + MoS_2	Titanium Carbide	1	10^{-5}	1250	2,180				4.1	2.7
Composite + MoS_2	Titanium Carbide	2	10^{-5}	1250	1,260				2.8	5.7
Composite + MoS_2	Chromium Carbide	1	10^{-5}	1250	1,465				3.6	3.7
Composite + MoS_2	Chromium Carbide	2	10^{-5}	1250	1,415				2.6	4.8
Composite + MoS_2	Tungsten Carbide	1	10^{-5}	1250	730				3.0	7.0
Composite + MoS_2	Tungsten Carbide	2	10^{-5}	1250	1,220				2.6	3.7
Composite + MoS_2	Alumina (Norton)	2	10^{-5}	1250	695				4.0	2.5
S8DR Design Verification Tests – Final										
Composite + MoS_2	Titanium Carbide	1	10^{-8}	1150	6,091	97		33	6.5	5.5
Solid P5 Carbon	Alumina	1	10^{-5}	1150	12,045	280	1,000	86	6.8	3.8
Solid P5 Carbon	Alumina	2	10^{-5}	1150	12,041	282	1,000	86	5.2	3.7
Solid P5 Carbon	Alumina	3	10^{-5}	1250	12,140	310	1,000	85	6.5	3.8
Solid P5 Carbon	Alumina	4	10^{-8}	1150	12,086	290	1,000	86	4.3	4.6

The bearing test with the MoS_2 dry-film-coated balls completed 1060 hours, and was terminated due to a vacuum system failure. The test with the solid carbon-graphite balls ran 2230 hours, and the test with the composite ball without the MoS_2 lubricant ran 5050 hours, prior to termination for examination of the bearing sets. No signs of any damage to bearing surfaces were visible, and carbon-graphite transfer films on the alumina-coated shaft surfaces indicated full contact and well distributed loading.

Two additional tests were initiated with the MoS_2-coated composite balls. The tests were conducted at 1150° F, one at 10^{-5} torr and one at 10^{-8} torr.

The low-vacuum test (10^{-5} torr) completed 10,095 hours at 1150° F, with a maximum starting friction-torque of 2.3 in.-lb. The test was interrupted several times due to vacuum system malfunctions, and this was reflected in periodic step changes in friction-torque. One of these malfunctions, after ~5500 hours at test, exposed the bearings for 25 hours to 950° F and ambient pressure. Heavy oxidation of the carbon-graphite bushings and the MoS_2 dry film observed at the end of the test are attributed to this oxidation. A small chip also occurred in the alumina-coated lip of the thrust ball. Close examination of the thrust bearing shaft revealed that all of the alumina coating had spalled off, locking the ball to the shaft. The ball-to-socket bearing surfaces, however, continued to provide satisfactory bearing action as indicated by lack of any step increase in the measured bearing friction.

The high-vacuum (10^{-8} torr) test completed 12,600 hours, with over 10,000 hours at 1150° F. An increase in friction after 5,000 hours occurred as a consequence of increasing the control drum weight from 26 to 31 lb. The test proceeded without incident, and post-test examination showed all bearing surfaces to be in excellent condition. The shaft journals had an even carbon-graphite transfer film indicative of low friction and wear. The MoS_2 coatings were well burnished, showing unrestricted oscillation of the balls within the bearing sockets.

c. S8DR Bearings

During development testing of the S8DRM bearings, the control drum design was modified, and resulted in a weight increase from 26 to 31 lb. At the same time, the reactor launch shock and vibration loads were substantially increased

to the present levels listed in Table 1. It was necessary to redesign the radial bearing assembly to carry the increased torsional loads on the shaft. The resulting S8DR bearing configuration is shown in Figure 29. The bearing shaft was increased in diameter, and the ball and socket enlarged to the size of the thrust bearing assembly. The S8DRM design used separate bearing shafts and drum mounting brackets, which required mating splines. The S8DR design was changed to an integral shaft and bracket assembly, and a simplified shaft was used for development testing. While changing the configuration, the alumina vs carbon-graphite and MoS_2-coated alumina vs alumina bearing couples were retained. A series of tests were initiated, to study performance under simulated reactor conditions.[5] Table 33 also summarizes these tests.

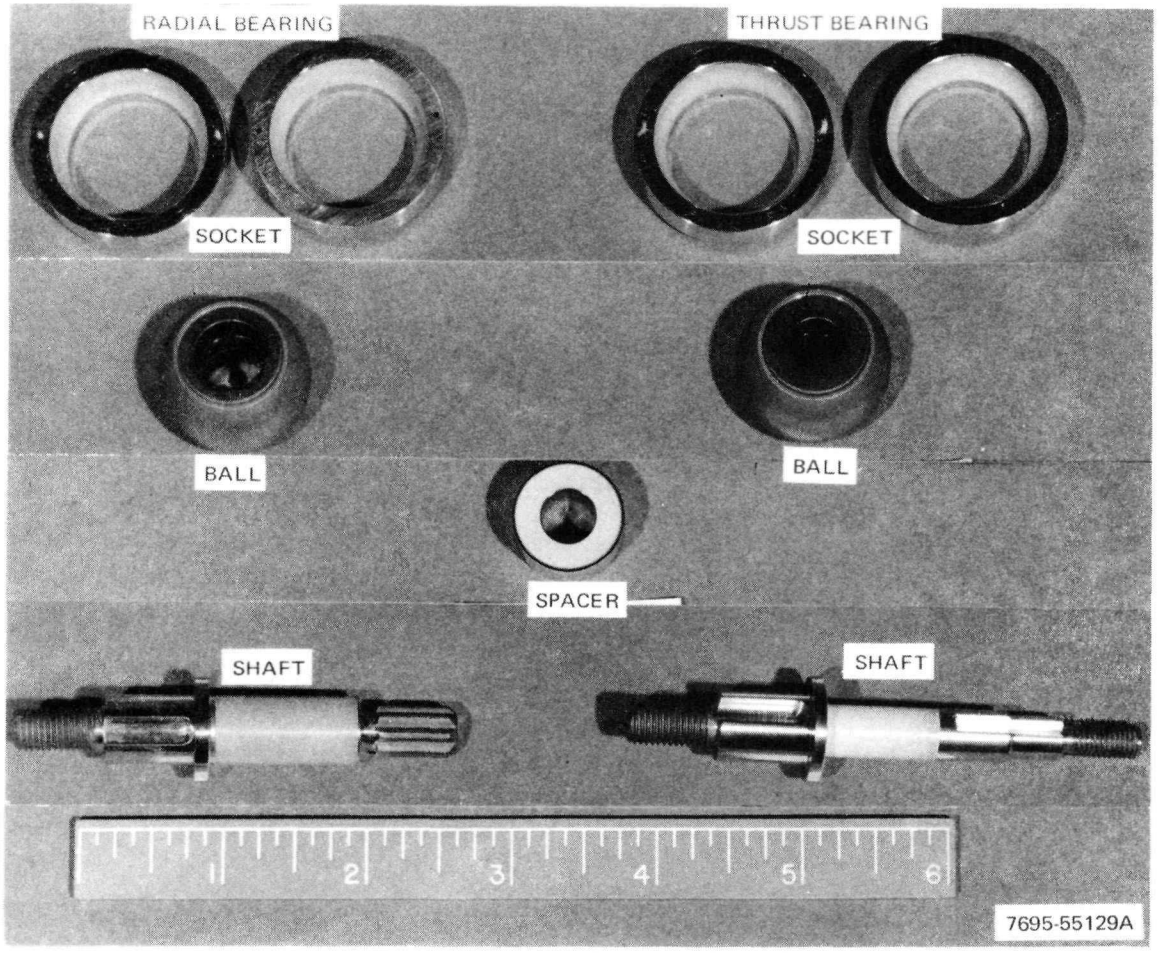

Figure 29. S8DR Bearing (Original Design)

Two test plans were formulated, each stressing one phase of reactor operation. Thermal cycle tests were designed to study the effects of numerous thermal transients produced by reactor startup and shutdown cycles. Operational life tests were designed to study the effects of intermittent bearing rotation with long-term dwell periods at temperature. Three thermal cycle and two operational tests were initiated. All five tests were conducted at 10^{-5} torr in the liquid nitrogen cold-trapped oil diffusion pumped systems. All tests were run at 1150° F, with the exception of the second operational test which accumulated time both at 1150 and 1250° F. The specified torque limit was 3.5 in.-lb at 1150° F. Two operational life tests were conducted, one with MoS_2 dry-film lubricant on the alumina surface of the ball OD's, and one without the dry film. This permitted a study of friction for nominal conditions and for worst-case conditions where all dry film had been lost.

(1) Test No. 1

Testing of Bearing Set No. 1 included 200 thermal cycles, a 1000-hour dwell, and 600 hours of the operational test. Maximum friction-torque was 3.4 in.-lb, occurring at the conclusion of the 1000-hour dwell. Maximum torque during the thermal cycle phase was 1.4 in.-lb, and during the 600-hour operational testing was 1.9 in.-lb. Following 600 hours of operational testing, a vacuum system malfunction occurred which resulted in shutdown of the test. The bearing set was removed for inspection, and the radial load shaft was found to be seized in the carbon-graphite insert bushing. Figure 30 illustrates the shaft, with the journal alumina broken off. Examination of the thrust shaft and all other coated surfaces was made, all were in excellent condition with no indication of cracking or chipping. Due to the redundant bearing (ball in socket) friction had remained satisfactory, with no indication of seizure during testing.

(2) Test No. 2

Testing of Bearing Set No. 2 was terminated after 200 thermal cycles, a 1000-hour dwell, and 2500 hours of operational testing to inspect the bearings for possible alumina coating failures. Maximum friction-torque during testing was 5.1 in.-lb compared to the 3.5 in.-lb design limit, and occurred following the 1000-hour dwell. Maximum torque during thermal cycling was 1.3 in.-lb and 2.0 in.-lb during the operational test phase. Inspection of the bearings showed no signs of cracking or other damage to the alumina coatings.

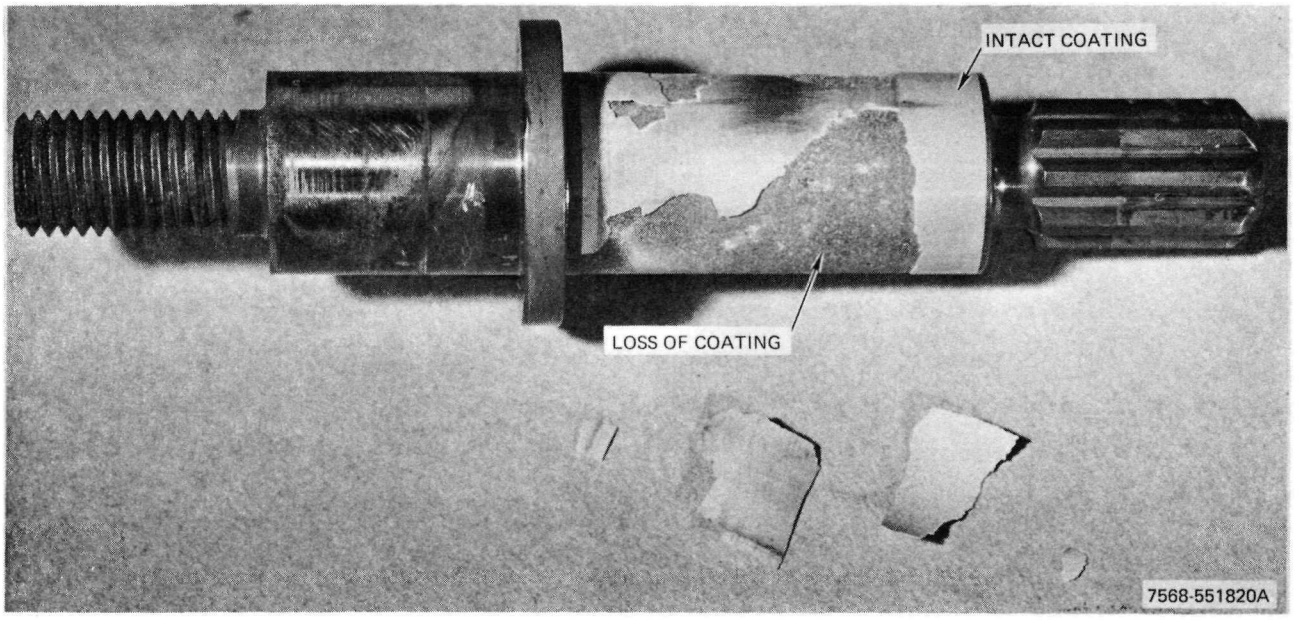

Figure 30. S8DR Shaft with Spalled Alumina

(3) Test No. 3

Bearing Set No. 3 was also terminated to inspect the bearings following 200 thermal cycles and a 1000-hour dwell. Maximum friction-torque was 3.8 in.-lb following the dwell, again greater than the specification limit, and was 1.8 in.-lb during the 200 thermal cycles. Inspection of the bearing alumina surfaces revealed no signs of cracking or impending failure.

(4) Test No. 4

Testing of the MoS_2 dry-film-coated bearing set included 10,116 hours at 1150° F. Maximum friction-torque during the test at 1150° F was 2.8 in.-lb, occurring after ~7500 hours. Two short duration and one 1000-hour dwell period were included in the first 4000 hours of testing. Friction throughout the test was somewhat erratic, but averaged around 2.5 in.-lb over the last 6000 hours. Following the test, the bearings were closely examined, and no sign of alumina coating damage or failure was visible.

(5) Test No. 5

The bearing test without MoS_2 dry film on the alumina surface of the balls resulted in a primary bearing couple of alumina vs carbon-graphite (ball-to-shaft)

and alumina vs alumina (ball-to-socket). The test was conducted in two phases, the first 5000 hours at 1150° F and the remainder at 1250° F. Friction-torque during the 1150° F test remained at or below 2.0 in.-lb and examination of the bearings showed little wear and no signs of alumina damage. During the 1250° F test phase, friction-torque reached 3.4 in. -lb through the first 2500 hours and inspection of the bearings revealed both shafts were seized in their respective balls. Again, due to rotation between the ball and socket couple, bearing operation had continued without significant increase in friction. Both the thrust and radial shafts had extensive loss of alumina, with all material in the bearing contact zone lost.

Failure of these shafts resulted in a total of three separate cases of alumina coating loss. Only one case, the S8DRM test, could be attributed to massive oxidation. All further S8DR testing was suspended, and effort was directed toward isolating the mode of failure of the alumina.

d. Shaft Materials Evaluations

Based on information gathered from the alumina failure analysis (Section II-C-1 above) it was concluded that the best course of action was to replace the alumina-coated, Inconel-750 ball with a solid, unimpregnated, P5 carbon-graphite ball. It had been determined that on existing balls, the process of replacing the P5-N carbon-graphite bushings with P5 would overstress and probably fail the OD alumina coating. Replacement with a solid P5 graphite ball would eliminate the problem and would result in a P5 carbon-graphite vs alumina combination, which had already proved to be a compatible, low-friction combination. Also, the alumina-coated shafts, thrust sleeves, and sockets could be retained.

To provide backup to the revised design, a series of materials was evaluated (as previously described), and tests were run to select an alternate bearing couple. The following coatings were chosen for evaluation on Inconel-750 bearing shafts for use with the existing composite ball (Al_2O_3-coated Inconel-750 with P5-N carbon-graphite bushings) and Al_2O_3-coated socket:

1) Cr_3C_2 flame-sprayed coating (LC-1)
2) WC flame-sprayed coating (LW-5)
3) TiC plasma-sprayed coating

4) Al_2O_3 plasma-sprayed coating (Noroc)

5) Haynes Alloy 90 hard facing.

Initially, two sets of Cr_3O_2 and WC, and one set of TiC and Al_2O_3 bearings were set up. Material compatibility tests showed the "Noroc" Al_2O_3 to fail in contact with the LiF-impregnated carbon-graphite in the same manner as the LA-2 type Al_2O_3. Due to the promising results of the TiC-coated specimens, the "Noroc" Al_2O_3 prototype shaft test was replaced with a second TiC-coated shaft test. The bearing sets, tested in the same fixtures as the previous tests, were subjected to operations at 1250° F with periodic thermal cycling. Friction-torque was measured throughout the tests, and results are summarized in Table 33.

Excluding the Al_2O_3-coated shaft test, which was eliminated for incompatibility, the Cr_3C_2-coated shaft tests resulted in the most consistently low friction-torque, with the TiC-and WC-coated bearings second and third. Following testing, the bearings were disassembled, and inspected for wear and possible failure or damage. Inspection of the bearings revealed fully developed carbon-graphite transfer film on all the shafts, and no signs of chipping, cracking, or other signs of shaft damage.

The TiC-coated Inconel-750 was selected as the backup shaft, due primarily to the results of the material compatibility tests. While its higher friction is not desirable, it can be compensated. The potential material incompatibility of Cr_3C_2-WC is totally unacceptable. The possibility of self-welding, due to the thin chrome layer at the carbon-graphite and coating interface, could jeopardize operation of the entire reactor system.

e. S8DR Design Verification Tests

The material evaluation tests confirmed the alumina and P5 carbon-graphite to be both a low-friction couple and metallurgically compatible under S8DR conditions. The tests also established the TiC and P5-N carbon-graphite to be the best overall alternate bearing couple. These couples were therefore chosen as the reference and backup material couples for the redesign of the S8DR bearing. Both bearing sets are of the same configuration, except for the shaft coating and the ball designs. The reference bearing uses Al_2O_3 coating on the shaft and the

solid P5 carbon-graphite ball, while the backup bearing uses TiC shaft coating while retaining the original S8DR composite ball (Inconel ball with alumina-coated OD and P5-N carbon-graphite bushings).

(1) Test Description

Except for the vacuum and nominal temperature, all tests were conducted as follows:

1) 30 thermal cycles between 450 and 1150° F (Test No. 3 at 1250° F, where plan shows 1150° F)
2) 500 hours at 1150° F
3) 500 hours at 1250° F
4) Continue at 1150° F to 5000 hours
5) 1000 hours at 1150° F, with 1 thermal cycle each 100 hours
6) 1000-hour dwell at 1150° F
7) Continue at 1150° F to 12,000 hours, with 1 thermal cycle each 100 hours.

(2) Friction Data Analysis

Starting and running friction torques of the bearing sets were measured, and starting torque (as a function of test duration) is shown for a typical test (No. 1) in Figure 31. A general consistency exists for the three 10^{-5} torr tests of the reference design. The torque level shows a gradual increase during the first 2000 to 4000 hours, after which a short period of stability is reached. A small decrease in friction then occurs, prior to the 1000-hour dwell. Following the dwell, the friction tends to again increase slightly. It is hypothesized that lubrication is initially enhanced by outgassing of the carbon-graphite; and, as the outgassing subsides, the friction increases until a carbon-graphite transfer-film is built up to a level where it, in turn, enhances the lubrication to decrease the friction. The same pattern, but with an accelerated increase in friction, occurred with the 10^{-8} torr bearing test. This could be accounted for by the lower system pressure, and hence, the greater outgassing rate.

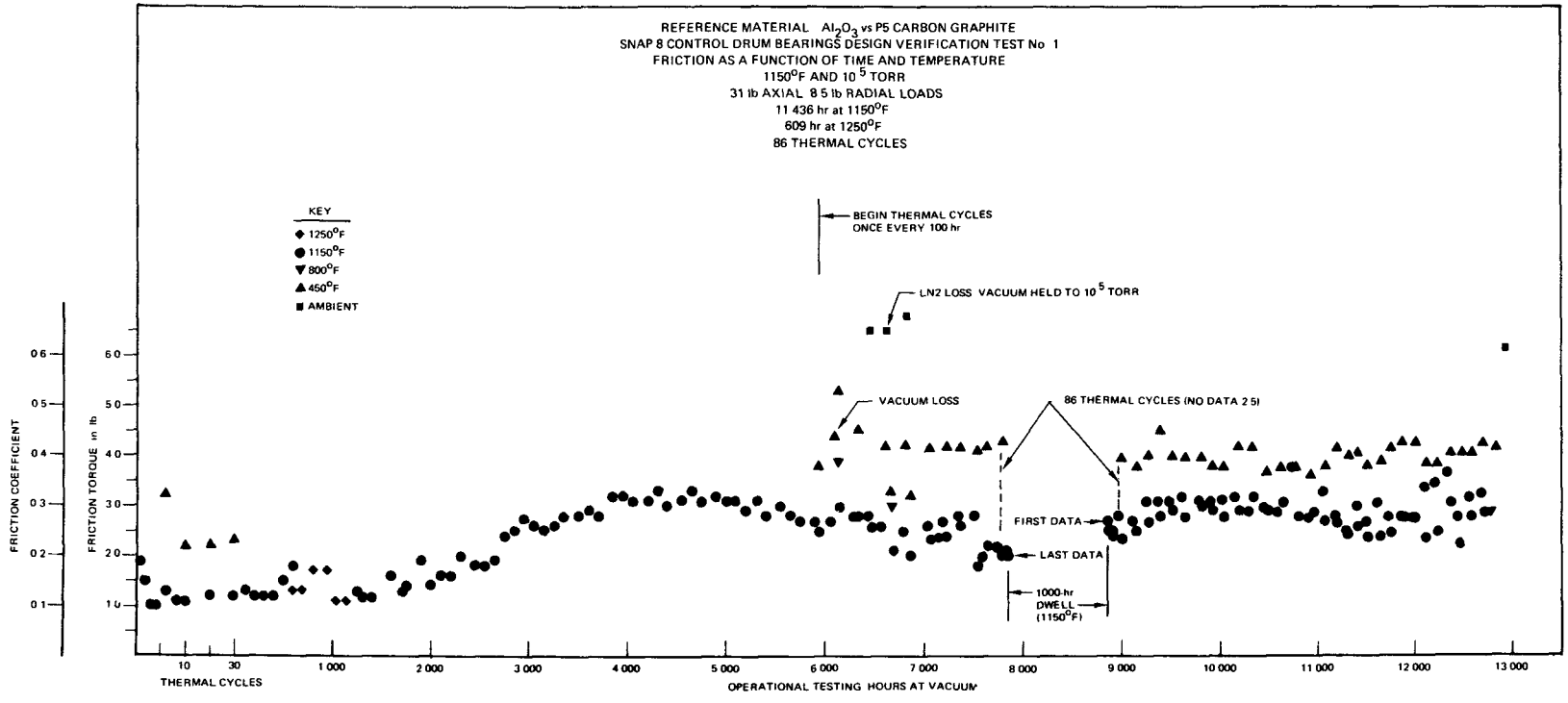

7759-25133

Figure 31. S8DR Design Verification Test Friction History, Test 1

Approximately 7000 hours into the test, vacuum was partially lost on Test No. 4 (10^{-8} torr), with the pressure rising to 10^{-4} torr at 400° F. As a precaution, bearings were disassembled, and inspected for possible oxidation damage. No damage was found, the bearings were reassembled, and the test resumed, with satisfactory performance for the balance of the test.

The friction torque profile of the backup bearing set shows initial low friction increasing to 4.0 in.-lb or above and stabilizing at that point. The test was terminated after 6000 hours, due to failure of the vacuum system. Inspection of bearings revealed cracks in the radial journal shaft TiC coating.

A summary of all test parameters and friction torque data for the five tests are given in Table 33.

(3) Post-Test Analysis

Following completion of the design verification tests, each bearing set was disassembled, and inspected for wear and condition of the bearing components.

(a) Reference Bearings

The post-test condition of a typical bearing set, Test No. 1, tested at 10^{-5} torr and 1150° F, is shown in Figure 32. The alumina-coated bearing shaft shows the light, but well developed carbon-graphite transfer film associated with even ball-to-shaft contact. All load-supporting alumina-coated surfaces were in excellent condition, with no signs of cracking or failure. Detailed inspection of the carbon-graphite balls showed the OD surfaces to be lightly pitted from oxidation during the 12,000-hour testing. Weight loss of each carbon-graphite ball was measured, and compared to calculated weight loss curves for fully exposed and bearing geometry enclosed carbon-graphite, assuming all weight loss during test was due to oxidation. The close agreement between data points for the 10^{-5} torr test and the calculated attenuated condition is shown on Figure 24. Examination of the carbon-graphite balls did not show any signs of chipping or damage due to testing.

Surfaces of the post-test carbon-graphite balls from the 10^{-8} torr test were shiny and smooth in contrast to the pitted surfaces of the balls from the 10^{-5} torr tests, and indicated considerably less oxidation for the lower pressure environment. Shiny rings around the balls indicated areas of contact with the

Figure 32. Post-Test Condition of S8DR Design Verification Bearing, Test 1 (Reference Bearing)

bearing sockets. The shaft alumina coating had a well developed carbon-graphite transfer film, and was typical of all the alumina-coated surfaces. Examination of both shafts, the thrust sleeve, and the sockets showed all the alumina surfaces to be in excellent condition, with no signs of cracking or chipping.

(b) Backup Bearings

Figure 33 shows the post-test condition of the backup bearing set (Test No. 5). The thrust ball shows the contact zone between the ball and the thrust sleeve, and the burnished areas of the ball OD show contact with the socket. Both appear in excellent condition. The thrust shaft and sleeve also appeared in good condition, with well-defined transfer films; however, close examination revealed three cracks in the TiC coating of the shaft. Essentially no clearance with the ball existed at post-test disassembly, and it is apparent the coating is partially loose from the substrate. This condition of the shaft coating and the

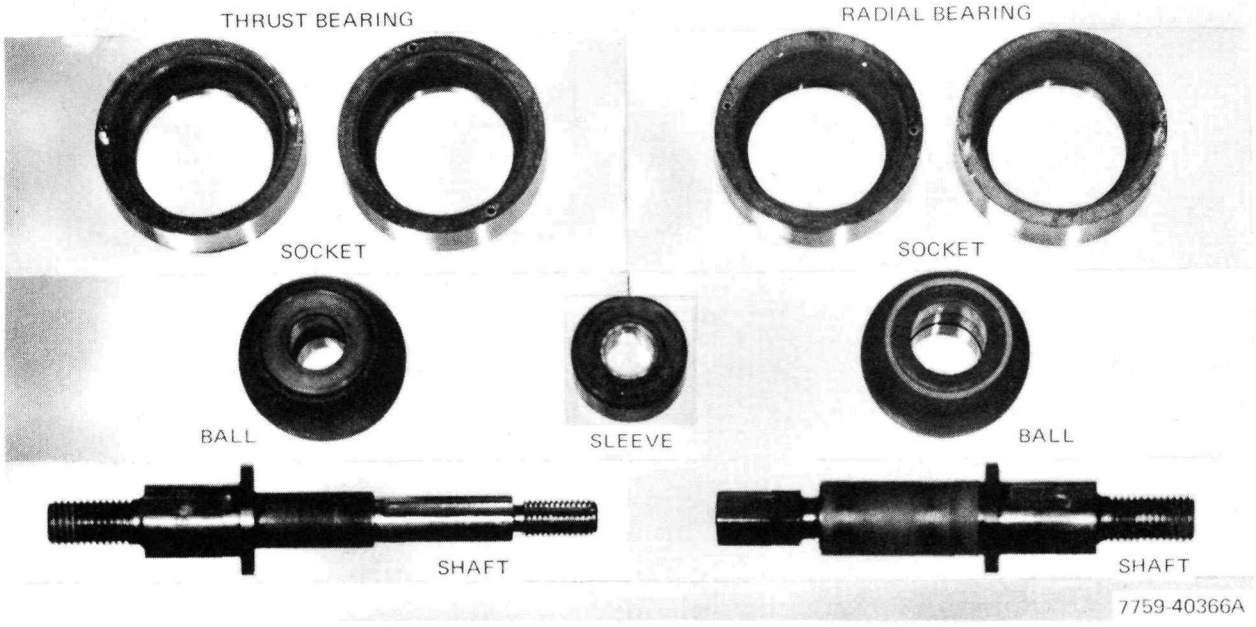

Figure 33. Post-Test Condition of S8DR Design Verification Bearing, Test 5 (Backup Bearing)

possible resulting loss of bearing motion did not cause failure of the bearing set, because of the redundant ball-to-socket bearing. Cause of the coating failure was not identified, nor further study conducted, due to the excellent performance of the reference alumina against the P5 carbon-graphite bearing couple.

f. Advanced ZrH Reactor Bearings

The advanced ZrH reactor bearings, while retaining the basic design of SNAP 8 bearings, were designed to operate at 1500° F in space for up to 20,000 hours. The P5 carbon-graphite against Al_2O_3 bearing couple was retained, with the Al_2O_3 shaft and socket substrate material upgraded by using Ta-10W for the 1500° F environment.[20]

Two bearing assemblies, identical except that one utilized a shaft with a builtin 2° offset to force oscillation of the ball, were subjected to a series of thermal vacuum testing. The offset shaft bearing set completed:

1) 27 thermal cycles between ambient and 1500° F

2) A parametric load test at ambient temperature, 800° F and 1500° F to study friction as a function of varying radial and thrust loads

3) 18,000 hours endurance testing at 1500° F including three thermal cycles and dwells at 1500° F of 1000, 1000, and 500 hours.

The bearing set was subjected to a total of 21,170 hours at 10^{-8} torr with 19,124 hours at 1500° F, 33 thermal cycles to 1500° F, 962 rotational cycles (equivalent to 280 in-out movements of a control drum), and dwells of 1000, 1000, and 500 hours at 1500° F.

The straight shaft bearing set completed a parametric load test duplicating that of the offset bearing.

(1) Thermal Cycle Testing

Bearings completed 27 thermal cycles during 2300 hours at 10^{-9} torr and accumulated 1050 hours at 1500° F during the test. A total of 180 bearing drive cycles, each 35° CW and 70° CCW, were run totaling 283 in. of bearing travel. Friction torque was recorded at ambient temperature, 800° F, and 1500° F of each thermal cycle during increasing and decreasing temperature ramps. Bearing temperature was stabilized at 800° F for approximately 20 min prior to taking data and was maintained at 1500° F for a minimum of 20 hours between increasing and decreasing portions of each cycle. Table 34 shows torque values and percentage scatter for data at each temperature.

TABLE 34

THERMAL CYCLE FRICTION TORQUE SUMMARY

Temperature	Friction-Torque (in.-lb)			
	Maximum*	Minimum	Scatter Band	
			Mean	Deviation (%)
Ambient	24.0 (0.75)	12.5	18.3	±32
800° F	15.0 (0.45)	5.5	13.5†	±11
1500° F	9.5 (0.28)	3.4	7.9†	±20

*(0.xx) corresponding friction coefficient
†Mean calculated after stabilization: Minimum at 800° F = 12.0 in.-lb; minimum at 1500° F = 6.2 in.-lb

(2) Parametric Load Tests

Bearing friction torque was measured at ambient temperature, 800° F, and 1500° F using a matrix of nine load points: 5-, 25-, and 50-lb radial loads and 25-, 75-, 150-lb axial loads. Figure 34 shows the friction torque for the 2° offset shaft and the straight shaft at 1500° F. Data have been corrected for system fixture friction. The curves seem anomalous because the friction torque with the offset shaft is less in some cases than the straight shaft friction. These curves are based on starting or breakaway torque which tends to be erratic causing the anomaly.

(3) Endurance Life Testing

Following the parametric test, the bearing with the 2° offset shaft was loaded to 25 lb radially and 75 lb axially and subjected to a simulated life test at 1500° F in 10^{-8} torr vacuum for 17,974 hours. Three thermal cycles and 215 equivalent revolutions of travel were accumulated. Figure 35 shows the breakaway friction measured during the endurance test and Table 35 summarizes the friction for all three phases of testing.

Two 1000-hour and one 500-hour dwell periods were imposed during the course of the test to see if measurable self-welding would occur. Table 36 shows pre- and post-dwell performance.

TABLE 35

STARTING FRICTION WITH 25-lb RADIAL AND 75-ft THRUST LOAD

	Maximum Breakaway Friction, μ^* at 10^{-8} torr (in. -lb)		
	Ambient	800° F	1500° F
Endurance (hr)			
10,000 to 17,947	21.4 (0.65)	14.2 (0.43)	7.1 (0.22)
5,000 to 10,000	-	-	7.1 (0.22)
0 to 5,000	-	-	7.1 (0.22)
Parametric Load Test, 100 hr	7.0 (0.21)	9.5 (0.30)	5.1 (0.15)
Thermal Cycle Test, 1050 hr	24.0 (0.73)	15.0 (0.45)	9.5 (0.29)

*(0. xx) corresponding friction coefficient

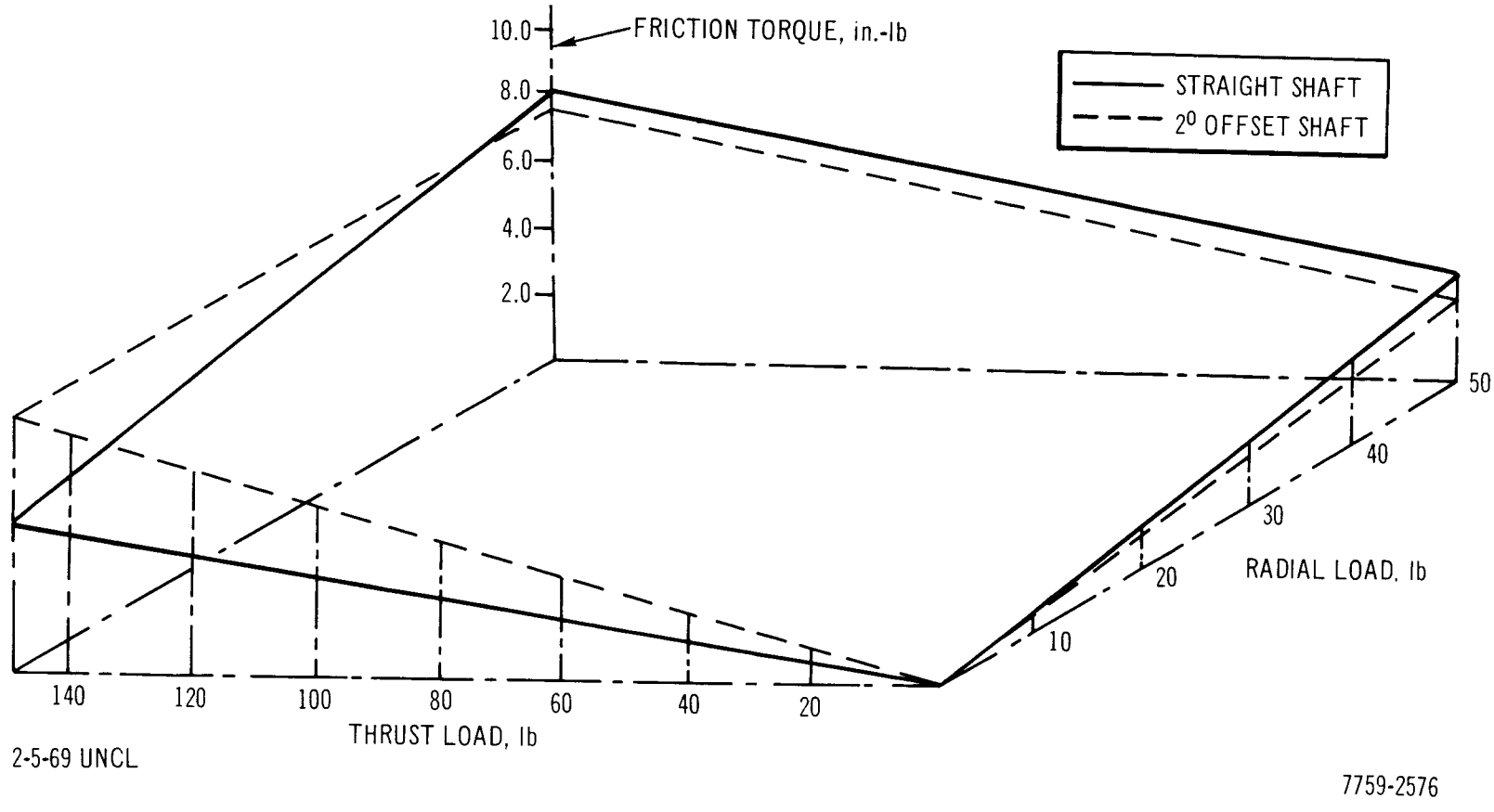

Figure 34. ZrH Reactor Control Bearing Breakaway Friction Torque vs vs Loads at 1500° F and 10^{-8} torr

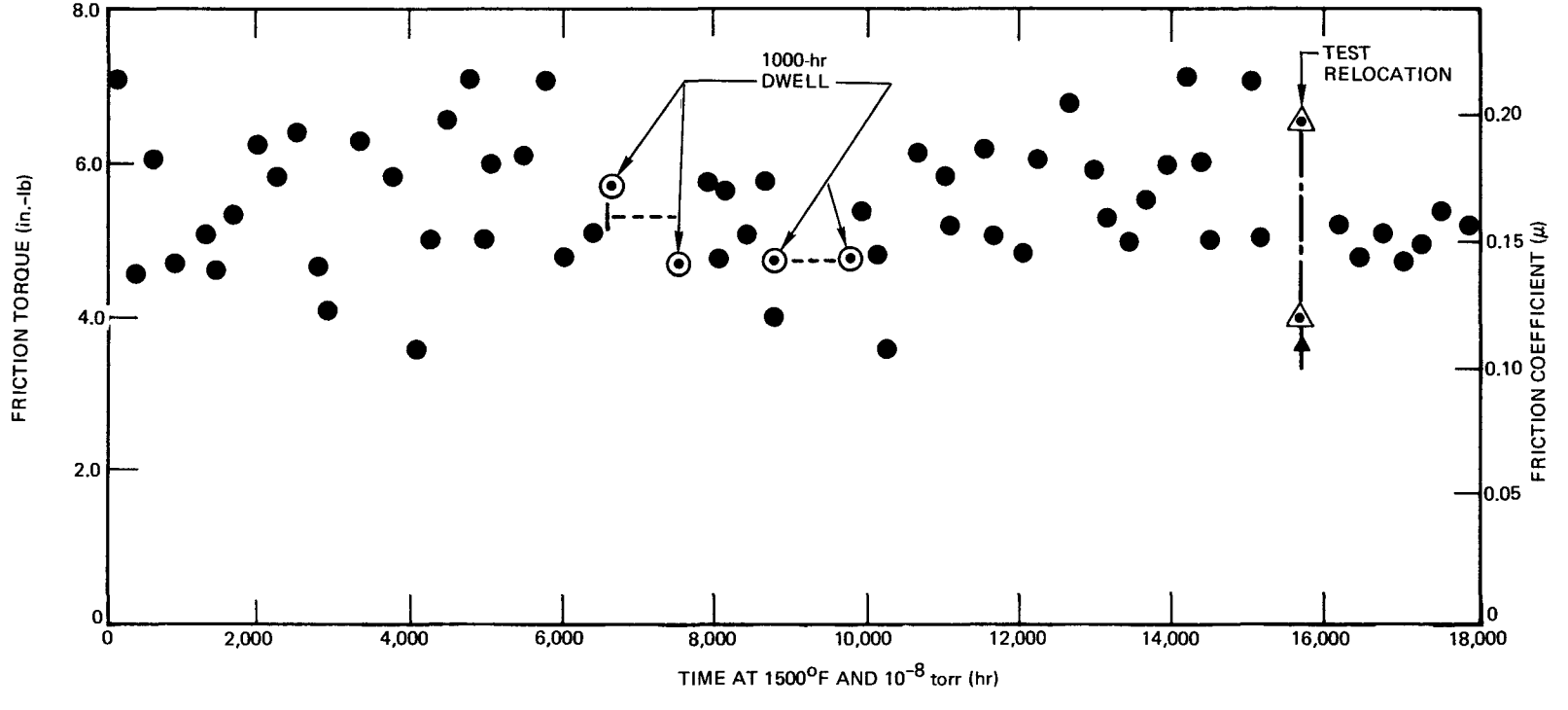

6531-5525

Figure 35. ZrH Reactor Bearing Life Test History, Al_2O_3 on Ta - 10 W vs P5 Carbon Graphite Breakaway Friction

TABLE 36

BREAKAWAY FRICTION TORQUE AFTER DWELL

Dwell Period (hr)	Friction Torque (in.-lb)	
	Pre-Dwell	Post-Dwell
1000	3.5	4.7
1000	4.6	4.7
500	5.7	3.5

It was expected that maximum torque values would be observed after the long dwells but the values are less than recorded during other phases of the test.

(4) Post-Test Inspection

Following each test phase, the bearing sets were disassembled and inspected for signs of wear or damage. Due to its limited testing, the straight shaft bearing set showed minimal evidence of the testing and was in excellent condition.

All parts of the offset bearing set were in excellent condition with no signs of excessive wear or detrimental effects due to thermal cycle, parametric, or endurance testing. Figure 36 shows the post-test bearing. Marks on the ball surface are due to machining and are not the consequence of testing. The concentric rings of carbon-graphite transfer-film on the sockets are the results of rotation between the ball and socket. The thrust sleeve corresponds to the burnished appearance of the ball thrust face. A uniform carbon-graphite transfer-film is present on the post-test shaft. Inspection of the shaft under a 90 power microscope shows no sign of cracking or failure of the Al_2O_3 coating.

(5) Test Facility

Testing of the Advanced ZrH Reactor bearing to 1500° F at 10^{-9} torr has required the design and fabrication of new test fixtures capable of reproducing space-thermal environments for periods up to 20,000 hours. Tests are conducted in the 2400 liter/sec ion-pumped system shown in Figure 37. Friction torque, temperature, and load data are printed and the entire test support fixture was fabricated from Ta-10W alloy. The heater and reflector assembly, also specifically designed for the ZrH bearing test and fabricated from tantalum, are

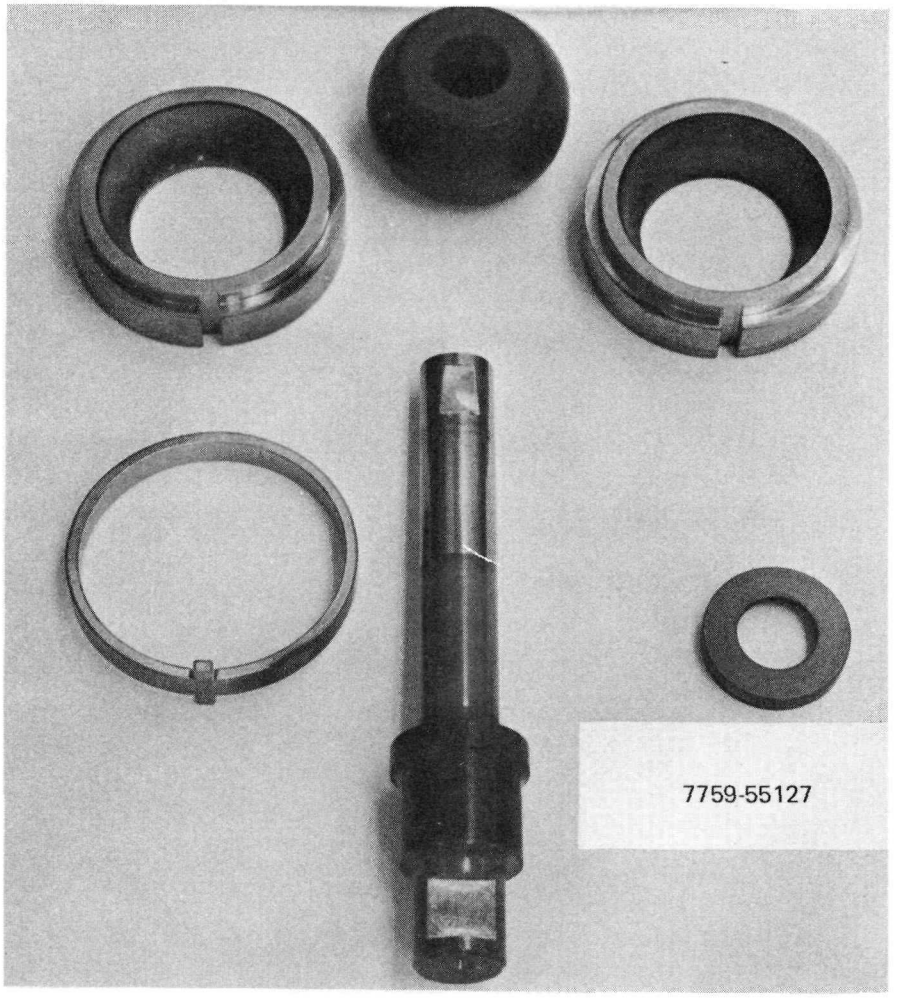

Figure 36. Advanced ZrH Reactor Control Drum Bearing Assembly – Post-Test

capable of maintaining temperatures in excess of 1800° F. During thermal cycling, temperatures are controlled by an SCR cam programmer. The test bearing and support assembly is carried by fixture bearings within the heater envelope, and radial and thrust loads are applied to the test bearing through sealed bellows. The torque arm is connected through the bellows assembly to an externally mounted force transducer. The bearing shaft is rotated through the magnetic drive unit and a force transducer measures the bearing sockets resistance to movement.

g. Launch Load Testing

Table 1 illustrates the changing launch load requirements as various space reactor systems evolved. The requirements for later systems were based on

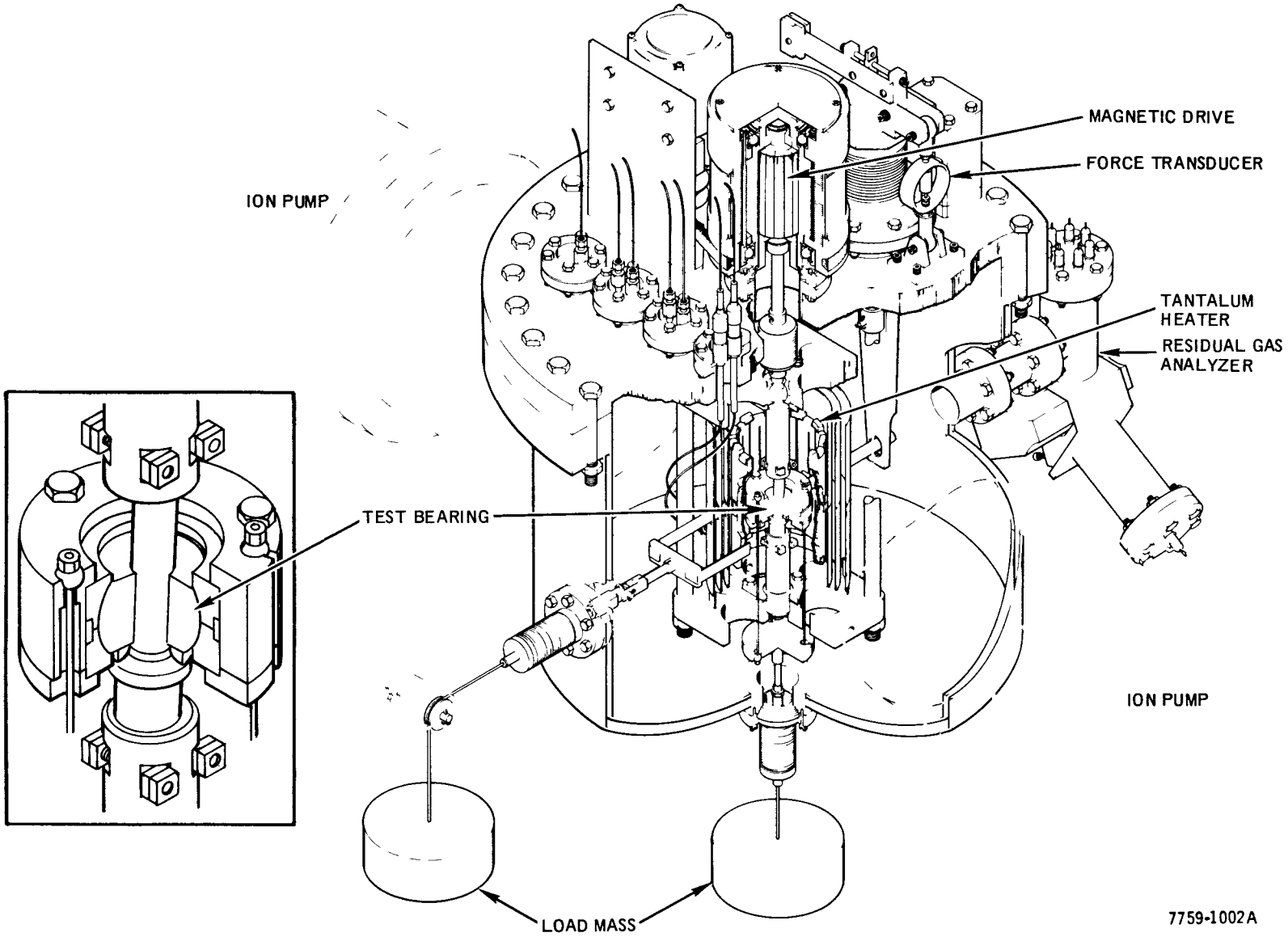

Figure 37. UHV Bearing Test Fixture

instrumentation records taken during launch of potential vehicles for the space reactor.

(1) SNAP 10A Shock and Vibration Tests

Eight bearing sets were subjected to shock and vibration tests per the SNAP 10A component requirements.[17] One of these sets was also subjected to two times the specified requirements. The tests were performed in the fixture shown in Figure 38 which simulates the drum mass with launch lockout conditions.

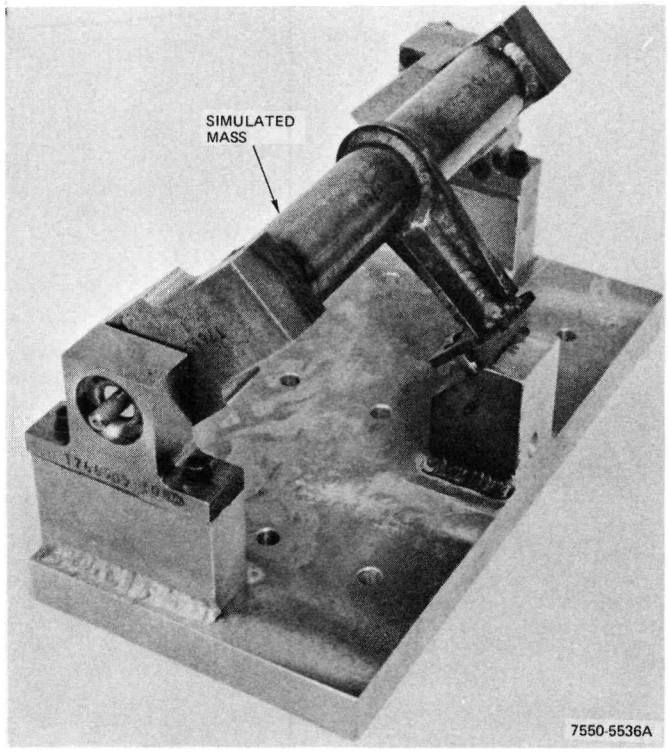

Figure 38. Drum Bearing Shock and Vibration Fixture

The aluminum oxide of the first shock and vibration test (Bearing Set 1) showed breakdown of the coated socket edges. The edges of all subsequent sockets were carefully chamfered to expose base metal and the breakdown problem has not recurred.

The balls of one set were found to be tight in their sockets after shock and vibration. These sockets had been dry-film-coated with Alpha Molykote X-15, which is sodium-silicate-bonded molybdenum disulfide plus graphite. Since this

test occurred during humid weather, swelling due to humidity was suspected. Before removing the bearings from the brackets, therefore, the assemblies were dried by heating then cooled to room temperature. Following this treatment, the balls were distinctly looser in their sockets. The assemblies were then subjected to humidity and again became tight. Visual inspection of the dry film showed there were compacted highs of dry film; apparently the bearing tightness was the result not only of swelling caused by humidity but also of sluffing and progressive localized compaction of the dry film. A special test was run of the dry-film cure cycle and 1-in.^{2} material samples were dry-filmed in a more complete cure cycle. Measurements of these samples through various humidity and drying cycles were inconclusive, but it appeared that either the improved curing had reduced susceptibility to swelling with humidity or the dry film problem had been largely caused by localized progressive compaction. A later improved curing cycle showed that proper dry-film application procedure and curing would reduce the sluffing and localized compaction as well as the swelling caused by humidity.

(2) SNAP 8 Vibration Tests

Two bearing sets, using the solid carbon-graphite balls, were subjected to simulated launch load shock and vibration testing in support of the SNAP 8 bearing development program.[5] The load test levels are listed in Table 1. The first test resulted in fretting of the spherical OD of the balls, and the buildup of carbon-graphite debris in the ball-to-socket bearing cavity.

A second test was run after coating the alumina socket surfaces with the MoS_2 dry-film lubricant. The dry-film layer cushioned the hammering of the ball in the socket, and the test was completed to design loads without fretting or other damage. The bearings were then tested to twice the design load level without any damage.

(3) Advanced ZrH Reactor Bearing Launch Load Tests

The Advanced ZrH Reactor bearings retained the same basic features as in SNAP 8 but the drum weight was 80 lb. Al_2O_3 against P5 carbon-graphite was retained as the reference bearing couple, but due to the increased temperature, Ta-10W was used as a substrate for the Al_2O_3 rather than the Inconel-750 used

on SNAP 8. Shock, vibration, and acceleration tests were conducted on prototype carbon-graphite balls to study the effect of the 80-lb drum on the bearings. Two types of carbon-graphite, the reference P5 and a finer grained AXF-5Q, were investigated. The tests were conducted using mocked up drum and bearing shafts, and prototype balls and sockets.

The testing was divided into two identical phases, testing the P5 carbon-graphite ball and the AXF-5Q carbon-graphite ball.[21] Testing was divided into three parts: (1) shock tests, (2) acceleration tests, and (3) determination of resonant frequencies followed by a 5-min dwell at the resonance.

(a) Shock Tests

Three 20-g shocks were applied in each direction of the x, y, and z axes (18 total shocks). Following the shocks no change in axial end play or residue from the carbon-graphite balls was detected. There was no visible damage to either the P5 or the AXF-5Q carbon-graphite balls.

(b) Acceleration Tests

The bearing fixture was placed in the centrifuge and the following accelerations were applied to the system:

6 g in the +x direction
3 g in the -x direction
±2 g in the y and z directions

Following the tests, no change in bearing axial play and no damage to either the P5 or the AXF-5Q carbon-graphite balls were found during visual inspection.

(c) Vibration Tests

Vibration testing consisted of determining the resonant frequences of the bearing-drum assembly and then conducting 5-min dwell tests at each resonance point. The resonant frequencies were determined by low level sinusoidal sweeps in each axis to ensure against damage to the bearings.

A series of 5-min dwells was then conducted at each resonant frequency with the input controlled to the response spectrum of Figure 39. No output was allowed to exceed the response level of the same figure. The resonant frequencies and their respective axes are shown in Table 37. The most prevalent

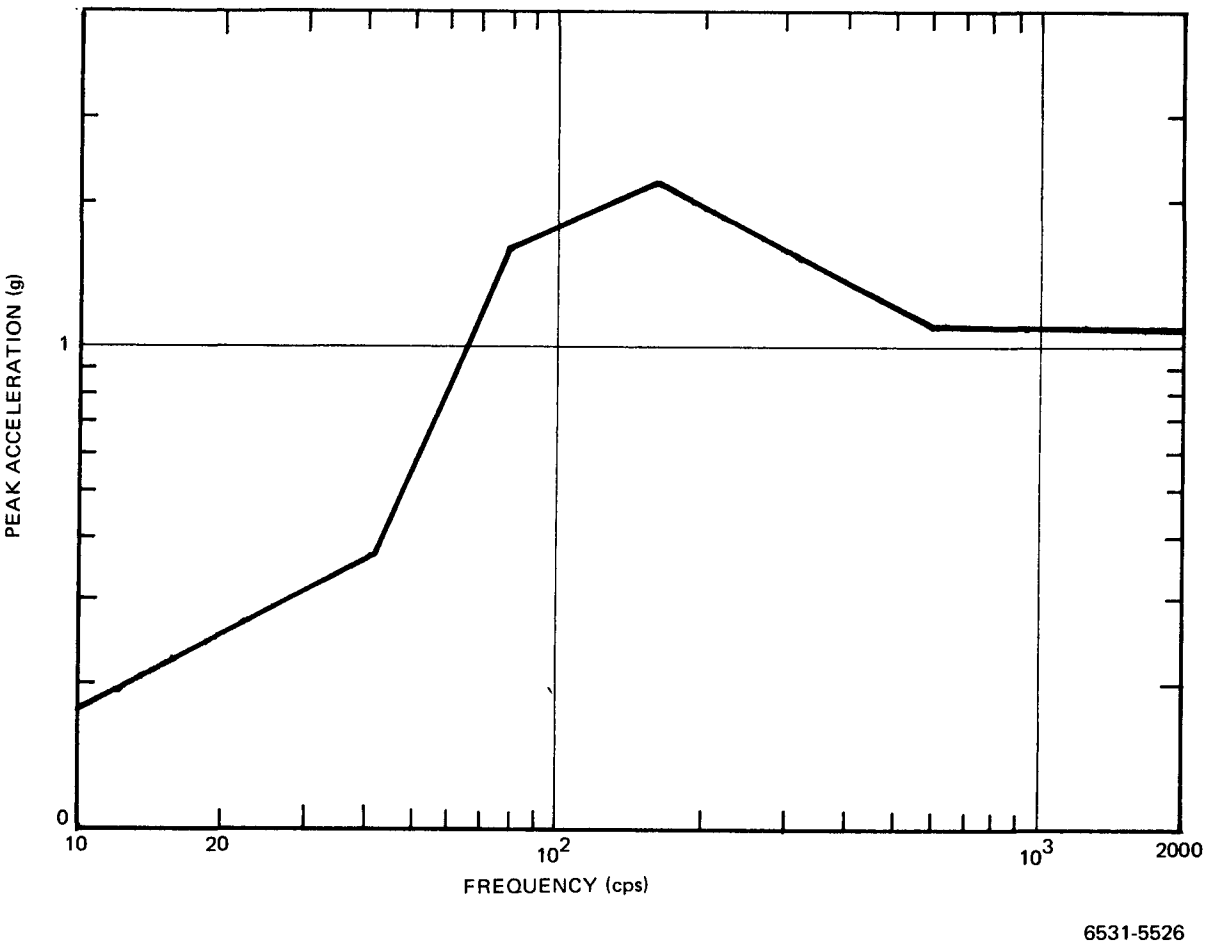

Figure 39. Resonant Dwell Response Level Limits

TABLE 37

EXPERIMENTALLY DETERMINED RESONANT FREQUENCIES

Input Axis	Resonant Frequency (Hz)	Acceleration Level (g)	Amplification Factor	
			AXF-5Q	P5
X	40 to 90	13	55	35
	500	11	5	5
	1500 to 1900	11	-	11
Y	40 to 90	4	7	16
	500	13	-	9
	1500 to 1900	11	7	10
Z	155	20	10	-
	500	13	56	35
	1500 to 1900	11	18	24

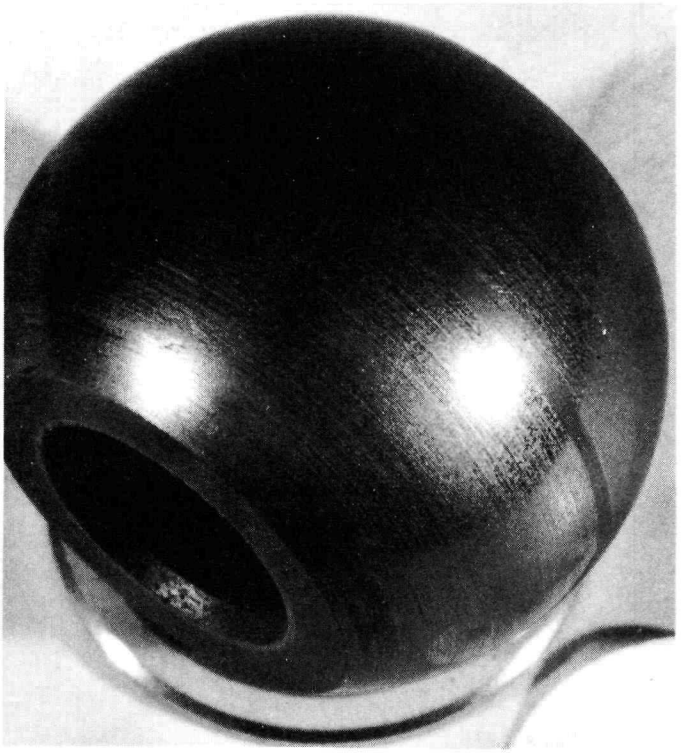

Figure 40. Post-Vibration Test, P5 Thrust Ball

7568-551341

frequencies were 40 to 90, approximately 500, and 1500 to 1900 Hz. Each graphite exhibited resonant frequencies of somewhat different frequencies and magnitudes.

Figure 40 shows the post-test P5 thrust ball, typical of all four bearings. General condition of the balls is excellent and neither the P5 nor AXF-5Q material appears to have been damaged by testing. There is no evidence of cracking or chipping of any of the balls. The thrust face of the ball shows lines of contact, but negligible wear. Note the ring on each ball along the center. This corresponds to the mating plane of the two socket halves. Ball ID's show several finite wear lines probably due to trapped graphite particles.

Both P5 and AXF-5Q carbon-graphites have been tested to Saturn-V launch shock, acceleration, and vibration loads using prototype bearings with mocked up shafts and drum. No damage to either graphite was detected and no sign of chipping or cracking of the balls could be seen. A slight degree of fretting occurred to the P5 carbon-graphite which was not evident with the AXF-5Q. The resonant frequencies of the mockup drum and bearing system were determined.

Tests were conducted later in the Advanced ZrH Reactor Development Program in which a prototype drum and drive system with prototype bearings were subjected to a resonance scan and a random noise vibration. The setup is shown in Figure 41. A sinusoidal sweep at one g resulted in a maximum amplification factor of 10 at 18 to 20 Hz. During the random noise test, a spurious input from the table imposed a 50 to 90 g load on the test assembly. No bearing failure was observed. The random inputs were 2.25 times specification level in Table 38.

TABLE 38
RANDOM SPECTRUM INPUT SPECIFICATION

20 to	42 Hz	at 0.001	g^2/cps
42 to	80 Hz	at +10	db/oct
80 to	160 Hz	at 0.0085	g^2/cps
160 to	700 Hz	at -6	db/oct
700 to	2000 Hz	at 0.0005	g^2/cps

Dynamic load test of 4 g at 18 to 20 lb for 3 min was performed. No damage to drum bearings resulted from the test.

4. Reactor and System Tests

Several tests were conducted in simulated space at operating temperatures on reactor or reactor-thermoelectric systems.

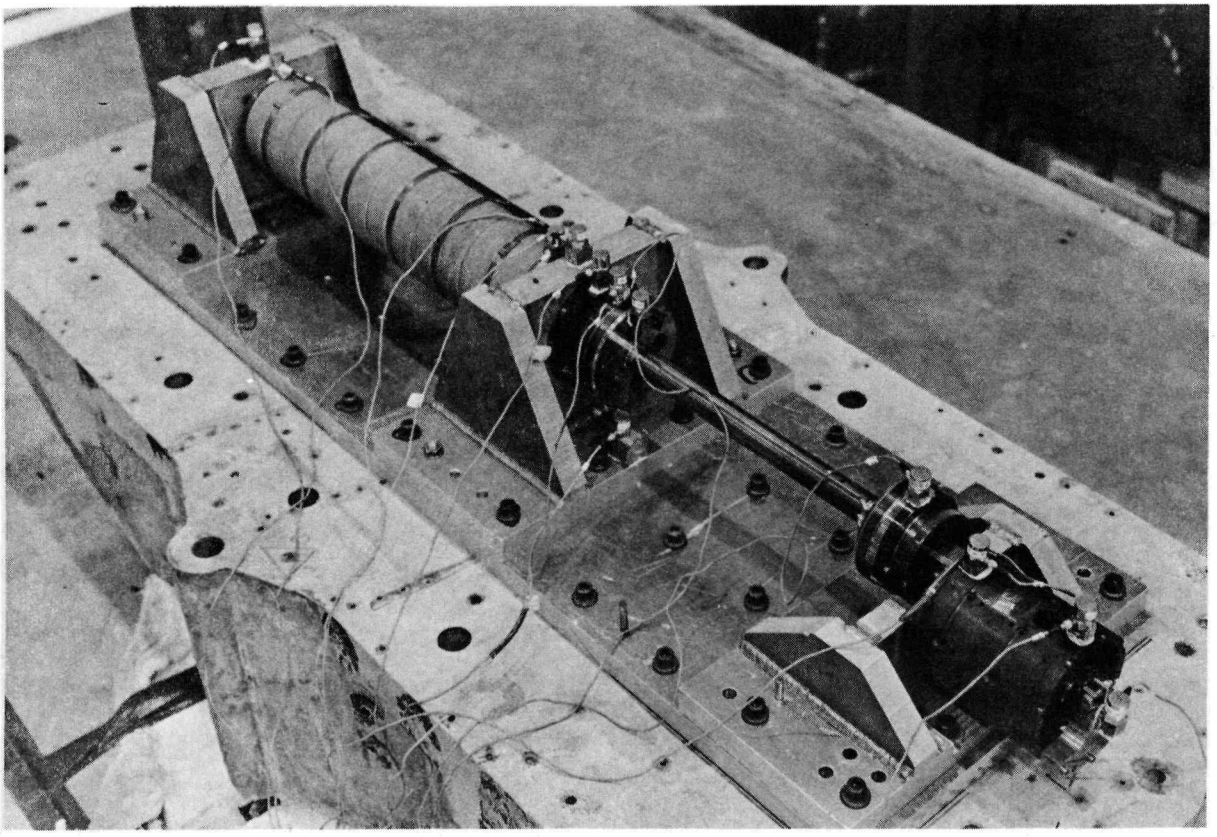

Figure 41. Drive System Vibration Test

Also one space flight was conducted on SNAP 10A. Table 39 lists several such tests which served to verify the performance of bearings under these conditions.

The SNAP 10DRM-1 was the first reflector assembly to be manufactured and tested. It was put through a series of startup simulation tests; qualification level shock, vibration, and acceleration tests; and a 90-day endurance test. The bearings performed as required during the tests.

The S10FS-3 system was identical to the flight systems. It was subjected to the complete spectrum of tests including initial performance measurements, full qualification-level shock and vibration, transient startup tests and a 10,000-hour endurance test in simulated vacuum. All bearing applications met performance requirements.

The S10FS-4 system was launched in a 700-mile earth orbit, and operated for 43 days or 574 orbits at full power. The control system, including the reflector bearings, performed satisfactorily to start up and operate the reactor as programmed.

The S2DRM-1 Reflector Assembly was ground tested to simulate hot critical thermal-vacuum checkout, launch vibration, and shock plus operational tests at temperature in vacuum. The critical checkout (performed twice) involved a heat-up to maximum temperature with control drums moved to full-in, a 4-hour dwell, and then movement of control drum to full-out during cooldown. The assembly was then vibrated in each of 3 axes to 7.5 g during a 45-min sinusoidal sweep. Two 5.5-g shocks in 8.8 msec were also imposed on the assembly. The thermal operation included a rise to full temperature, a 470-hour dwell and decrease to ambient temperature. Control drums were moved in during startup, oscillated 10° "out" to "in" each day, and moved out during shutdown. All bearings performed as required during all the tests.

The SNAP 8DRM-1 testing was intended to qualify the reflector and control components including bearings for flight use. The tests included extensive checkout at ambient conditions, low-level vibration surveys for resonant frequencies, nine startup sequences which involved firing squibs and stepping drums inward, a hot performance test at 1120° F (bearing at 469° F), and a qualification-level vibration and shock. A long-term endurance test was planned but cancelled when the effort was redirected. Results significant to bearing development were:

TABLE 39

REACTOR SYSTEM TESTS WITH SPACE BEARINGS

System Test	Test Type	Time at Operating Temperature (hr)	Temperature (°F)		Vacuum (torr)	Vibration and Shock
			Bearings	Core		
S10DRM-1	Nonnuclear Ground	2,800	600	1025	10^{-5}	To Specification (Table 1)
S10FS-3	Nuclear Ground	10,000	620	1025	10^{-4}	To Specification (Table 1)
S10FS-4	Nuclear Earth Orbit	1,032	600	1025	700 mi orbit	Actual Launch
S2DRM-1	Nonnuclear Ground	500	900	1150	10^{-5} to 10^{-7}	To Specification (Table 1)
S8DRM-1	Nonnuclear Ground	50	469	1120	10^{-5}	To Specification (Table 1)
S8DR	Nuclear Ground	7,023	900	1300	10^{-5}	None

1) Response of 8.75 g was measured at the bearing housing with 1 g vibration input.

2) The MoS_2 on one bearing had powdered and packed into the tight clearance to prevent drum rotation. This spurred development of better curing procedures for the sodium silicate binder.

3) No bearings in any component suffered damage from conditions imposed including the qualification-level vibration and shock. The bearing with packed MoS_2 mentioned above was cleaned before this test and operated satisfactorily afterward.

The S8DR nuclear ground test was run in a 10^{-5} torr vacuum for 7023 hours at power levels of 300, 600, and 1000 kwt of which 6688 hours were at 600 kwt. The reflector assembly including bearings were a flight-type design and performed properly throughout the test while nominally at 800° F.

B. BEARINGS FOR REACTOR COMPONENTS

Based on the development work conducted for the control drum bearings, it was concluded that a carbon-graphite against Al_2O_3 bearing couple should be used where practicable for all other reactor applications. At temperatures of 1000° F or less, many materials are a suitable substrate for the Al_2O_3 coating. All other reactor component bearing applications required only simple radial or radial-thrust bearings without self-aligning features. Again due to simplicity, journal bearings were retained on all rotating components. The following is a list of bearing applications common to all the SNAP reactor systems:

1) Control Drum Stepper Motor — S10, S2, S8, 5 kwe:
Hyperco 27 shaft, alumina coated at bearing areas; P5N or P5 bushings shrunk fitted into end bells

2) Drive Gears, Position Sensors, or Limit Switches:
Alumina on Inconel 750 for SNAP 8, on Rene 41 for the Advanced Reactor design, and on Inconel 718 for the 5-kwe reactor against carbon-graphite

3) Ground Test Kits
On both S10A and SNAP 8 ground test kits, alumina against carbon-graphite.

For several bearings or rubbing areas it was not possible to use carbon-graphite. In these cases a material or coating which retained a good degree of hardness at operating temperatures was used as a substrate for the sodium silicate bonded MoS_2. Examples are:

1) SNAP 10A Control Drum Bearings

2) Gear Teeth for All Reactors

3) Actuator Brake Faces (Anti-Self Weld)

4) Advanced Reactor Locking Cam

5) 5-kwe Ball Screw and Nut.

IV. 5-kwe-TE SYSTEM REFLECTOR BEARINGS

A. DESIGN SELECTION

The 5-kwe thermoelectric reactor, Figure 2, is similar in operation to previous SNAP reactors, except that the reflector control segments slide vertically, parallel to the reactor core. The reflector drive mechanism, a ball bearing screw, is supported at both ends by spherical self-aligning bearings and the movable segment is supported by the ball nut and screw, and by a spherical bearing. These three self-aligning bearings, are typical SNAP-type bearings using Al_2O_3 vs P5 carbon-graphite couple. The 5-kwe design requirements, Table 1, result in a bearing operating at 800° F in the space environment. The Al_2O_3 substrates are Inconel-750 for the sockets and Inconel-718 for the shaft. Inconel-750 was retained from SNAP 8 technology due to the considerable test experience with the Al_2O_3 coating on the socket configuration. A shaft of Inconel-718 was used because of design requirements for the ball screw shaft. At room temperature, the shaft-to-ball clearance is 0.0035 to 0.0045 in. and the ball-to-socket clearance in 0.0020 to 0.0030 in. At operating temperature, these clearances become 0.0019 to 0.0029 in. for the shaft to ball, and 0.0050 to 0.0060 in. for the ball to socket. The resulting bearing is smaller in size than the SNAP 8 bearing due to severe space limitations and lighter loading.

B. TEST HISTORY

Testing of the prototype bearing has not been conducted, but SNAP 8 bearings using Al_2O_3-coated Inconel-750 sockets and P5 carbon-graphite balls were used in two tests to evaluate MoS_2 dry-film life on ball screws at 800° F and 10^{-5} torr. The bearings underwent typical operation and dwell cycles expected on 5-kwe operation and performed satisfactorily. No further testing is currently planned.

BLANK

V. COMPONENT FABRICATION

Closely controlled materials and fabrication methods are required for repeated satisfactory performance of proven design bearing. These material controls and fabrication methods have been developed as part of this program. Specifications for materials were prepared, and processes tested and verified. Some salient features are listed below:

A. CARBON GRAPHITE

1) Procure to Pure Carbon Co. specification for Grade P5 with a material certification. Some impregnants used in carbon can react with alumina or its substrate.

2) Use clean handling and machine dry (no oil) with diamond tools. Water coolant sometimes used with a bakeout afterward.

3) Design with radiused edges or corners to prevent stress concentration.

4) Design for shrink fits that will not loosen at the maximum operating temperature. A shrunk-in bushing must be fully contained on the periphery in the housing (an overhang causes a stress transition and is a source of fracture).

5) Surface may be rubbed with MoS_2 powder to reduce friction slightly.

B. ALUMINA

1) The substrate should have a 60 finish or better and have finished heat treatment.

2) Clean part with vapor degrease, abrasive clean with clean 60-mesh alumina powder and clean ultrasonically in chlorinated solvent.

3) Coat areas by Linde "D" gun process to 0.006-in. thick minimum with 99% pure alumina material. Hardness to be 850 (VPN-300 gram) minimum.

4) Finish-machine with diamond or silicone carbide tools and water coolant.

5) Do not ultrasonically clean after coating.

C. SODIUM-SILICATE-BONDED MoS_2 – SPRAY COATING

1) Use material that conforms to the Naval Aeronautical Materials Laboratory Sodium Silicant Lubricant.

2) Vapor degrease and ultrasonically clean substrate with chlorinated solvent and dry in clean 10^{-4} torr vacuum at 1150° F for 1 hour. Cool parts.

3) Handle with clean nylon gloves.

4) Coat parts 0.0004 to 0.0011 in. thick.

5) Air dry 30 min and bake at 180° F for 2 hours. An infrared heat source is recommended. Cure further at 400° F for 3 hours.

6) Specimens coated with the parts are to be tested for adherence.

7) Coated surfaces may be burnished with nylon cloth to obtain precision thicknesses or fits with mating parts.

REFERENCES

1. F. P. Bowden and D. Tabor, The Friction and Lubrication of Solids, (Clarendon Press, Oxford, 1950)

2. L. G. Kellogg, "SNAP Reactor Materials Development, Self-Weld Studies," NAA-SR-9643, June 1964

3. W. J. Kurzeka, "Bearing Materials Compatibility for Span Nuclear Auxiliary Power Systems," NAA-SR-6476, September 1961

4. L. Kellogg, "SNAP Reactor Materials Development, Ultrahigh-Vacuum Friction Studies," NAA-SR-9644, June 1964

5. P. H. Horton, "SNAP 8 Control Drum Bearing Development," AI-AEC-12964, August 1970

6. M. E. Merchant, "The Mechanism of Static Friction," J. Appl. Phys. 11, No. 3, March 1940, p 230

7. D. V. Keller, "Metallic Adhesion," ASMA/ASLE Aerospace Council, N. Y., May 1963

8. E. Rabinowicz, "Practical Use of the Surface Energy Criterion," Conference on the Fundamental Mechanisms of Solid Friction, Kansas City, Kansas, September 1963

9. M. E. Sikorski, "The Adhesion of Metals and Factors that Influence It," Conference on the Fundamental Mechanisms of Solid Friction, Kansas City, Kansas, September 1963

10. F. P. Bowden and J. E. Young, "Friction of Diamond, Graphite, and Carbon and the Influence of Surface Films," Proc. Royal Society of London, 208A (1951)

11. E. E. Bisson, "Boundary Lubrication and Adhesion Theory of Friction," Bearing Technology, 1961

12. J. C. Simons, Jr., "Effects of Extreme Altitudes, and the Need for Simulation," Inst. of Environmental Sciences, 1960

13. W. Brainard, "The Thermal Stability and Friction of Disulfides, Diselinides, and Ditellurides of Molybdenum and Tungsten in Vacuum (10^{-9} to 10^{-6} torr)," NASA TN D-5141, April 1969

14. V. Hopkins, et al, "Development of New and Improved High Temperature Solid Film Lubricants," ML-TDR-64-37, Part II, April 1965

15. J. G. Asquith (ed.), "SNAP Reactor Programs Progress Report, May-July 1969," AI-AEC-12870, September 1970

16. J. Susnir, "SNAP 10A Reactor Design Summary," NAA-SR-8679, February 5, 1963

17. W. J. Kurzeka, "SNAP 10A Component Development Summary," NAA-SR-9898, Vol I, II, III, 1964

18. Puls, et al, "SNAP Reactor Control Drum Drive Summary," NAA-SR-9615, August 24, 1964

19. W. J. Kurzeka, "Functional Design Description and Test Summary of SNAP 8 Development Reactor Mockup-1," NAA-SR-12300, February 24, 1967

20. D. G. Mason (ed.), "SNAP Reactor Programs Progress Report, February - April 1969," AI-AEC-12819, June 29, 1969

21. "SNAP Reactor Programs Progress Report, February - April 1969," AI-AEC-12953, June 15, 1970

APPENDIX
PROPRIETARY MATERIALS SOURCE LIST

Designation	Composition (wt %)	Source
Coatings and Platings		
LA-2	99 + γ (gamma) phase Al_2O_3	Linde Division, Union Carbide
LC-1A	85 Cr_3C_2 + 15 Ni-Cr binder	Linde Division, Union Carbide
LC-1C	93 Cr_3C_2 + 7 Co binder	Linde Division, Union Carbide
LW-1N	84 to 87 WC + Co binder	Linde Division, Union Carbide
LW-5	25 WC + 7 Ni + mixed W, Cr carbides	Linde Division, Union Carbide
Noroc	99 + γ Al_2O_3	Norton Company
Ceramics and Cermets		
K96	WC base	Kennametal, Inc.
K162B	64 TiC, 25 Ni + Mo, CbC, TaC	Kennametal, Inc.
LT-2	60 W, 25 Al_2O_3, 15 Cr	Haynes Stellite Division, Union Carbide
LA 687	Al_2O_3 (hot pressed)	Norton Company
Firth CR-2	Cr_3C_2	Unknown
Carboloy 608	Unknown	General Electric
Composites		
Grafoil	Pyrolytic graphite	Unknown
Mykroy	Glass-bonded mica	Unknown
Micaceram	Mica-bonded mica	Unknown
Deva 3N-12	Ni + carbon	Deva Metals, Inc.
Deva 3F-12	Fe + carbon	Deva Metals, Inc.
108M	65 MoS_2 + 25 Ta + 10 Mo	Boeing Aircraft Corporation

APPENDIX (Continued)

Designation	Composition (wt %)													Source
Carbon-Graphites														
CDJ - 83	Unknown impregnated graphite													National Carbon
Purebon P-5	Unimpregnated 60% graphitized carbon-graphite													Pure Carbon, Inc.
Purebon P-5N	LiF impregnated 60% graphitized carbon-graphite													Pure Carbon, Inc.
Purebon P-02	LiF impregnated 60% graphitized carbon-graphite													Pure Carbon, Inc.
Purebon P-03N	Unknown													Pure Carbon, Inc.
Purebon P-03NHT	Unknown													Pure Carbon, Inc.
Purebon ZTA	Unknown													Pure Carbon, Inc.
Purebon 3293	Unknown													Pure Carbon, Inc.
Graphitar 16	Unknown													Unknown
AXF-5Q	Unimpregnated, 60% graphitized fine grain carbon-graphite													Poco Graphite Company
Dry-Film Lubricants														
Drilub 861	WS_2 base													Drilube, Inc.
Drilub 867N	Ceramic + $MoSe_2$ base													Drilube, Inc.
Lubco 6001	MoS_2 base													Lubco, Inc.
Lubco 6021	MoS_2 base													Lubco, Inc.
Molykote X-15	MoS_2, graphite base													Alpha-Molykote Corporation
Metals	Fe	Cr	Ni	Mo	Co	C	W	Cb	Al	Si	Mn	Ti	Other	
Hastelloy B	4.0-7.0	1.0	Bal	26.0-30.0	2.5	0.5				1.0	1.0		0.2-0.6 V	Haynes Stellite Division, Union Carbide
Haynes 25	3.0	19.0-21.0	9.0-11.0		Bal	0.05-0.15	14.0-16.0			1.0	1.0-2.0			Haynes Stellite Division, Union Carbide
Haynes 90	Bal	27.0				2.75				1.0	1.0		2.0	Haynes Stellite Division, Union Carbide
Stellite No. 3	3.0	30.5	3.0		Bal	2.45	12.5			1.0	1.0			Haynes Stellite Division, Union Carbide
Stellite 6B	3.0	30.0	3.0	1.5	Bal	1.0	4.5			2.0	2.0			Haynes Stellite Division, Union Carbide
Inconel 718	18.0	19.0	52.5	3.0		0.04		5.2	0.6	0.2	0.2	0.8	0.1 Cu, 0.007S	International Nickel
Inconel 750	5.0-9.0	14.0-17.0	70.0		0.7-1.2	0.08			0.4-1.0	0.5	1.0	2.5	0.5 Cu, 0.01S	International Nickel
Vicalloy	Fe, Co base alloy													Unknown
Ta-10W	90% tantalum, 10% tungsten													Several vendors